PREDICTION OF THE EFFECTS OF CREEP OF CONCRETE

UNDER NON-UNIFORM STRESS

PREDICTION OF THE EFFECTS OF CREEP OF CONCRETE UNDER NON-UNIFORM STRESS

by

David C. Gray, B.Sc.

A Thesis
Submitted to the Faculty of Graduate Studies
in Partial Fulfillment of the Requirements
for the Degree
Master of Engineering

McMaster University
Hamilton, Ontario

December, 1968

MASTER OF ENGINEERING (1968) McMASTER UNIVERSITY

(Civil Engineering) Hamilton, Ontario

TITLE: PREDICTION OF THE EFFECTS OF CREEP OF CONCRETE UNDER NON-UNIFORM STRESS

AUTHOR: DAVID C. GRAY, B.Sc. (Glasgow)

SUPERVISOR: DR. R. G. DRYSDALE

NUMBER OF PAGES: v, 138

SCOPE AND CONTENTS: The problem of predicting the stresses and strains in a plain concrete member subject to sustained non-uniform stress is investigated. Two theoretical methods of solving this problem are presented. Both were used to predict the strains and stresses of four eccentrically-loaded plain concrete prisms which formed a part of an experimental program. The experimental program also furnished data necessary for both of the theoretical approaches. It is concluded that the two methods are useful, and that they may be easily modified to deal with problems involving the sustained load characteristics of reinforced concrete members.

TABLE OF CONTENTS

ACKNOWLEDGEMENTS

The author would like to express his gratitude to Dr. R. G. Drysdale for his advice and guidance throughout the course of this research.

The author also takes this opportunity to thank McMaster University for awarding him a scholarship and an assistantship.

CHAPTER 1

INTRODUCTION

1.1 Foreword

Creep of concrete has many important effects in engineering structures. This is particularly true in cases in which the concrete is subjected to a non-uniform stress distribution (i.e. when the concrete is subjected to a stress gradient) since such cases are commonest in practice. Some practical examples of cases where stress gradients arise are given in section 1.4. The important point about creep in such cases is that it brings about a redistribution of stress. In view of the importance that these effects can have, it is somewhat surprising that comparatively little has been published on creep of this type. The purpose of the investigation described in the following pages was to analyse this particular type of creep, and to devise and test methods of predicting its effects.

This first chapter is intended as an introduction to the topic, and as an outline of background material.

1.2 Definitions

Only a few definitions are required at this stage and these appear below; other terms will be defined or explained as they arise.

Creep:- When concrete is loaded it undergoes two kinds of deformation

(i) immediate deformation

(ii) time-dependent deformation which begins at once and continues for years, though at a decreasing rate. This second type of deformation is known as creep.

"True" or "Basic" Creep:- True or basic creep of concrete is creep which occurs under conditions which prevent moisture movement to or from the surrounding medium.

"Specific" Creep:- The specific creep at a given time is the creep strain at that time per unit of applied stress. (Typical units of specific creep would thus be inches per inch per p.s.i.).

Elastic Strain of Concrete:- The term "elastic" strain is used in this report to mean that strain which occurs immediately on application of stress. The term does not necessarily mean that all such strains will be recovered on removal of the applied stress. It is used to distinguish such instantaneous strains from the creep strains defined above. Note also that this definition does not necessarily imply a linear stress-strain relation. Values of elastic strain used in this report were taken from short-term cylinder tests.

1.3 The Nature of Creep

A short description of the theories of creep, and of factors affecting creep, is given. The purpose of this brief review is to provide a background against which the McMaster investigation can be described. For a complete list of references describing creep and related topics, the reader is referred to the excellent Bibliographies published by the American Concrete Institute[1] and the Cement and Concrete Association[2].

1.3.1 The Structure of Concrete

Since any description of the mechanism of creep presupposes some knowledge of the structure of concrete, a brief outline will be given here.

Our interest is principally centred on the physical nature of the products of the hydration of cement.

Fresh, hardened cement paste is mainly composed of various hydrates (known as "gel"), of crystals of calcium hydroxide, and of particles of unhydrated cement. These components form a firm matrix which serves to connect the aggregate particles. This matrix, however, also contains various spaces in which water resides.

The largest spaces are termed capillary pores; they are minute channels in the paste whose diameter has been estimated[3] to be of the order of 5×10^{-5} inches. Permeability studies suggest that they form an interconnected network within the paste.

The fact that such pores exist is important in the hydration process. Water supplied to the concrete (e.g. by wetting its surfaces) can pass along these tiny channels, allowing the hydration process to continue in the interior regions of the concrete mass. In time, the formation of hydration products often blocks up capillary pores, causing them to become segmented and discontinuous.

Interstitial voids between the fibrous particles of the gel also contain water. These voids are termed gel pores. They are much smaller than capillary pores, having a diameter of between 15 and 20 Angstrom units.

1.3.2. Theories of Creep

A great many "theories" of creep have been proposed, most of them being hypotheses which fit some known facts and are in disagreement with others. It seems likely that a composite theory will ultimately emerge from the individual hypotheses outlined below.

(i) Plastic Theory of Creep

This theory holds that creep of concrete is due to crystalline flow. That is, creep is due to slipping along certain preferred planes in the crystal lattice, and to local rupture of the cement paste.

It may be noted that, while in metals undergoing plastic deformation, the volume change experienced is fairly slight, a fairly large decrease in volume occurs as concrete creeps. In addition, if this theory were completely true, creep of concrete would be wholly irrecoverable. This is not the case in practice.

Thus, plastic flow cannot be wholly responsible for creep.

(ii) Viscous Theories of Creep

In these theories, creep is assumed to be a viscous flow, or movement of particles over each other.

Thomas[4] considers the concrete to consist of two parts:

(a) cement gel, which behaves in a viscous manner when loaded, and

(b) aggregate particles, which do not flow under load.

On loading the concrete, the natural tendency of the cement gel to flow is impeded by the relatively rigid aggregate particles. The latter then experience an increase in stress owing to their resistance to the gel flow. Meanwhile, the stress on the gel decreases, giving a corresponding decrease in flow (i.e. a decrease in the rate of creep).

Using this theory, researchers have attempted to conclude that the rate of creep will depend on the cement gel properties, but will be independent of the properties of the aggregate, which is considered to be rigid. It has been pointed out*, however, that the amount and rate of creep deformation also depend on the aggregate's elastic modulus and porosity.

It should be noted that if creep were due entirely to viscous flow, the volume of the concrete would remain constant. The fact that this is not even approximately true has already been mentioned.

(iii) Delayed Elastic Theory

The cement gel is assumed to consist of both elastic and viscous phases which can interact causing delayed elasticity. That is, under the action of an external load, flow of the viscous phase takes place, thereby throwing an increasing percentage of the load on the elastic phase. This results in an increase in elastic deformation with time.

Creep of concrete, however, exhibits such behaviour only to a limited extent. This theory cannot explain the observed influence of moisture exchange on creep.

(iv) The Seepage Theory of Creep

The seepage theory suggests that the equilibrium of the concrete's solid phase with the external load is determined by the vapor pressure of the gel water. This vapor pressure equilibrium is disturbed by the application of any load increment. The applied stress is considered as forcing sheets of cement gel together, and thus putting pressure on the

* See section 1.3.3 "Factors Affecting Creep:.

gel water. Equilibrium is gradually restored as moisture seeps through pores in the concrete to the member's surface. The process involves a loss of water from the gel pores. Adjacent surfaces in the pores are now closer to each other and are attracted by stronger van der Waal's forces. This increased attraction can cause some deformation of the matrix. Surface tensions may also play a small part in the deformation, since surface menisci exert a force on the surrounding material.

Objectors to this theory have stated that the loss of moisture during creep straining should be similar to that experienced during shrinkage of the same magnitude. Experiments have shown that this is not so[14]. Powers[5], however, pointed out that the water loss during creep is likely to be about one-hundredth of that which would occur under equal shrinkage. The following example, used by Powers, illustrates this:

The following experimental data refer to the shrinkage of a mortar specimen drying from the saturated state to a state approximately equilibrium at 50 per cent relative humidity:

Item	Notation	Quantity
water/cement ratio	w/c	0.47 by weight
drying shrinkage	$\Delta L/Lo$	880×10^{-6} in/in
volumetric shrinkage	$\Delta V/Vo$	2640×10^{-6} in^3/in^3
amount of water lost	$\Delta w/Vo$	.103 c.c. per c.c. of specimen

Consider an identical specimen in a totally saturated state, and subjected to uniaxial compression without drying. Let the load be such that the measured creep strain amounts to 880×10^{-6} in/in. By the seepage theory, water will tend to relieve the stress on itself by moving out of a stressed region. Since the specimen is saturated, this means that water must move out of the specimen. For the given conditions, the amount of water lost will be virtually equal to the reduction in volume of the specimen. (Otherwise some water in the specimen will remain under compressive stress, and the specimen's dimensions will depend partly on the stress).

Let μ = Poisson's ratio

Then $\Delta V/Vo = (1 - 2\mu)\ \Delta L/Lo = \Delta w'/Vo$

where $\Delta w'$ = water lost due to creep

Thus $\Delta w'$ can be calculated for any value of μ. Taking $\mu = 0$ will give the greatest value of $\Delta w'$, viz

$$\frac{\Delta w'}{Vo} = \Delta L/Lo = 880 \times 10^{-6} \text{ c.c.}$$

$$\text{Thus, } \Delta w'/\Delta w = \frac{880}{103{,}000} = \frac{1}{117}$$

Hence, the creep strain requires less than one-hundredth the loss of water for equivalent drying shrinkage. Powers also pointed out that water should still be lost even if the creep prism was not initially saturated.

A further objection to this theory is the fact that concrete exhibits creep even when no moisture exchange with the surrounding medium is possible. There is, however, a body of opinion which holds that in this case water seeps from regions of high pressure to regions of lower pressure within the concrete.

Creep recovery can also be explained in terms of this theory. Removal of the applied load allows an instantaneous recovery of elastic strain, following which moisture may slowly return to the areas from which it was previously expelled. The water molecules act against the cohesive forces holding the gel particles closely together. The gel particles are thus forced further apart. A similar mechanism accounts for the swelling of concrete when immersed in water.

The seepage theory is attractive in that it can explain many of the observed features of creep of concrete.

Of the various theories, it appears that the seepage theory, although not yet universally accepted, best accounts for observed creep behaviour.

1.3.3. Factors Affecting Creep of Concrete

A great many investigations have been carried out in order to ascertain the effects of individual variables on the magnitude of creep. The following section represents a summary of the results of many test programs.

(i) Magnitude of Applied Stress

Creep depends first of all on the magnitude of the applied stress. The relationship is generally taken to be linearly proportional for stresses up to about 50% of the crushing strength, although the exact limit of proportionality is disputed, and has been estimated to be considerably lower[10].

At stresses higher than this limit, creep increases at an increasing rate with stress, as shown qualitatively in Fig. 1.1. It is known that at stresses of about 40 to 60% of the crushing strength internal micro-cracking of the concrete begins. This change in the

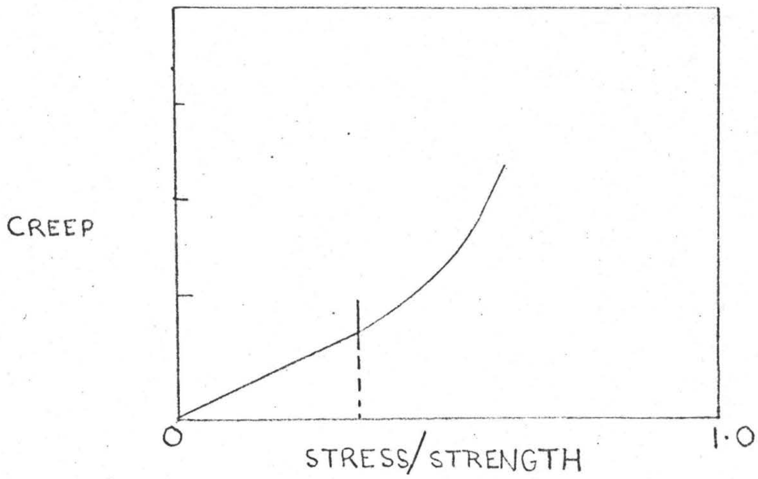

Fig. 1.1.

concrete's internal structure may partially account for the increasing slope of the CREEP v. STRESS/STRENGTH curve at high stress levels.

For a uniformly applied stress higher than about 80% of the concrete strength, creep will lead to failure of the concrete.

(ii) Mix Proportions

The type, quantity, and maximum size of the aggregates used influence creep.

The aggregate acts as reinforcement for the cement paste; as such it tends to restrain the paste's volume changes. The amount of restraint which the aggregate can offer is principally determined by

(a) the amount of aggregate present in the mix

(b) the Young's Modulus of the aggregate.

Experimental evidence[7] has confirmed that high aggregate content and an aggregate with a high Young's Modulus both lead to lower creep.

In addition, highly porous aggregates have been connected with comparatively high creep, and this has lent some weight to theories of creep based on the movement of moisture within the concrete (see section 1.3.2. (iv)). The situation is not clear, however, since highly porous aggregates frequently have a low Young's Modulus. Thus, the high creep might be at least partly caused by the low value of "E".

Concretes made with different types of cement and subjected to the same applied stress at the same early age will exhibit different creep characteristics. This is because the various types of cement differ in the fineness to which they have been ground, and also in the proportions of the cement compounds which they contain. Therefore, they have different rates of hydration and unequal strength gains for similar degrees of hydration. Their creep characteristics are functions of degree of hydration and strength.

In general, concrete containing Type IV (Low Heat) cement will creep more than that containing Type I (Ordinary Portland) cement, which will in turn creep more than that containing Type III (Rapid-Hardening) cement, (i.e. for the same age at loading, the lower the strength of the concrete, the higher the creep). The differences are small, however, if the concrete is loaded at a considerable age after pouring.

The amount of creep increases with increased water/cement ratio (aggregate/cement ratio being constant). The relationship is not clearly defined. This increase is evident only above a certain minimum percentage of water, but does apply for the range of water/cement ratios normally used in practice.

(iii) Age of Concrete

The age of concrete at loading is known to influence creep. The degree of hydration and strength of concrete normally increase with age and thus reduce creep. If no significant variation in the degree of hydration occurs with time; the age at loading does not influence creep. For mature dry-cured concrete, the age at which the load is applied has a comparatively small effect on creep. In addition, for other concretes, the rate of creep at later ages is largely independent of the age at loading.

If, however, hydration is allowed to proceed, the gel matrix becomes progressively stiffer with time, due to the addition of more gel. In practical cases, therefore, when load is applied to wet-cured concrete at a fairly early age, the age at the time of loading is an important factor.

(iv) Ambient Relative Humidity.

It has been demonstrated[12] that creep increases with a decrease in ambient relative humidity. Fig. 1.2. illustrates this effect qualitatively. The numbers on the plots refer to the ambient relative humidity.

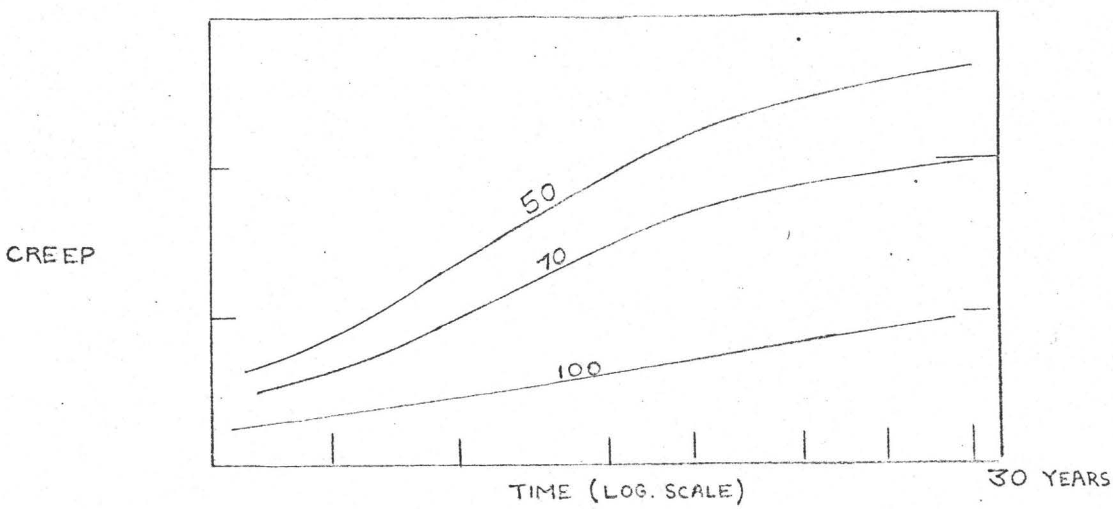

Fig. 1.2.

If, in accordance with the seepage theory of concrete creep (described in section 1.3.2.), creep can be described as a sort of stress-induced shrinkage, the influence of low relative humidity in aiding the process can easily be visualized.

It may be noted that alternating the relative humidity of the surrounding medium between two limits will yield higher creep than that observed at some constant value of relative humidity between these limits[13]. Ali and Kesler[14], have explained this phenomenon in the following way. Let the terms shrinkage and swelling denote volume changes due to egress and ingress respectively of gel water with or without applied load. In the absence of applied load, such volume changes will be termed free shrinkage and free swelling. Ali and Kesler then state the following rules describing concrete's behaviour under various conditions of moisture exchange and applied load.

(a) Free shrinkage is less than shrinkage under an applied compressive stress.

(b) Free swelling is more than swelling under an applied compressive stress.

Now creep is usually defined as the difference between the time-dependent deformations of a loaded specimen and an unloaded control specimen. According to this definition and the behaviour described in (a) and (b), creep would be expected to increase with moisture exchange, irrespective of the direction of the moisture movement.

(v) Temperature

Creep is known to increase with increasing temperature, the greatest increases taking place in the range of 70°F to 180°F. The seepage theory of concrete creep (see section 1.3.2.(iv) suggests that creep involves seepage of gel water. This water, existing within the gel in layers only a few molecules thick, has quite different properties from larger volumes of water. Its viscosity, for example, is several thousand times that normally exhibited by water[5]. It is possible that high temperatures may produce increased creep by reducing the viscosity of the gel water, thus making it more mobile.

(vi) Curing Conditions

The curing conditions for the concrete affect its creep behaviour, presumably through their effect on the concrete's degree of hydration and on its internal structure. That is, curing conditions affect both the strength of the concrete and the permeability of the gel. The latter factor is important if creep takes place by seepage of gel water, as the seepage theory (section 1.3.2. (iv)) suggests.

In this connection, it may be noted that creep of high-pressure steam-cured concrete is known to be comparatively low[7]. It is also known that such curing produces concrete with a vastly different internal structure, as indicated by specific surface measurement.[3]

(vii) Member Size and Shape

Size and shape affect the shrinkage characteristics of a concrete member.

Mattock and Hansen[8] have made the assumption that their influence on creep is confined to that creep which is accompanied by moisture exchange with the surrounding medium, (i.e. 'Basic Creep' is unaffected by member size and shape).

Fig. 1.3. is taken from their work, and illustrates the relationships derived from their test program.

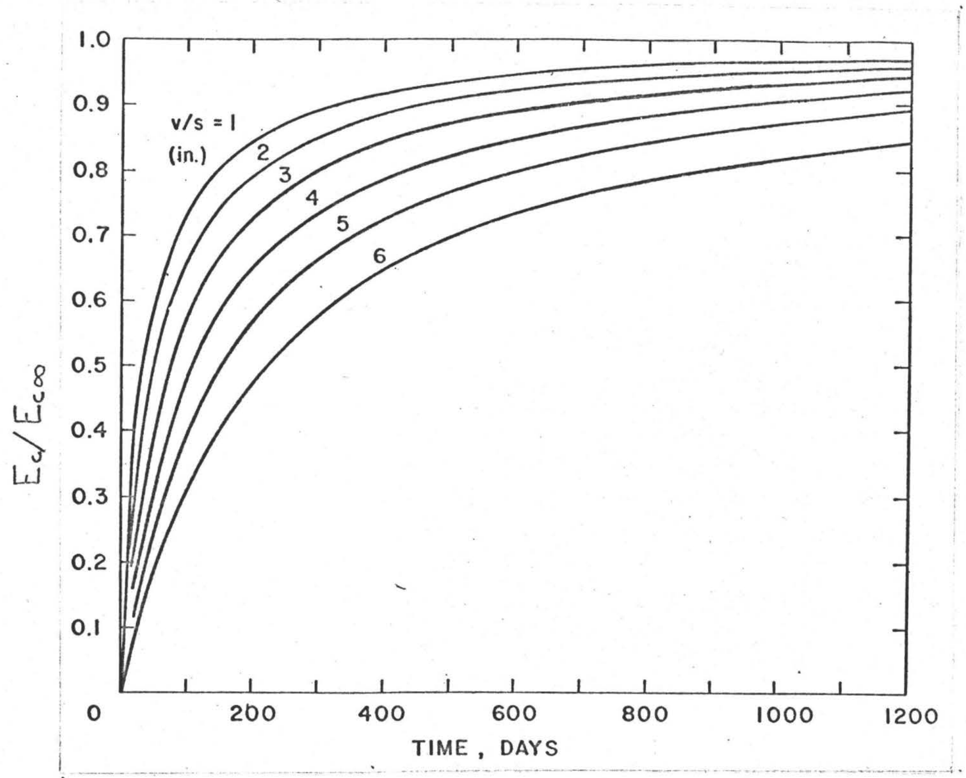

Fig. 1.3.

The vertical axis gives values of $E_c/E_{c\infty}$ where

E_c = creep strain

$E_{c\infty}$ = ultimate value of creep strain (i.e. creep at time $t = \infty$) predicted from the formula of Ross (see Chapter 3).

"V/S" stands for the volume/surface area ratio of the various members tested. It is seen that a lower proportion of the ultimate creep is attained at a given time for higher values of this variable.

Consideration of the foregoing section should indicate the difficulties involved in comparing data compiled in different research programs. Many, if not all, of the variables mentioned above will have different values in any two sets of tests. A meaningful comparison will thus require much knowledgeable and skilled work. Because of the lack of complete and accurate documentation, such comparison may have to be only qualitative rather than quantitative.

For similar reasons, results of creep tests performed in the laboratory cannot be blindly applied in the field. For example, laboratory tests performed at constant relative humidity would often under-estimate creep under conditions of exposure to the elements.

For any large test program, it is desirable to have a high degree of similarity between the various test conditions.

1.4. Creep Effects in Engineering Structures

Creep of concrete has important effects in engineering structures, affecting the stresses and deflections of structural members.

Some of the effects of creep may be considered beneficial, as when creep brings about a relief of stresses caused by concrete shrinkage. Some other effects, however, are less desirable, and examples of these are not hard to find.

Steel reinforcement in compression areas of beams or columns may undergo major stress increases when creep, sometimes in conjunction with shrinkage, causes a transfer of stress from the concrete. In addition, the ultimate or long-term deflections of reinforced concrete beams may be several times the initial deflections, with the difference being largely due to creep effects.

In prestressed members, creep causes a gradual loss of prestressing force. Although this effect can be partially offset by using a higher initial prestress, it is nonetheless an important factor, and one which cannot be neglected.

Creep effects in statically indeterminate structures are sometimes helpful to the designer. If, for example, there is some movement of the abutments of a two-hinged arch, creep in the concrete will tend to offset its effects and partially restore conditions to those calculated by the designer.

In other cases, the creep effects can constitute an additional complication which the designer must take into account. In a prestressed portal frame, for example, creep shortening of the beam changes the horizontal reactions at the column bases, giving rise to secondary moments. In the case of an eccentrically-loaded long column, creep deflection of the column will add to the eccentricity of the load. The additional moment, although secondary in name, may be of prime importance in effect.

It may be noted that most of the cases mentioned above involve creep of concrete where there is a stress gradient across the member in question. An important feature in calculating the effect of creep where there is a strain gradient is that, due to the non-linearity of creep versus stress, there is a redistribution of stress. That is, the elastic portion of the total strain is no longer linear, and, therefore, the shape of the stress block is changed.

1.5. Creep of Concrete under a Stress Gradient

As the previous section indicates, the creep of concrete under a stress gradient has practical effects which can be of considerable importance in engineering structures. In practice, it may be necessary to compute the redistributions of stress and strain caused by creep of the concrete. These redistributions will be investigated here for the case of a member having no reinforcing steel.

A plain concrete prism of rectangular cross-section is subjected to an external load P applied parallel to the prism's length, and with eccentricity "e" from one axis of symmetry of the prism's cross-section. The concrete will experience initial stresses f_i, and initial strains E_i, as indicated in Fig. (a).

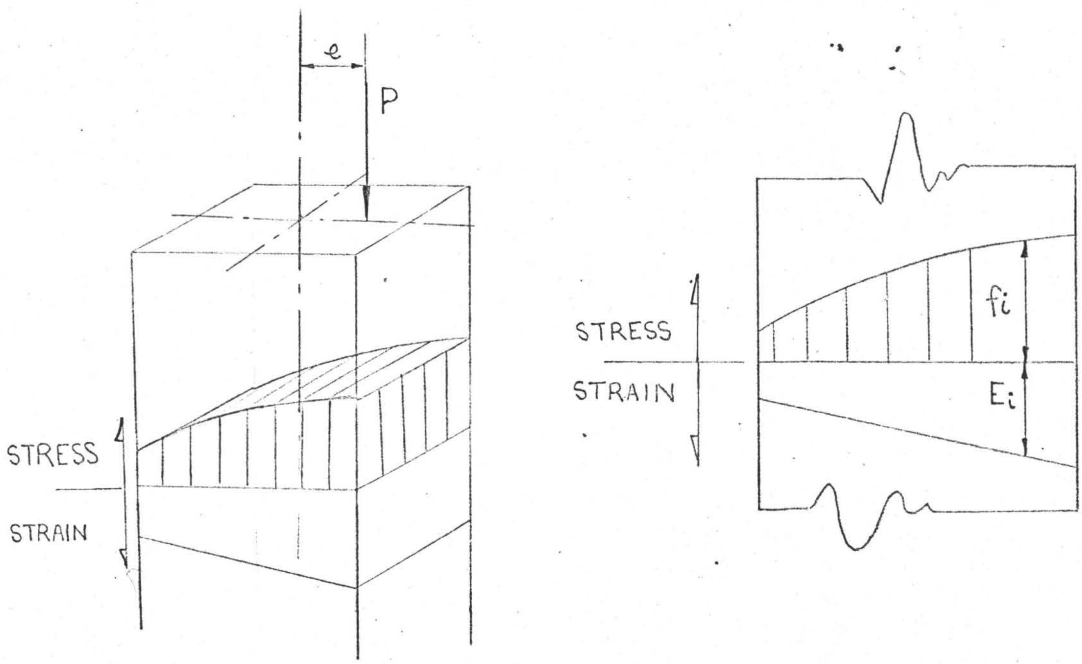

Fig. (a)

The stress distribution may have both linear and non-linear portions, while the strain distribution will be linear (in order to satisfy the condition that plane sections remain plane).

Let each element across the cross-section now creep independently of the others during a time interval, due to its portion of the applied load. The stress distribution will be unchanged, but the strain distribution will alter to some form such as that shown in Fig. (b). The additional (creep) strains will be referred to as Ec.

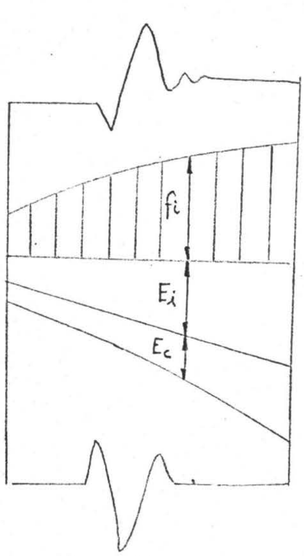

Fig. (b)

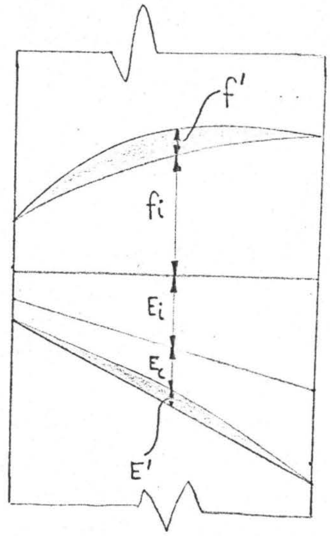

Fig. (c)

It is apparent that the usual condition that "plane cross-sections shall remain plane" has been violated. Therefore, forces F_i must be applied to the individual fibres of the prism to bring them into position and so satisfy this requirement. Figure (c) shows the new strain and stress distributions after application of F_i. The additional stresses are f', and the added strains are E'.

Having restored the various fibres to a bonded state, the forces F_i are now removed to satisfy statics (a process equivalent to applying a force system $-F_i$ to the bonded cross-section). The stresses induced by this last step are f", the corresponding strains being E".

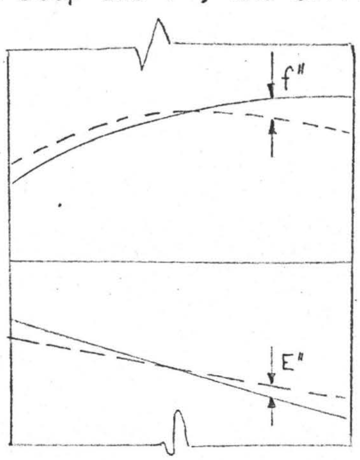

Fig. (d)

The final stresses and total strains appear in Fig. (d). The elastic strain distribution is no longer linear, due to the change in the stress distribution.

Thus, the final total strain is Et, given by

$$Et = E\mathit{i} + Ec + E' + E''$$

and the final stress is ft, given by

$$ft = f\mathit{i} + f' + f''$$

It will be convenient to remember the four main stages of the solution:

(i) determination of elastic strains.

(ii) determination of "free" creep (each fibre allowed to creep under its portion of applied load).

(iii) restoration of plane section (apply a force system $F\mathit{i}$ to the individual fibres).

(iv) satisfy statics (apply a force system $-F\mathit{i}$ to the bonded cross-section).

Step (ii) is carried out assuming that the stress and elastic strain distributions remain constant, or nearly constant, during the chosen time interval.

The details involved in calculating the values of the component stresses and strains will be considered more fully in Chapter 3.

CHAPTER 2

THE TEST PROGRAM

2.1. Introduction

In order to obtain creep information for concrete subjected to uniform sustained stresses, four concentric creep tests were carried out. These tests involved loading 6" x 6" x 22" plain concrete prisms. The stresses applied were 750 p.s.i., 1500 p.s.i., 2250 p.s.i., and 3000 p.s.i. These applied stresses were chosen to provide creep data for the range of stresses which would be found in four additional eccentrically-loaded creep test specimens.

The eccentric-load tests were performed on prisms of the same dimensions as those used in the concentric tests. For the eccentric tests, the load was applied on one axis of symmetry of the prism's cross-section, and at a distance of 3/4" from the other axis of symmetry. The average stresses (= load/area) applied in the eccentric tests were 750 p.s.i., 1000 p.s.i., 1500 p.s.i., and 1750 p.s.i.

The creep specimens were given identification numbers which consisted of either the letter "C" (denoting concentric load) or the letter "E" (denoting eccentric load) followed by a number equal to the average stress applied to the specimen in p.s.i. Thus E-750 identifies the prism loaded eccentrically to an average stress of 750 p.s.i.

The creep test prisms were kept under sustained load for 137 days. The only exception to this was the 1,000 ps.i. eccentrically-loaded prism which was kept under load for only 67 days. This came about because one eccentrically-loaded prism was inadvertently overloaded at the time of application of the load, and failed by crushing of the concrete.

The prism E-1000 was cast and made ready at a later date as a replacement; hence, its period under load had, of necessity, to be somewhat shorter than those of the other specimens.

All the creep prisms were sealed with wax at the age of 31, 32, or 33 days, and all were loaded at the age of 36 days. The wax sealing was intended to eliminate the influence of varying atmospheric humidity during the test period.

A record was kept of the prisms' length changes from the age of one day up to the time of loading. A record was also kept of the length changes of companion unloaded prisms which had been cured and sealed in the same way as the creep prisms. These prisms were also stored in the test area.

The concrete's crushing strength and stress-strain relationship were obtained from cylinder tests. Such tests were performed at various ages of the concrete in order to determine how the concrete's strength and stress-strain properties altered with time. The cylinders were waxed at the same age, and in the same manner as the creep prisms.

2.2. The Concrete Mix

In the initial concrete pour, ten 22" x 6" x 6" prisms, seven 12" x 6" x 6" prisms, and twelve 12" x 6" diameter cylinders were cast. In a second pour, 11 weeks after the first, three 22" x 6" x 6" prisms and six cylinders were cast.

2.2.1. The Concrete Mix Proportions

The weights and percentages of the constituent materials are tabulated below (Table 2.1.).

TABLE 2.1.

CONCRETE MIX CONSTITUENTS

Material	Weight per batch (lbs.)	Percentage by weight
Ordinary Portland Cement, Type I	63.6	14.0
3/8" Maximum Size Crushed Limestone	135.5	29.9
Concrete Sand (washed sand of fineness modulus = 2.74)	212.2	46.4
Water	44.0	9.7
TOTAL	455.3 lbs	100.0

The volume of each batch was approximately 3 cubic feet.

The aggregates used were subjected to a moisture analysis. The weights in the above table were obtained using the results of this analysis. Thus, the "Water" entry is the sum of the actual weight of water added and the weight of water present in the sand and crushed stone.

2.2.2. Mixing and Pouring Procedure

A "butter" batch equal to roughly one third of a regular batch was first made in order to condition the 4 cubic foot capacity horizontal-drum mixer. The concrete from this batch was thrown away.

In the first pour, three regular batches were then made. The various forms and cylinders were filled in three layers, each layer being composed of the concrete from one batch. Each layer was vibrated using a a hand-held poker-type vibrator. The poker was not allowed to penetrate any further than just into the surface of the preceding layer.

In the second pour, only one batch was required. The forms were filled and vibrated in three stages as before.

Since it was considered desirable to make the concrete in the cylinders as much like that in the prisms as possible, the cylinders from both pours were also mechanically vibrated.

The slumps for the three batches of the initial pour were 3 1/8 in., 3 3/4 in., and 3 in. The slump of the second pour was 3 in.

In each case, after the last layer of concrete had been placed in the forms, excess concrete was trowelled off the upper face. A smoothly-trowelled surface was obtained without addition of water or excessive working which would cause migration of water to the upper surface. One half-inch diameter brass gauge points, each with a number 60 reference hole in its centre, were set in the exposed face of each of four of the large prisms from the first pour. The points were placed on a 10 in. gauge length. After about 7 hours, initial readings were taken from these points using a "Soiltest" mechanical strain indicator (see section 2.2.3. for a description of this gauge).

At the age of about 8 hours, all of the test specimen were covered with wet burlap. At the age of one day, all the prisms and cylinders were removed from their forms or molds. This procedure was adhered to for both pours.

The prisms were cast in wooden forms which were lined with polyethylene plastic sheet in order to give the concrete a smooth finish.

The dimensions of the forms were carefully checked for accuracy, and all dimensions were correct to within 1/32 of an inch.

2.2.3. Curing of the Concrete and Preparation of the Test Prisms

The specimens were cured under moist burlap for 21 days. From this time until they were put under load at the age of 36 days, the prisms stood in the Concrete Laboratory of the Engineering Building. During this period for the first pour, the atmospheric temperature was maintained at near 70°F and relative humidity varied approximately from 50% to 70%. For the second pour, the range of temperature during this period was 70°F to 80°F, the relative humidity varied between approximately 60% and 80%.

In the five-day period from 29 days to 33 days, the cylinders were capped, and "Demec"† gauge points were affixed to the creep prisms. The arrangement of the gauge points on the creep prisms is shown in Fig. 2.1.

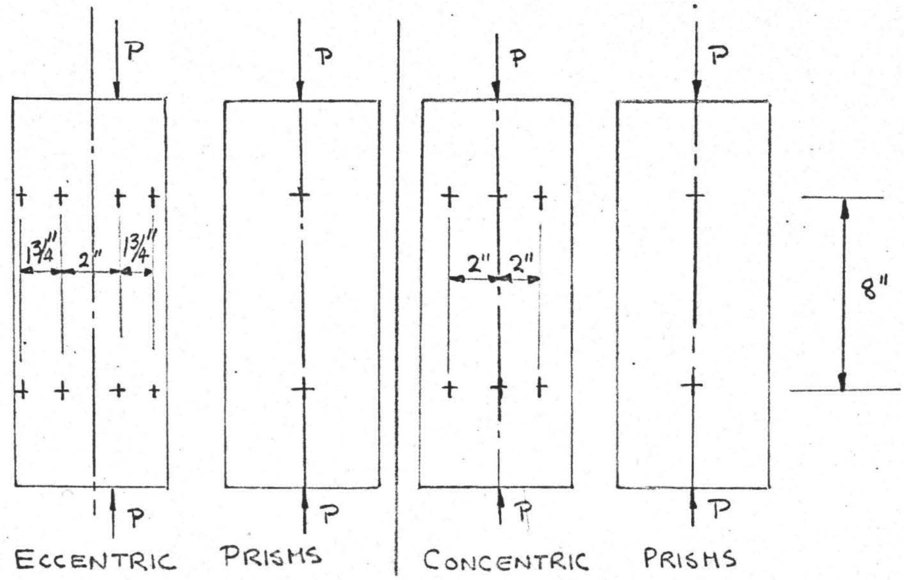

Fig. 2.1. Arrangement of Gage Points on Creep Prisms

† The "Demec" is a demountable mechanical strain gauge described in section 2.3.3.

Points were also affixed to several of the cylinders in order that the concrete's stress-strain curve could be obtained during tests for compressive strength.

The set-in gauge points on the prisms which were to serve as shrinkage control specimens were augmented by further sets of points glued on to the other three faces of the prisms.

All points were glued to the concrete using a two-part epoxy glue.

Next, all of the concrete test specimens were coated with Esso microvan 1400 wax, in order to prevent further loss of moisture. The coating was achieved by blowing air from a hot-air gun onto a large slab of the wax, and allowing the molten wax to flow evenly onto the concrete surface. The melting point of this wax is 140°F.

2.2.4. Concrete Properties

(a) Strength and stress-strain relationship.

As has been mentioned previously, a number of the concrete cylinders were fitted with gauge points in order that the concrete's stress-strain curve might be determined.

Each such cylinder had two sets of points attached, the sets being diametrically opposed. At the age of 36 days (i.e. at the same time as the creep tests commenced) one of these instrumented cylinders was tested. The test procedure was standard, except that loading was stopped for a few seconds at various load levels in order that the concrete's strain might be determined. Strain readings were taken up to a stress of roughly 90% of the concrete's ultimate strength.

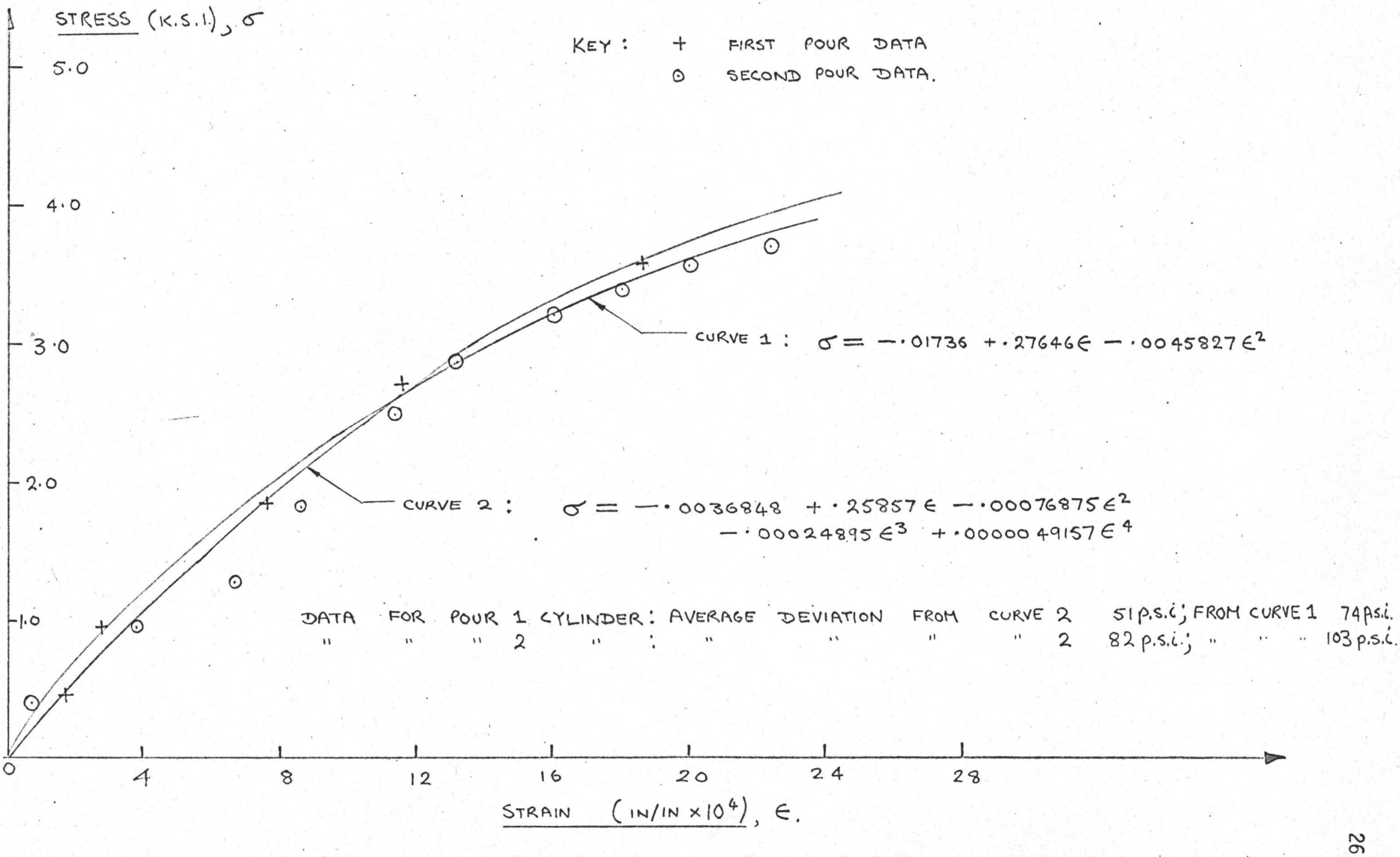

Fig. 2.2. STRESS - STRAIN CURVES

TABLE 2.2.

STRESS-STRAIN DATA FOR CONCRETE AT AGE 36 DAYS

POUR			
FIRST		SECOND	
Stress (KSI)	Strain (in/in x 10^4	Stress (KSI)	Strain (in/in x 10^4
0.0	0.0	0.0	0.0
0.354	1.812	0.352	0.800
0.886	2.880	0.850	3.900
1.240	5.063	1.200	6.800
1.770	7.750	1.760	8.600
2.656	11.625	2.120	9.800
3.540	18.875	2.480	11.400
ULTIMATE STRENGTH = 4.09 KSI		2.830	13.100
		3.010	14.600
		3.180	16.000
		3.350	18.000
		3.520	20.100
		3.690	22.500
		ULTIMATE STRENGTH = 3.86 KSI	

The difference in strength of the instrumented cylinder from one loaded continuously to failure at the same age was fairly small. (.28 KSI, or about 6%). It was, therefore, concluded that the effect of stopping the cylinder test at various stages in order to take strain readings was slight. A comparison of many more tests performed by Drysdale[11] also indicated that no strength reduction occurred.

The points obtained in this way appear on the stress-strain graph Fig. 2.2. The stress-strain readings are entered in Table 2.2. Strain was obtained as the average of the two values given by the two sets of gauge points. A cylinder from the second pour was similarly tested at 36 days, and the points obtained are also plotted on Fig. 2.2 and entered in Table 2.2.

The strain readings obtained from the two sets of points on each cylinder were normally fairly close (within 10%). A maximum difference of 24% for the final reading was, however, recorded. This discrepancy could have been due to the onset of failure on one side of the cylinder; it might also indicate that the cylinder was subjected to some slight eccentricity of load.

A least-squares fit of the stress-strain data was undertaken by computer. This allowed the stress-strain to be expressed as a 4th degree curve (curve 1 on Fig. 2.2) and also as a 2nd degree curve (curve 2 on Fig. 2.2.). These formulations were used in the analyses outlined in Chapter 3. The average deviations of points obtained by measurement from those given by the least-squares plots are indicated on Figure 2.2.

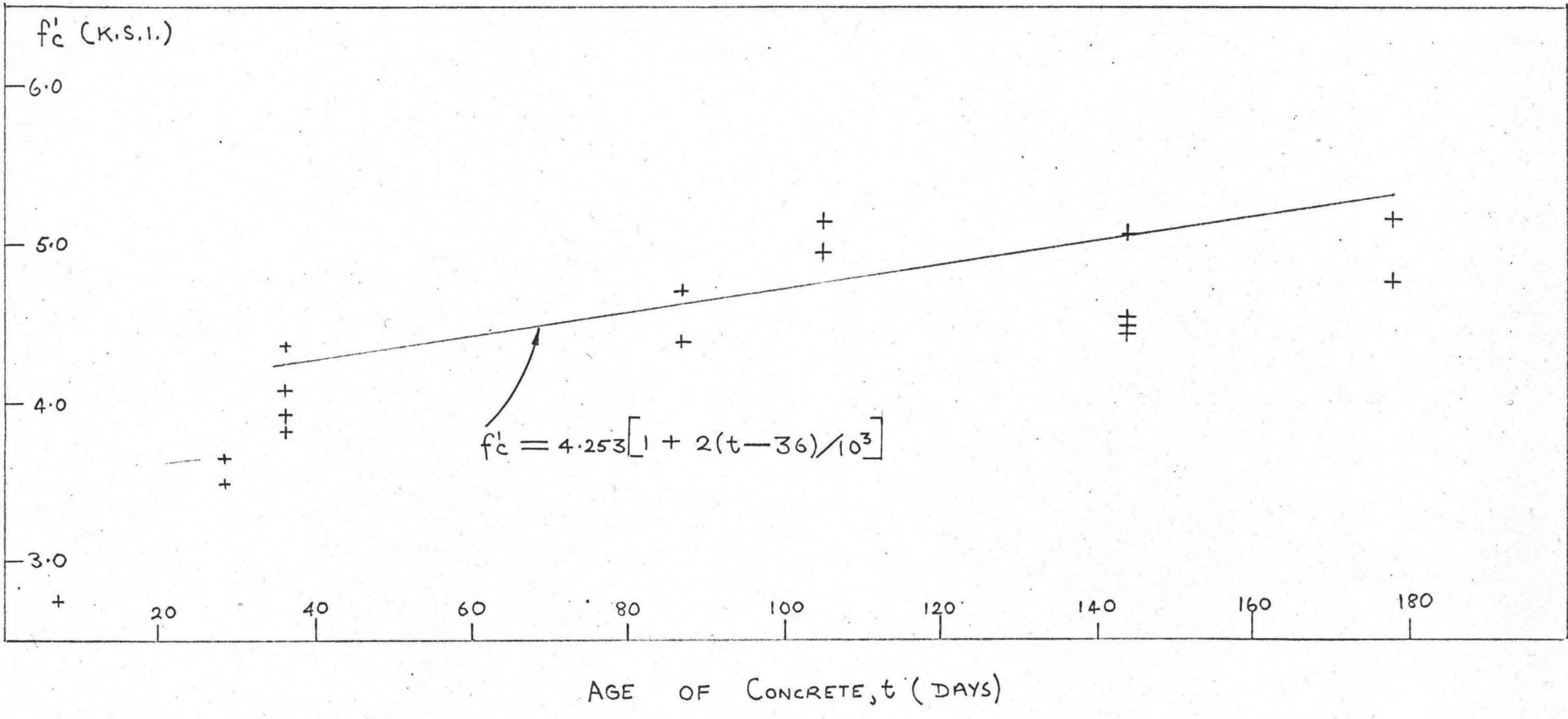

FIG. 2.3. CONCRETE STRENGTH AT DIFFERENT AGES

TABLE 2.3.

CONCRETE STRENGTH AT DIFFERENT AGES

Age (days)	Pour No. 1		Pour No. 2	
	Individual Cyl. Strengths (KSI)	Average Strengths (KSI)	Individual Cyl. Strengths	Average Strengths
7	2.73	2.73	-	-
28	-	-	3.65	3.58
			3.57	
36	4.09	4.23	3.92	3.89
	4.37		3.86	
87	-	-	4.68	4.53
			4.38	
105	5.15	5.02	-	-
	4.89			
142	4.52	4.61	-	-
	4.48			
	4.36			
	5.09			
178	4.74	4.95	-	-
	5.16			

It may be noted that the points obtained from the two cylinders are very similar for stresses below about 3.25 K.S.I. In addition, it can be seen that the stress-strain relationship is very nearly linear up to a stress of 2.25 K.S.I. It appears that the strain at ultimate strength was about .0026 in/in. in both cases.

Table 2.3. contains the results of cylinder tests at various ages of the concrete. As indicated, the average strength at the time of loading the creep prisms (36 days after pouring) was 4.253 K.S.I. The gain in strength with time is evident from the Table 2.3., and is illustrated by Figure 2.3. It can be seen that the points in Figure 2.3. show considerable scatter.

The concrete strength is expressed as a function of time by the formula

$$f'_c = 4.253\ (1 + 2(t - 36)/10^3)$$

for ages greater than 36 days.

f'_c is in K.S.I. and t is the age of the concrete in days.

It was recognized that this formula did not give a perfect fit of the experimental data; at no point, however, did the cylinder strength given by the formula differ from the average value measured at that time by more than 8%.

It was assumed that the stress-strain relationship of the concrete was linearly dependent on strength. If over a given period the concrete cylinder strength had increased to "n" times its 36-day value, it was assumed that the ordinates (i.e. the stress values) on the stress-strain curve had also increased to "n" times their former values.

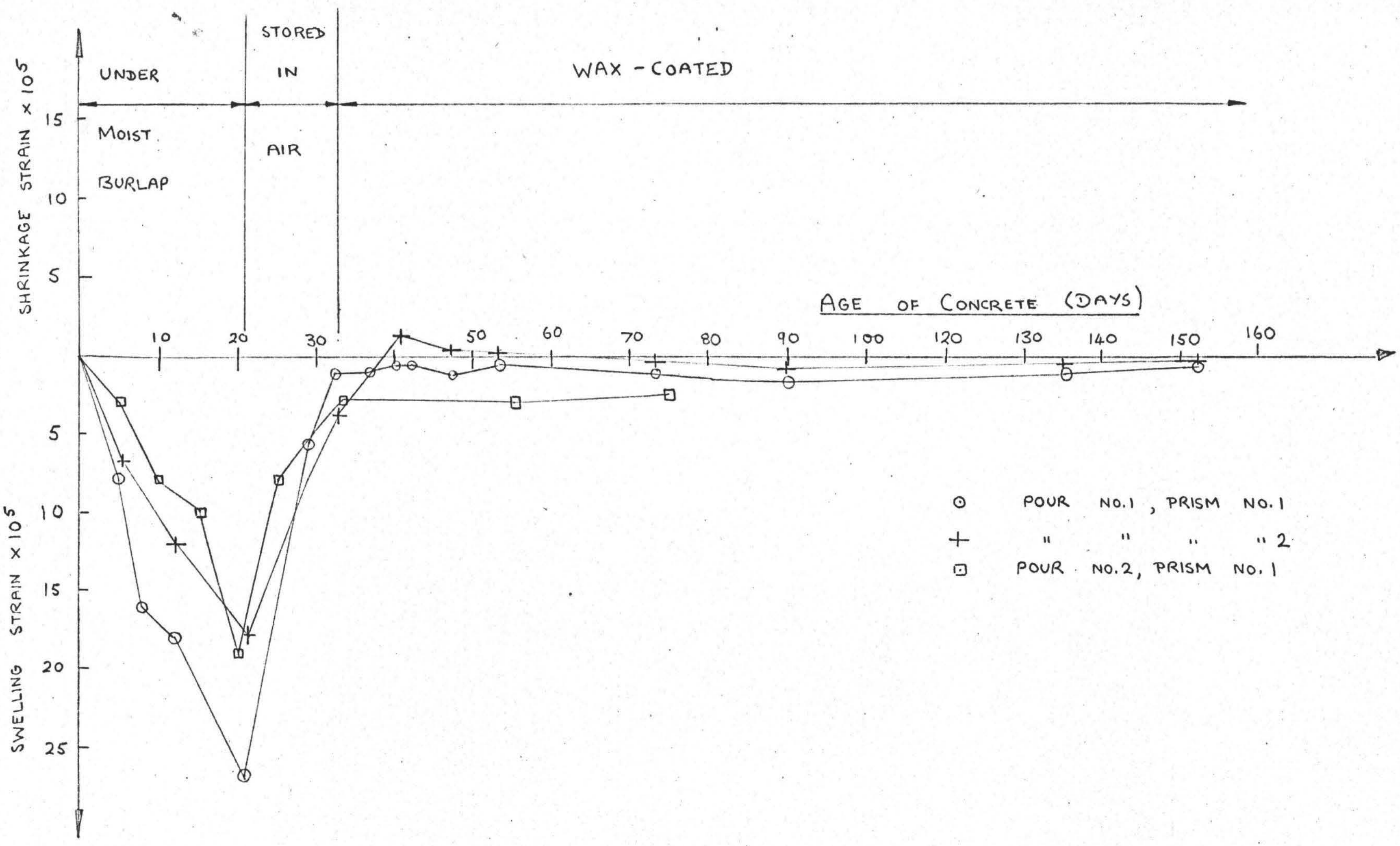

FIG. 2.4. SHRINKAGE STRAINS OF THE CONCRETE

TABLE 2.4.

SHRINKAGE STRAINS OF UNLOADED PRISMS (in/in x 10^6)

Age (days)	Pour 1 No. 1	Pour 1 No. 2	Pour 2 No. 1	Storage Conditions
0	0	0	0	Under Moist Burlap
5	- 80	- 60	- 30	
6	-110	-120	-	
8	-160	-140	-	
10	-	-	- 80	
12	-180	-120	-	
15	-	-	-100	
20	-	-	-190	
21	-270	-180	-	
25	-	-	- 80	In Air
26	-240	-120	-	
29	- 60	- 80	-	
33	- 10	- 40	- 20	Wax-Coated
36	- 10	- 20	-	
40	- 5	- 15	-	
41	- 5	+ 10	-	
47	-12.5	+ 2.5	-	
53	- 5	0.0	-	
55	-	-	- 30	
73	- 10	- 5	-	
75	-	-	- 25	
88	- 15	- 10	-	
125	-12.5	- 5	-	
142	- 10	- 5	-	

It was known that this assumption was not completely accurate. Comparison of a stress-strain curve obtained from an instrumented cylinder loaded at the age of 142 days with one computed from the 36-day curve using the above assumption showed that the maximum error in the range of stress of interest (up to 3KSI) was 9%. Both of the curves appear in Fig. 2.2.

No attempt was made to trace the stress-strain relationship for strains beyond that at the ultimate stress. For the tests under consideration, stresses were always well below the ultimate strength.

(b) Concrete Shrinkage

A record of the length changes occurring in two unloaded prisms identical to the creep prisms was kept for the duration of the test period. A third prism, taken from the second pour was also used to check length changes. The recorded strains are plotted against time in Fig. 2.4. The shrinkage strain readings at various ages are entered in Table 2.4. It can be seen that after wax-coating, practically no further strains occurred. It was, therefore, unnecessary to apply any correction to the creep strain readings to account for non-load-induced strain.

2.3.1. The Loading Frame

Eight identical load frames were used in the test program. The features of a load frame are shown in Fig. 2.5. It is basically an assembly of four identical steel plates, four steel rods, and four steel springs. The creep prism is loaded by jacking off plate (1) down onto plate (2). The four rods are thus placed in tension, while the springs and the creep specimen are placed in compression. When the compressive

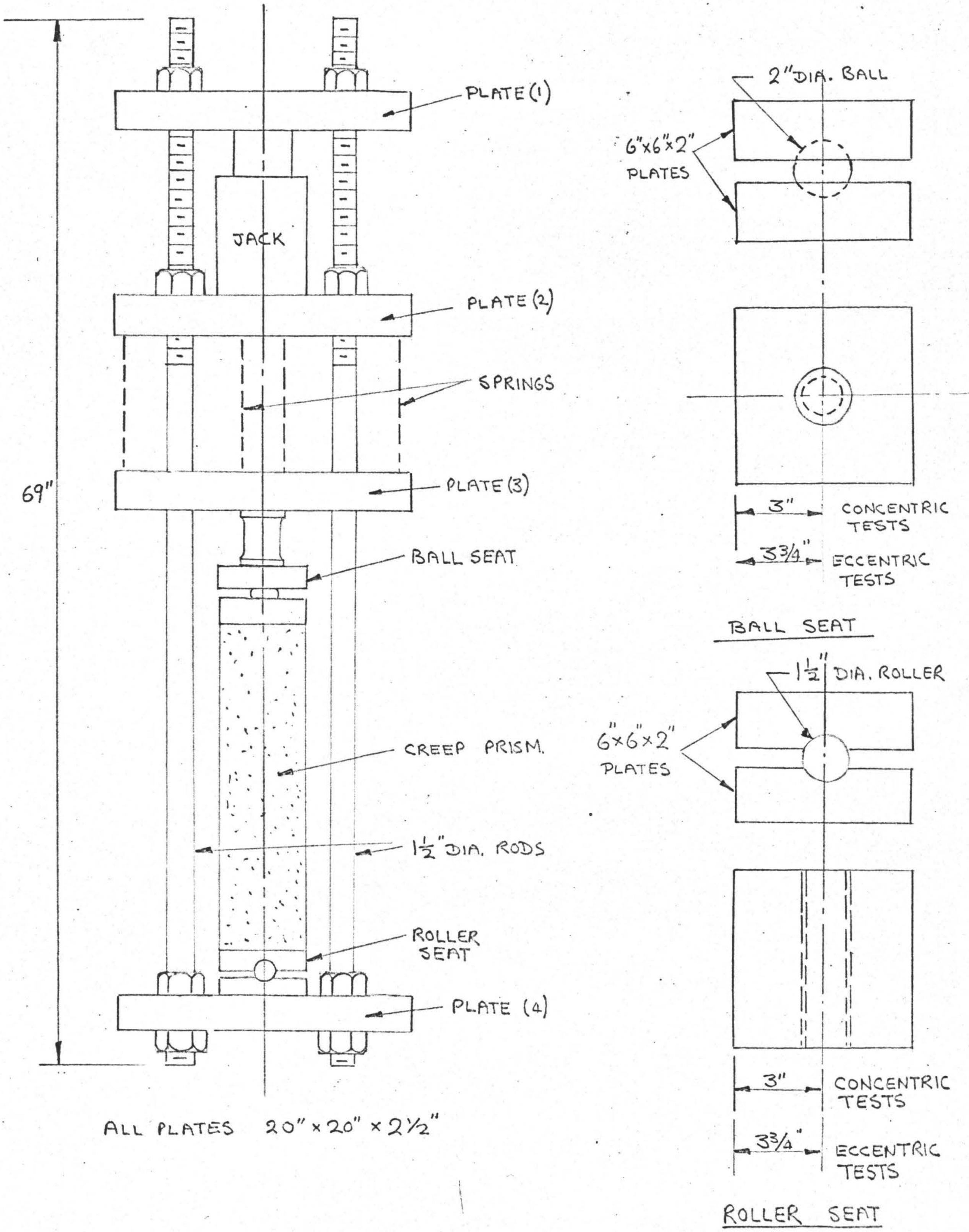

Fig. 2.5. THE LOAD FRAME

load on the concrete, as indicated by the load cell, has reached the desired level, the nuts above plate (2) are screwed down into contact with (2). The jack force can now be released and the jack removed.

The load would fall off quite drastically due to the concrete's deformations if the springs were not incorporated in the apparatus. The use of springs restricts the loss of load in a given time to approximately 4 x (deformation of concrete) x (spring constant).

The spring characteristics are as follows:

Free length = 9"	Spring constant = 13.5 k/in.
Solid length = 6"	Weight = 50.5 lbs.
No. active turns = 1.69	Rod diameter = 1 5/8"
Outside diameter = 9"	Inside diameter = 5 3/4"

The load was applied to the concrete prism through load seats, which are also shown in Fig. 2.5. The load seat at the top of the prisms used on arrangement of a ball set between two plates, while the lower seat used a roller bearing. It was felt that a ball seat was necessary at one end in order to reduce the possibility of applying the load with an eccentricity in a direction at right angles to that intended.

The load seat plates were attached to the prisms using plaster of Paris. When the applied load is fairly low (below 54 kips, say) it is possible to adjust the load by moving the nuts above plate (2) with a wrench. At high loads, the friction between plate (2) and the nuts is too great to permit such a method of adjustment. To change the load in such cases, the jack must be used.

The rods were designed as tension members. The plates were designed for bending, considering them to be loaded over an area in the center, and simply supported at the rods.

A 60 ton capacity hydraulic "Simplex" jack was used to apply the loads.

A photograph of an assembled load frame, with the creep prism and the jack in position appears in Fig. 2.6.

2.3.2. The Load Cells

The loads applied to the various creep prisms were determined by the use of load cells.

The dimensions of these components appear in Fig. 2.8. The steel used was "Ultamo 6", which is a high yield steel with good creep characteristics. Four Budd C6-181-B "Metafilm" electrical resistance strain gauges were attached to each cell using GA-5 heat-cured epoxy cement. The arrangement of two gauges positioned vertically and two horizontally (with members of like pairs being diametrically opposite) constituted a full bridge.

The load cells were calibrated in the 120 kip capacity Tinius Olsen testing machine. For the calibration, the strain readings indicated by the gauges on the cells at various loads were recorded. The calibration procedure involved loading and unloading cycles for each cell. This process was carried out at least three times. If the calibration curve and zero load reading continued to vary after several cycles of loading, the strain gauges were replaced. The calibration curves (graphs of strain versus load) were plotted for all the cells. In all

Fig. 2.6. Assembled Load Frame

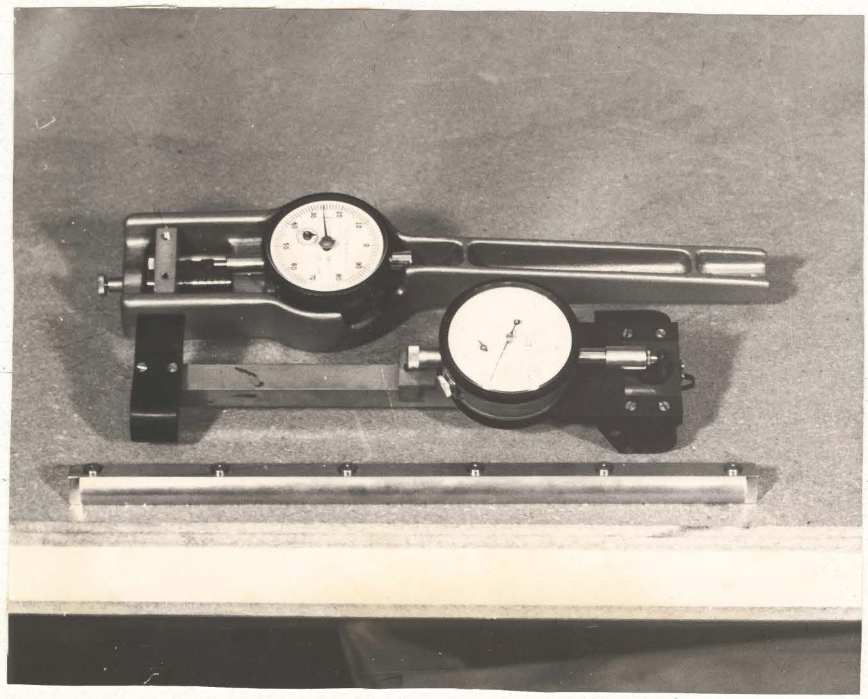

Fig. 2.7. The "Soiltest" (top) and "Demec" gauges.

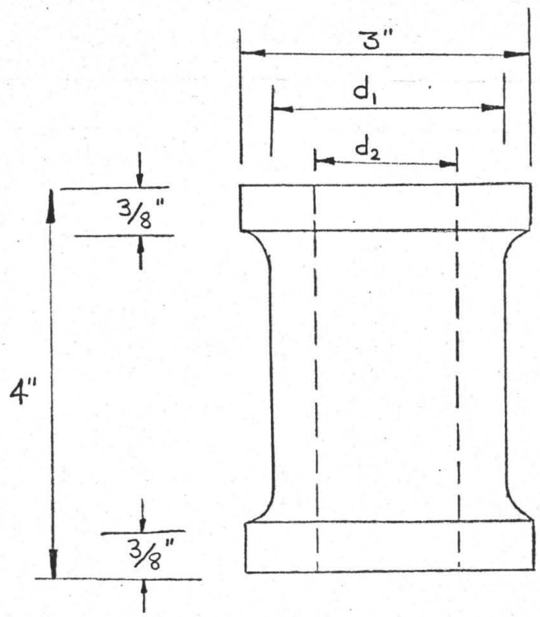

Specimen Cell Used With	C-750; E-750; E-1000	E-1500 C-1500	C-2250 E-1750	C-3000
d_2	1 3/8"	1 1/4"	1"	3/4"
d_1	2 1/4"	2 1/4"	2 1/2"	2 1/2"

Fig. 2.8.

Load Cell Dimensions

cases, the graphs were very nearly linear. The calibration units (lbs/microinch/inch) for the load cells were found to be as follows:

Specimen	C-750	C-1500	C-2250	C-3000	E-750	E-1000	E-1500	E-1750
Load cell Calibration Units	47.5	42.0	45.0	55.0	30.0	37.0	45.0	50.0

For the creep tests, the eight load cells were connected to a Budd SB-1 portable switch-and-balance unit. This unit was connected in turn to a Budd portable strain indicator.

After the creep tests had been completed, the load cells were removed from the load frames and re-calibrated as a check on their accuracy over the test period. The recalibration procedure was as follows:

(1) Each load cell was loaded until the indicated strain was that which had originally represented the applied load for its specimen. The load for this strain reading was then noted.

(2) The load was released, and the strain reading for zero load noted.

It was found that none of the "at load" strain readings had altered significantly. The greatest error obtained for the sustained load level was 1.6% of the applied load. The load cell used for specimen E-1000 was found to be unserviceable 60 days after the commencement of loading. Until this time, the cell had given no indication of being defective, and it has been assumed that the readings over this period were accurate.

A check on the load at 60 days was made by measuring the length of the springs in the load frame. The values of spring deflection multiplied by spring constant, although only a rough guide, indicated that the load was at approximately the correct level.

2.3.3. The "Demec" and "Soiltest" Strain Gauges

A photograph of these two strain indicators appears as Fig. 2.7. The "Demec" gauge was used to take all creep and elastic strain measurements. It is a demountable mechanical strain gauge of British manufacture. The smallest division on the scale represents a strain of 10 microinches per inch. The gauge has an 8-inch gauge length. It was found possible to repeat readings to one half of a division.

The "Soiltest" gauge is also of the demountable mechanical type. Again, the smallest division is equivalent to a strain of 10 microinches per inch. The gauge has a 10-inch gauge length. It was used to measure some of the shrinkage strains. Generally, it did not consistently repeat the readings taken to within less than one division.

Both gauges were used in the same way. Two readings were taken, one from a standard invar bar, and one from the points glued to the concrete's surface. Any change in the difference between these two readings indicated a change in the strain of the concrete.

The errors involved in using these gauges are discussed in Chapter 4.

2.4. Experimental Procedure

The load frames were assembled lying on their sides and were hoisted into position using a 2,000 lb. capacity workshop crane. Plate (3) was held up initially by means of temporary clips.

The polished ball-and roller-bearings in the load seats were well-coated with grease.

The creep specimens with their load seats and load cells were then aligned in the frames, and held vertically by means of short lengths of wood. Next, the temporary clips restraining plate (3) were slackened, allowing the weight of plates (2) and (3), plus that of the springs, to bear on the specimen and hold it in place.

Initial readings were then taken with the "Demec" gauge.

The specimens were loaded 36 days after casting, and measurements of the strains were taken immediately after loading.

Further measurements of strain were made in the next few days. The frequency of taking readings decreased as the experiment proceeded, until 37 days elapsed between the last two sets of readings.

The load on each specimen was checked every few days, and a record kept of fluctuations. The loads on all specimens tended to diminish with time, and in each case, the load was brought back up to the desired level once a week, or as necessary to prevent the load from dropping by as much as 5% below its initial value. Actually, the loads seldom departed by more than 3% from their nominal values. The variations in load for each of the test specimens are illustrated in the graphs in Figs. 2.9. and 2.10. Increased deformation of the springs with time under load indicated creep in them. This did not change the recorded values of load. One of the original eight creep prisms was accidentally overloaded at the time of first loading, and this led to crushing of the concrete, as mentioned in the Introduction. The prism was replaced by one taken from the second pour which became prism E-1000.

The specimen E-1750 was subjected to an initial overload as shown in Fig. 2.10. E-1750 was subjected to an average stress of 2250 p.s.i. at first. The stress was reduced to 1750 p.s.i. after four days.

All the creep prisms were unloaded on the same day; the specimen E-1000 had then been under load for 61 days, and the other specimens for 137 days. To unload a specimen, plate (2) was first jacked downwards in order to free the nuts immediately above it. These nuts were then screwed up well clear of the plate, so that when the jack force was released and the jack removed, plate (2) was pushed up freely by the springs. Only the weight of plates (2) and (3) plus that of the springs remained on the specimen at this stage. Plates (2) and (3) the springs were then raised a fraction of an inch using the workshop crane. This allowed the load cell and the creep prism to be removed. Strain readings were taken immediately after the removal of the prisms from the load frames.

Inaccuracies in the experimental set-up and their effect on the results are considered in Chapter 4. Chapter 4 also considers the effects of the scatter of points in the various least-squares plots. Chapter 3 contains the results from the concentric creep tests. Chapter 5 contains results from the eccentric creep tests.

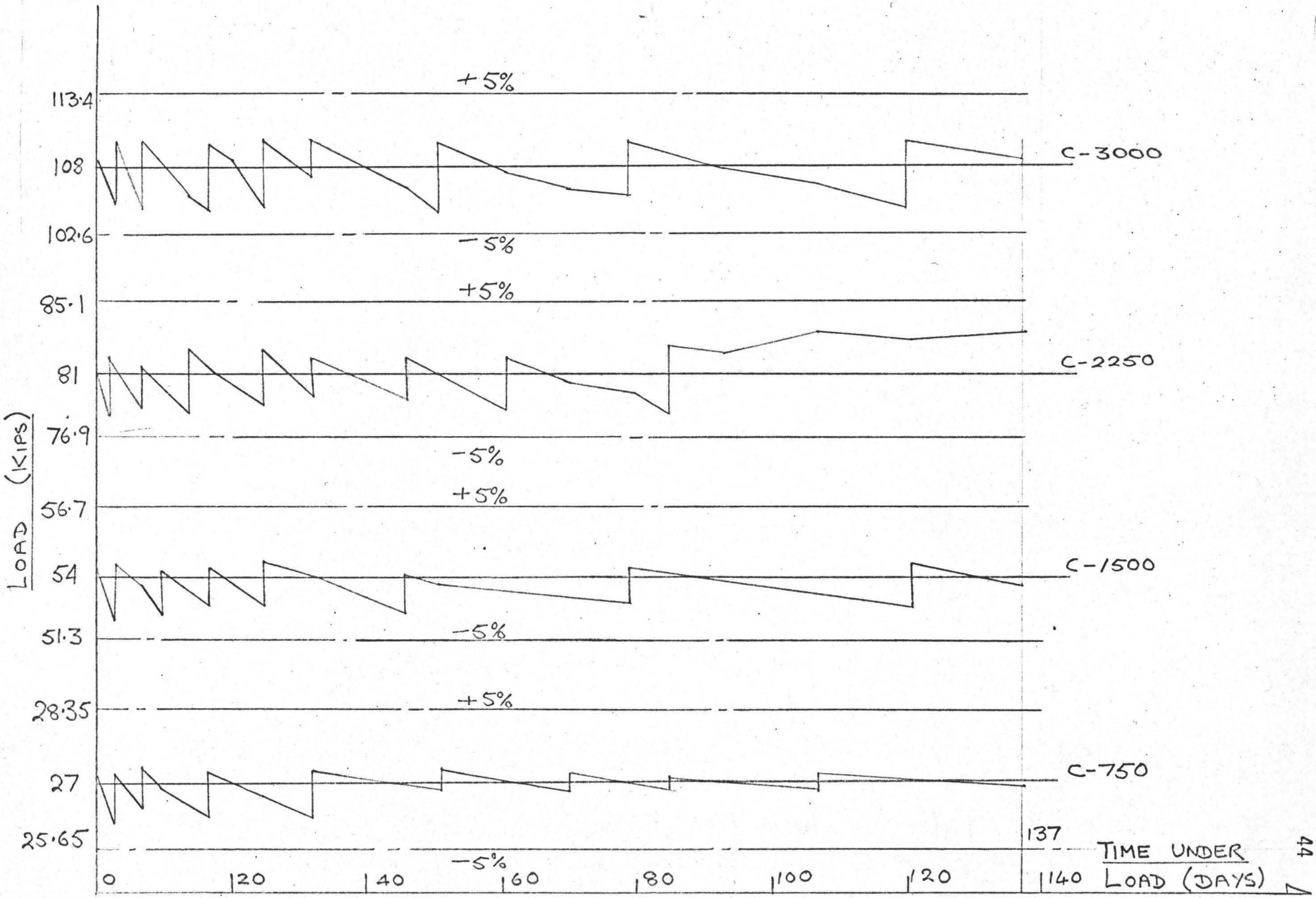

Fig. 2.9. LOAD VARIATIONS - CONCENTRIC CREEP PRISMS.

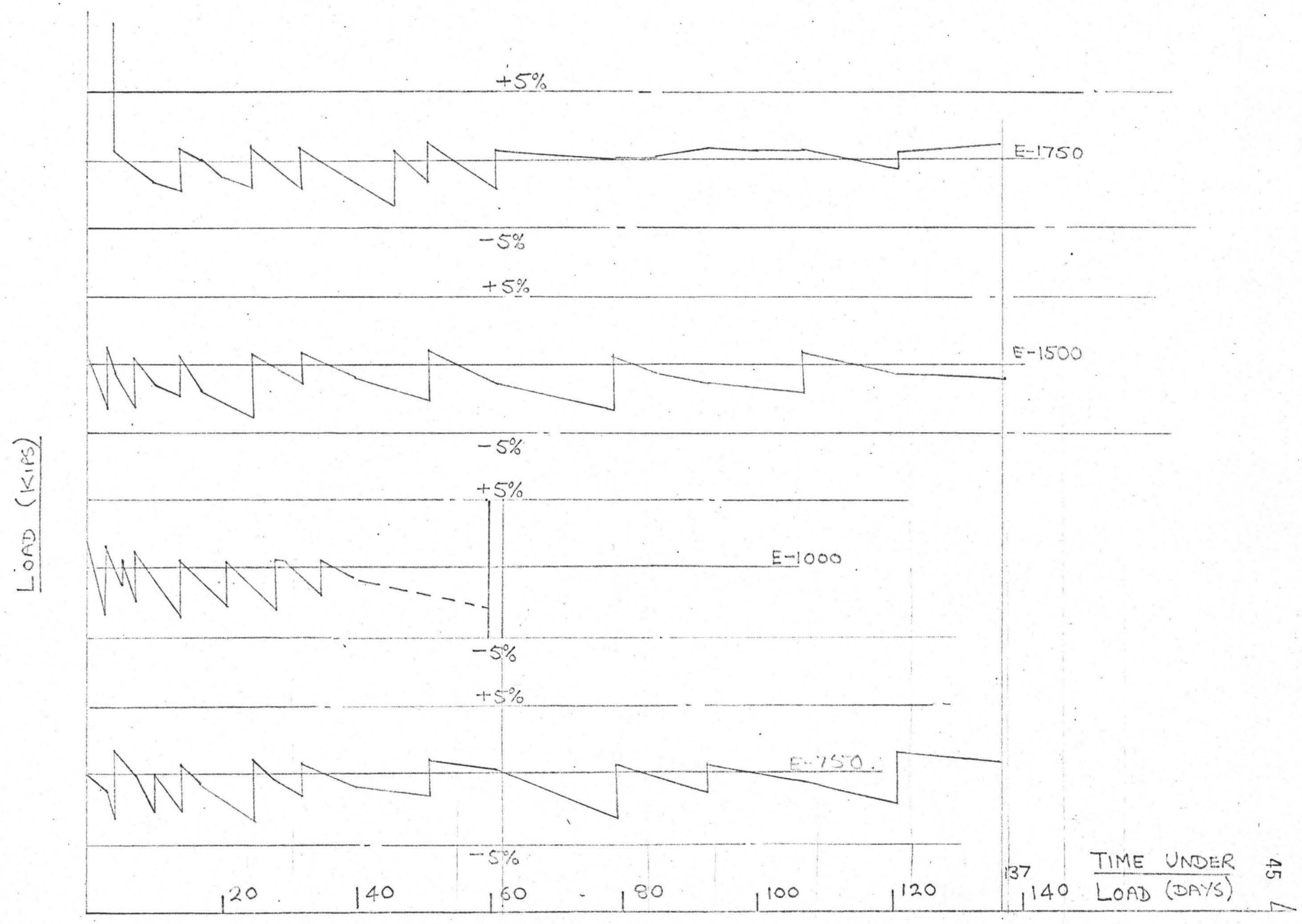

Fig. 2.10. LOAD VARIATIONS – ECCENTRIC CREEP PRISMS

CHAPTER 3

PREDICTION OF THE EFFECTS OF CREEP IN A MEMBER SUBJECT TO A STRESS GRADIENT AND PRESENTATION OF CONCENTRIC CREEP DATA.

3.1. Introduction

The general method of calculating the strains and stresses in a plain concrete prism subjected to a long-term eccentric load was described in Chapter 1. It will be recalled that the method had four distinct stages:

(1) Determination of the initial elastic strains necessary to produce resisting stresses equal to the applied load and moment.

(11) Determination of "free" creep corresponding to the distribution of stress across the section.

(111) Restoration of plane sections. The creep strain plus "elastic" strain must result in a linear distribution of total strain.

(1V) Alteration of total strains in order that the "elastic" portion satisfies statics.

These four basic steps are common to the two methods of analysis presented here, although each method tackles these steps in its own way. The first method, called the "element" method, is essentially numerical in character. The strains at various points across the member cross-section are determined in a computerized process. The element method considers the prism to be made up of a number of smaller concentrically-loaded prisms, held togethqr in such a way that plane cross-sections remain plane.

The second method, called the "continuous" method, seeks to find mathematical functions which describe the creep strain and total strain distributions across the member. It differs from the "element" method in that it considers the member cross-section as one unit, rather than as an assembly of smaller elements.

Both methods require certain data to be represented by convenient formulae. The data required consist of creep results from concentric load tests, shrinkage results of unloaded prisms, the concrete stress-strain relationship, and the way in which this and the concrete strength vary with time. The treatment of all but the creep results has been considered in Chapter 2. The formulation of this data will now be considered before the two methods are described.

3.2. Representation of Creep by Standard Formulae

The two methods of presenting creep data used in the analyses will be described. Both formulae were devised empirically to fit observed creep results.

3.2.1. The Method of Ross[9]

The equation suggested by Ross has the form

$$C = t/(a + bt)$$

where c = creep strain t days after application of load, and "a" and "b" are constants. The units of "a" are those of time, while "b" is dimensionless. Any factor which affects the creep observed at a given time will also affect the values of "a" and "b". Thus both constants are functions of the magnitude of the applied load. That is, "a" and "b" may be expressed as functions of stress or of initial elastic strain, both of which are measures of the magnitude of the applied load.

The above relation may be rearranged to give

$$t/c = a + bt$$

A plot of t/c against t is a straigth line, as shown in Fig. 3.1. The constant "a" is then the intercept on the t/c-axis, while "b" is the gradient of the line.

The formula of Ross is frequently used for predicting creep. Having established the constants from a relatively short sustained load test, long term creep strains can be conveniently extrapolated. It may be noted that at time $t = \infty$, $c = 1/b$. Thus, Ross is stating that creep tends to a finite limit.

3.2.2. The Semi-Logarithm Method

In this method, creep strain is expressed by a formula of the type

$$C = A + B \log (T)$$

where C = creep strain T days after application of load, and A, B are constants. Both "A" and "B" have units of strain.

Thus, a plot of creep strain (to a natural scale) against time (log scale) should be a straight line, as in Fig. 3.2. Logarithms to any base may be used. The values of "A" and "B" for a particular test are easily obtained from such a plot. Again, these creep constants are both functions of the level of the applied load. Thus, "A" and "B" can both be expressed as functions of either stress or initial elastic strain.

The use of the Ross and Semi-log formulae in this investigation is discussed in section 3.3.

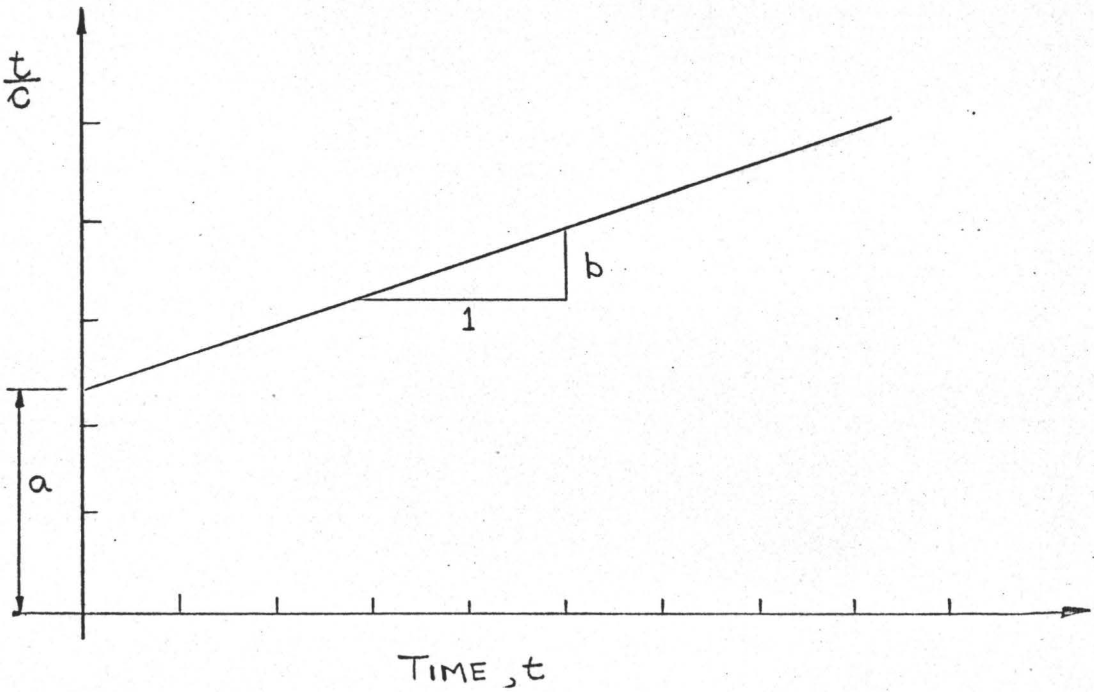

Fig. 3.1. Graph of t/c v. t, showing Ross creep constants.

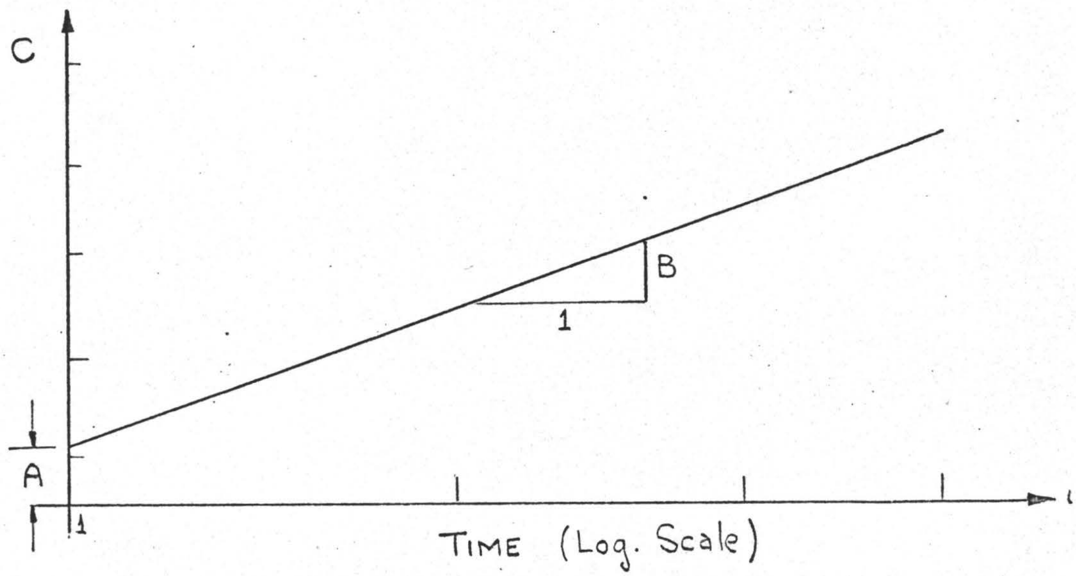

Fig. 3.2. Graph of C v. log (T), showing the Semi-log Method creep constants.

3.2.3. Presentation of Experimentally-obtained Concentric Creep Data

The concentric creep results are plotted to natural scales of creep strain and time in Fig. 3.3. The strain at a given time was calculated by taking the average of the strains indicated by the eight sets of gauge points fixed to each prism. It was thought that this practice would minimize the effects of any unintentional eccentricity in the applied load.

"Creep strain" is here taken to mean a change in strain after the instantaneous or "elastic" strain. The creep strain readings taken from the concentrically-loaded prisms appear in Table 1 of Appendix III.

Creep proportionality is shown by the results for prisms C-750 and C-1500; at any time, creep strain of the latter is roughly twice that of the former. That is, the ratio of creep is approximately equal to the ratio of stress. This relationship does not extend to the results for prisms C-2250 and C-3000. This is illustrated by the graph Fig. 3.4., which shows the relationship between applied stress and creep strains measured at various times after application of the load. Linear proportionality is seen to hold approximately at least up to a stress/initial strength ratio of .353.

In order to attempt to predict the creep behaviour of the eccentrically-loaded prisms, it was necessary to express the creep data from the concentric tests in the form of standard equations. Both the Ross and Semi-log methods were tested to gauge their usefulness in this regard.

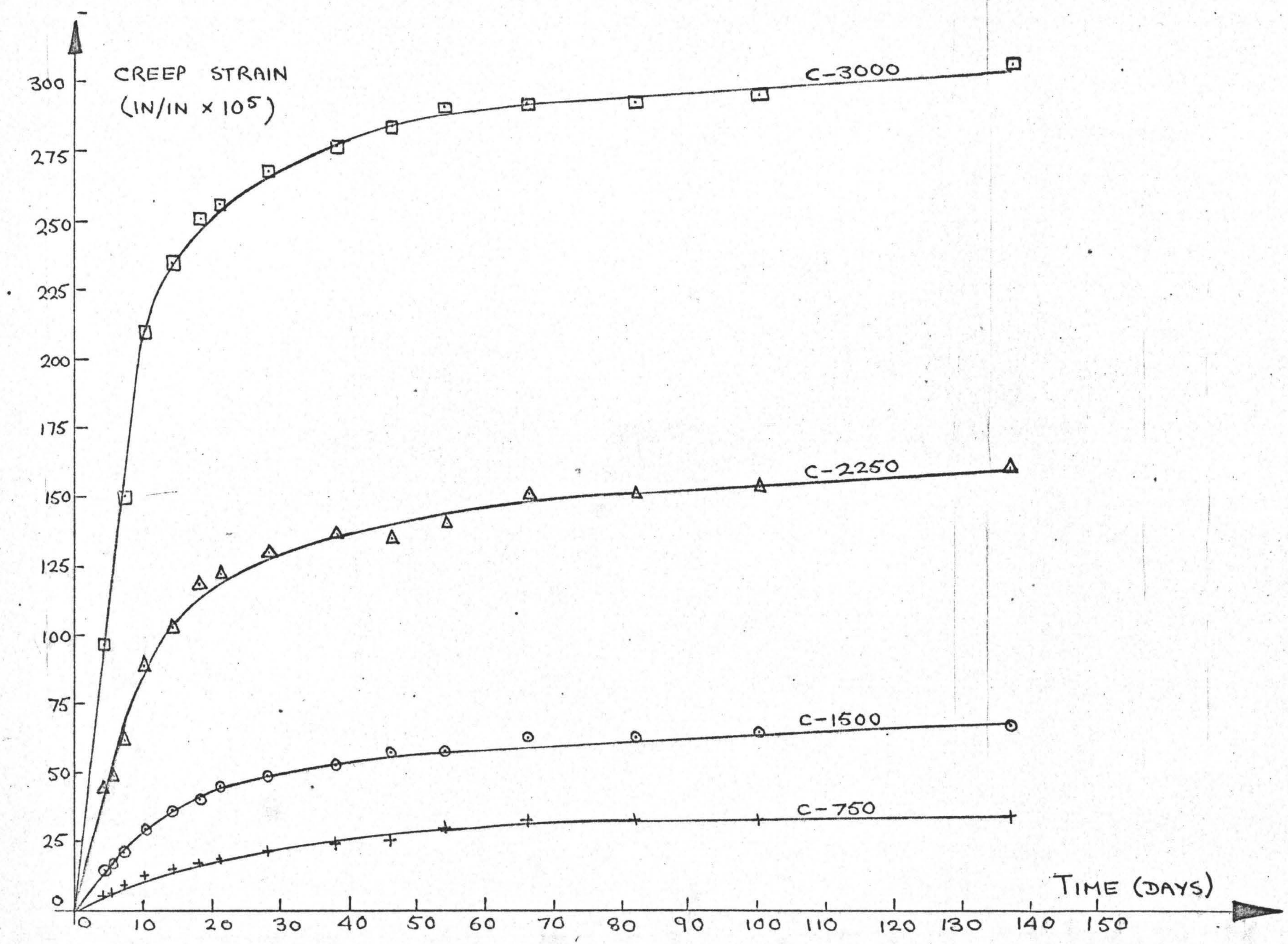

Fig. 3.3. CREEP OF THE CONCENTRIC PRISMS

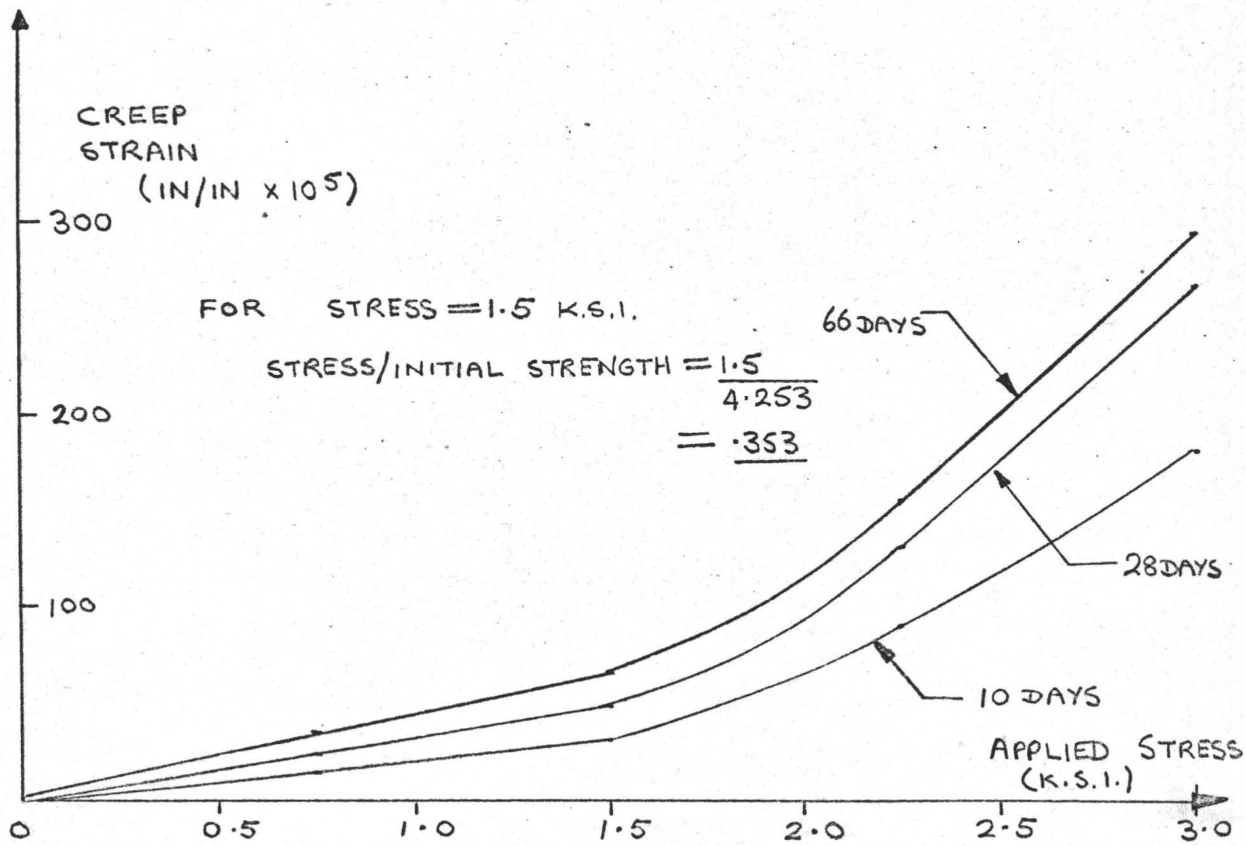

Fig. 3.4. COMPARISON OF CREEP FOR VARIOUS APPLIED STRESSES AT 10, 28, AND 66 DAYS AFTER LOADING.

A computer subroutine, DLESQ, available at the McMaster Uinversity Computer Centre, was used to give a least-squares fit of the data for the various straight line plots, which appear as Fig. 3.5. (Ross plots) and Fig. 3.6. (Semi-log plots, using logs to the base "e"). Both methods were found to give a reasonable fit of the concentric creep data.

In order to interpolate the creep data and apply it to intermediate stress levels, it was necessary to express the creep constants from both formulae as functions of the applied load. To this end, these constants were plotted against initial "elastic" strain, this being a convenient measure of the level of the applied load. Thus, the Ross constants, "a" and "b", were plotted against initial elastic strain, ε_E, as were the Semi-log constants, "A" and "B". Again, the computer subroutine DLESQ was used, this time to fit a curve of second degree in ε_E through the experimentally-obtained points. These plots and the equations of the four curves appear in Figs. 3.7. and 3.8. Second degree curves were used firstly because they gave a sufficiently good fit of the data, and secondly because use of higher degree functions would increase the complexity of the analysis described in the next section. The plot of the semi-log constant "A" against "elastic" strain shows the worst scatter of points. This constant, however, is always numerically less important than the term $B\log_e(t)$, especially for high values of "t".

It should be possible to accurately predict the creep of an identical prism subjected to a uniform stress of, say, 1000 p.s.i., by picking the corresponding elastic strain off the stress-strain curve, and using this to obtain the values of the creep constants. It would then

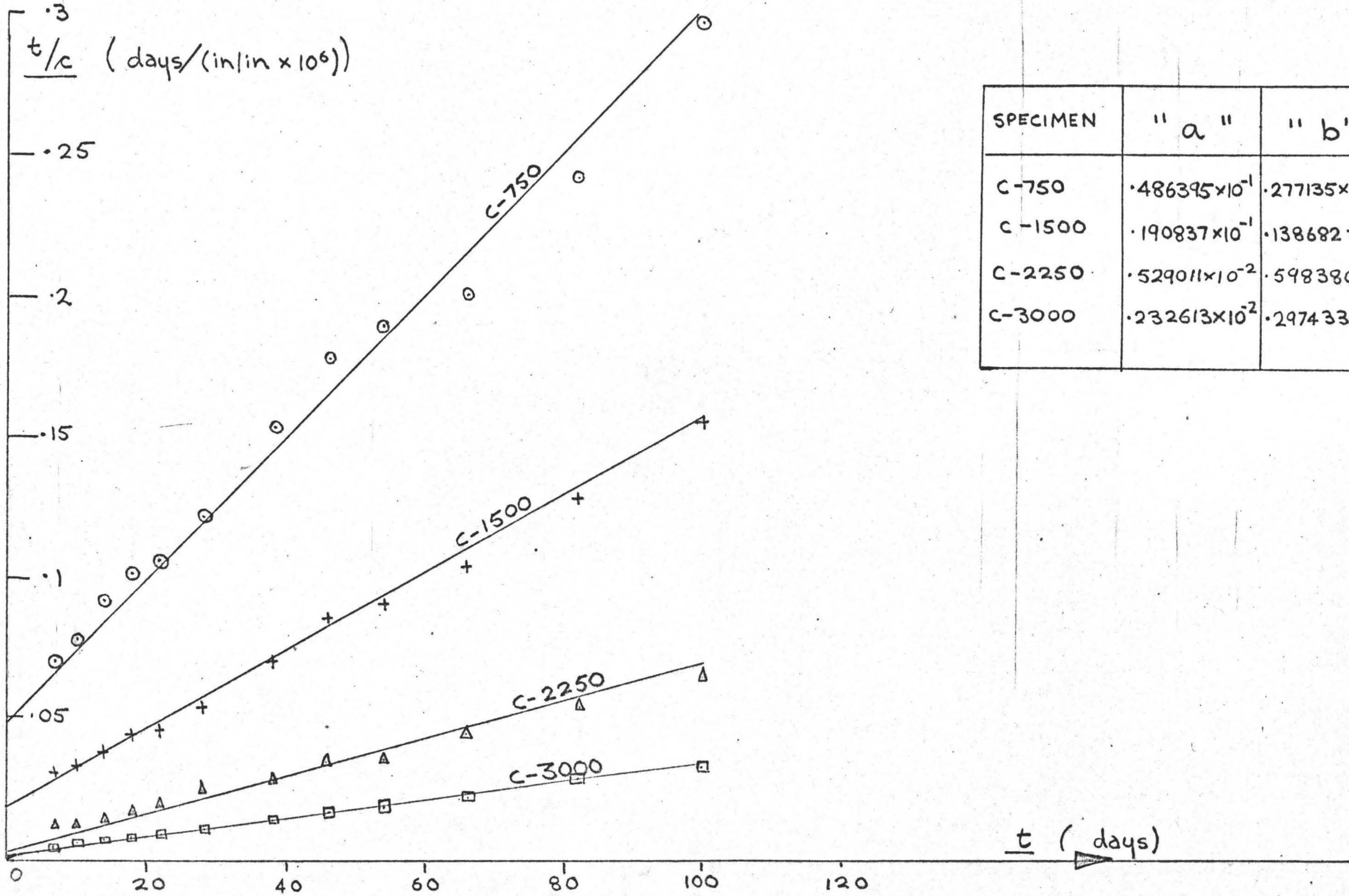

SPECIMEN	"a"	"b"
C-750	$\cdot 486395 \times 10^{-1}$	$\cdot 277135 \times 10^{-2}$
C-1500	$\cdot 190837 \times 10^{-1}$	$\cdot 138682 \times 10^{-2}$
C-2250	$\cdot 529011 \times 10^{-2}$	$\cdot 598380 \times 10^{-3}$
C-3000	$\cdot 232613 \times 10^{-2}$	$\cdot 297433 \times 10^{-3}$

Fig. 3.5. Ross Plots of Concentric Creep Data

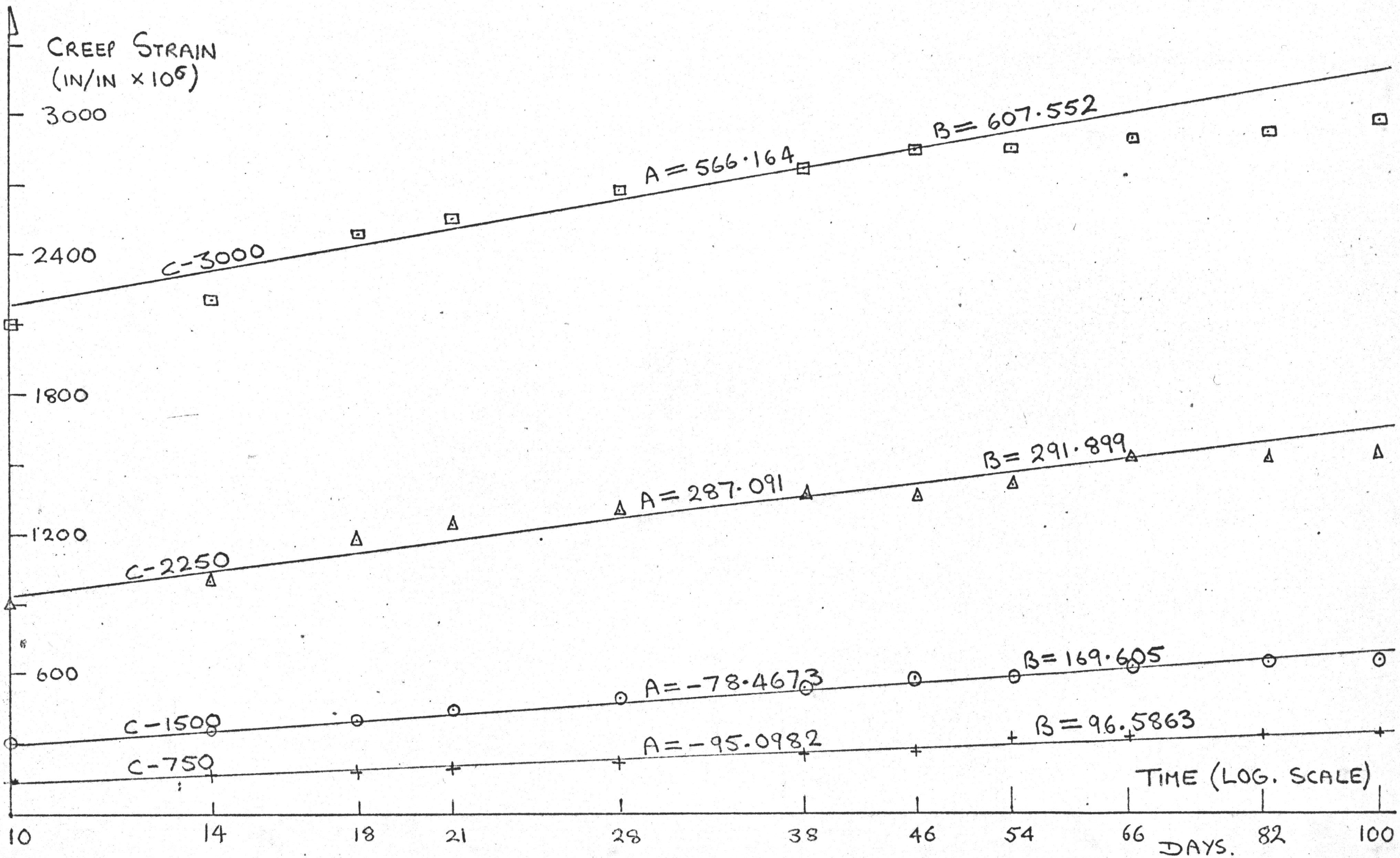

Fig. 3.6. SEMI-LOG PLOTS OF CREEP DATA

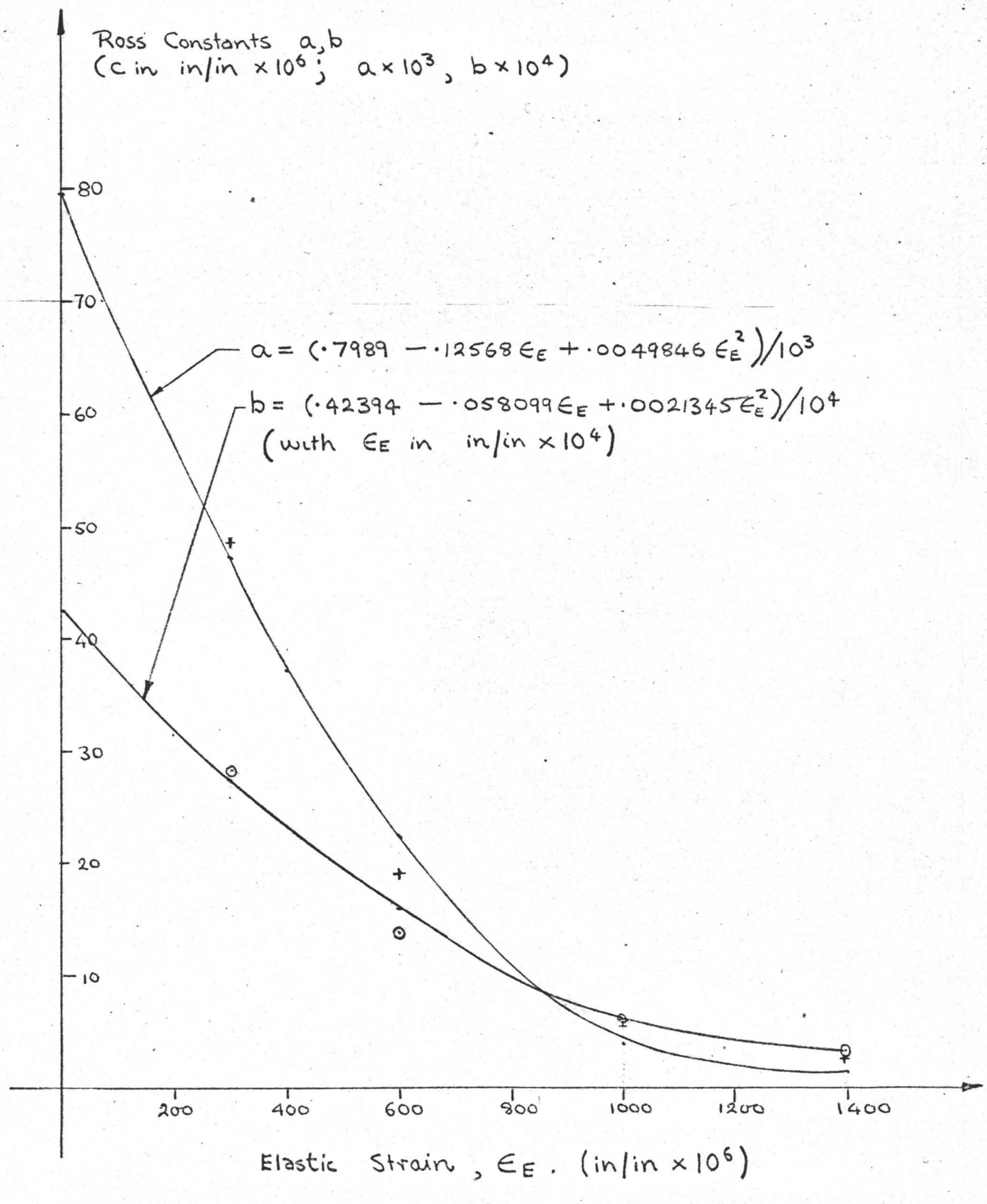

Fig. 3.7. Ross Constants against Initial Elastic Strain.

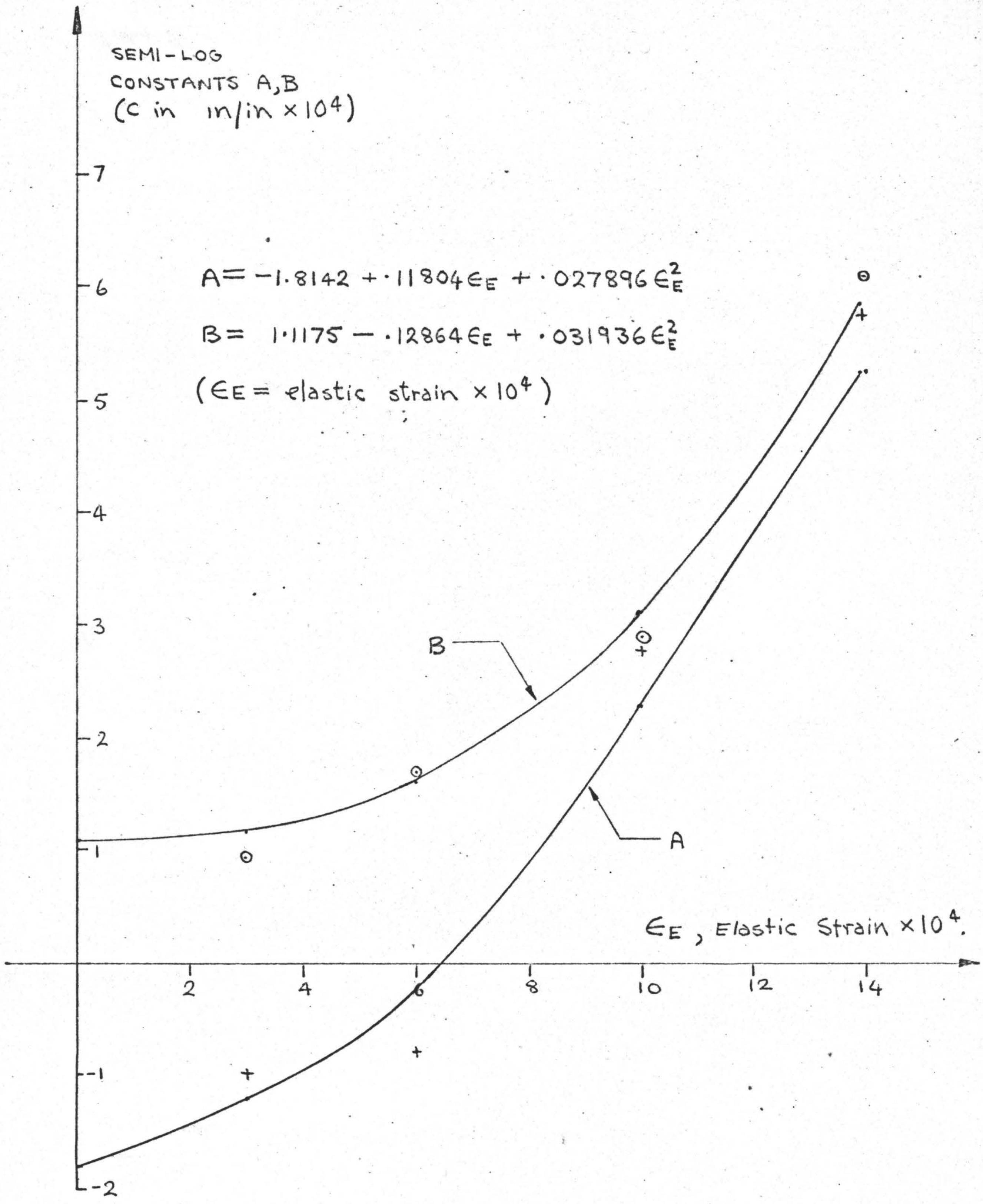

Fig. 3.8. SEMI-LOG CONSTANTS AGAINST INITIAL ELASTIC STRAIN.

be a simple matter to compute the predicted creep strain at any time. A procedure similar to this was used in applying the concentric creep data to the prediction of the creep of the eccentrically-loaded prisms, as detailed in the next section.

3.3. Methods of Predicting Eccentric Creep Effects

Both of the methods described below were used in conjunction with the IBM 7040 computer at the McMaster Computer Centre to predict the total strains of the eccentrically-loaded creep prisms used in the experimental program.

3.3.1. The "Element" Method

An "element" method was presented by R.G. Drysdale[11] and used by him in a study of sustained loading effects on long, slender columns. Some of the refinements incorporated in the original method were not used in the present analysis.

The basic purpose of the method, as used here, is to compute the creep of an eccentrically-loaded plain concrete prism from the following data:

(i) the member's cross-section properties

(ii) the concrete's stress-strain relationship, and the effect of increasing age in the stress-strain curve

(iii) the applied load and its eccentricity

(iv) the results of concentric creep tests covering the same stress range

The total strain as distributed between creep strain and elastic strain, and the stress distribution after some time under load are the unknowns of interest.

The information from (iv) is used by expressing the creep constants as functions of the initial elastic strain, as described in the previous section. The Ross creep formula was used initially. Later, the Semi-log method was incorporated in order to compare the accuracy of results obtained using the two creep formulae.

The method is a computerized process, and the main components of the program are:

(i) computation of creep and new total strains

(ii) adjustment of strains to satisfy external load and moment conditions.

The member cross-section is divided into a number of elements or strips, as shown in the sketch below.

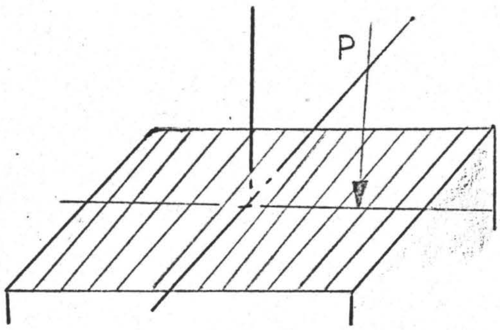

The number of strips used in this case was 20. The number of strips chosen represents, essentially, a compromise between accuracy of solution and amount of computer time and storage used in the calculation. (The number was not found to be critical, and little gain in accuracy was obtained by using a larger number of strips than 20. A discussion of the effect of the number of elements is contained in reference 11).

The stages of the element method can easily be identified with the main features of the basic approach outlined in Chapter 1.

(i) Determination of Elastic Strains

Initial "trial" values of elastic strain are read in as data, and are adjusted by two subroutines, ALOAD and XMOM, until they are compatible with the external load and moment conditions. This process may be described as follows.

Since the elastic strains on all elements are initially known as some proportion of the assumed strains at the extreme fibres of the prism, the forces on the elements may be calculated using the concrete's stress-strain relationship. The forces from all strips may be summed to give the calculated force, PCAL. (The stress resulting from the strain at the centroid of each strip is assumed to be constant over the width of the strip).

PCAL is compared with the known applied load, P. If PCAL differs from P by more than a pre-set allowable error, the strain distribution across the section is adjusted. The strain in the extreme fibres are either increased or decreased by an amount dependent on the size and sign of the error term (P - PCAL).

If, for example, the elastic strain distribution initially read in has the form shown in Fig. 3.9., and the equivalent resultant force PCAL is greater than P, then the extreme fibre strains, UC and UT, are both reduced by an amount UP, which is dependent on the magnitude of the discrepancy.

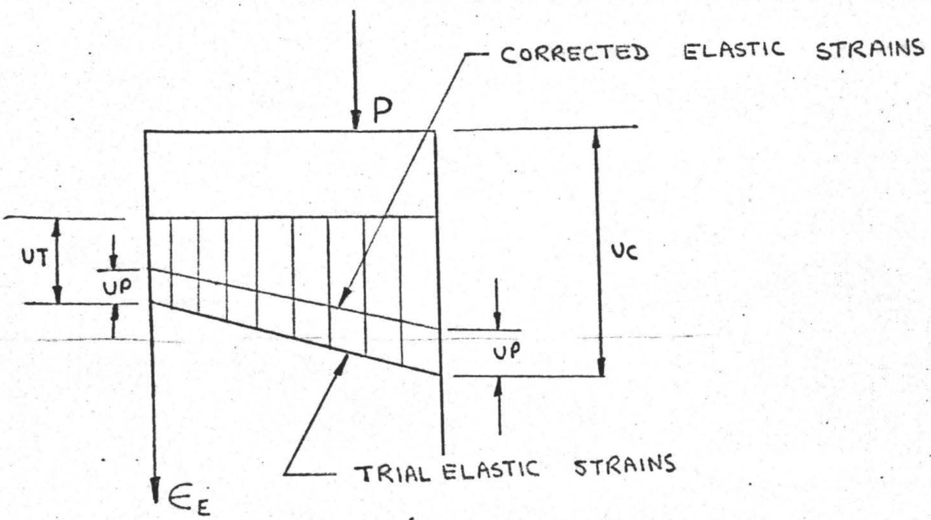

Fig. 3.9.

A similar process is applied in the moment-balancing sub-program. Using the new elastic strain distribution, the moment contribution of each strip is calculated, and all such contributions are summed. (The force in each strip is assumed to act at its centroid). The calculated moment is then compared to the known applied moment in a similar way to that in which PCAL is compared to P. Here, however, the strain correction applied is such as to alter the position of the resultant force. That is, the strain correction is added at one extreme fibre and subtracted at the other.

For example, consider a case where the calculated moment, BMXCAL, is greater than the known applied moment. This error is equivalent to having the correct load at too great an eccentricity. The correction, UM, is accordingly added to UT, and subtracted from UC, as shown in Fig. 3.10.

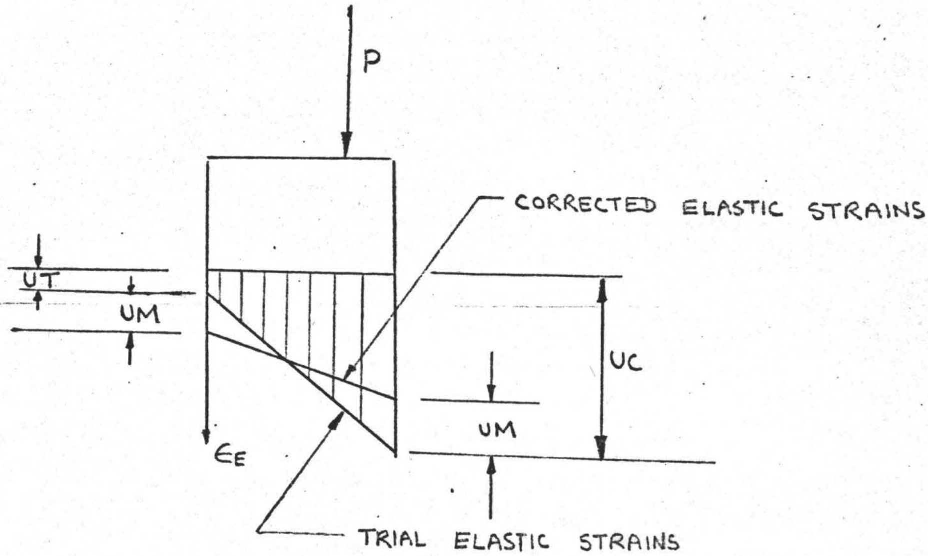

Fig. 3.10.

If either PCAL or BMXCAL is in error by more than a preset amount (usually 1%) the process was repeated. The strains converged monotonically in an asymptotic manner on their "correct" values. A typical series of load- and moment- balance cycles is shown in Fig. 3.11. The figure illustrates the way in which PCAL converges on P from one side.

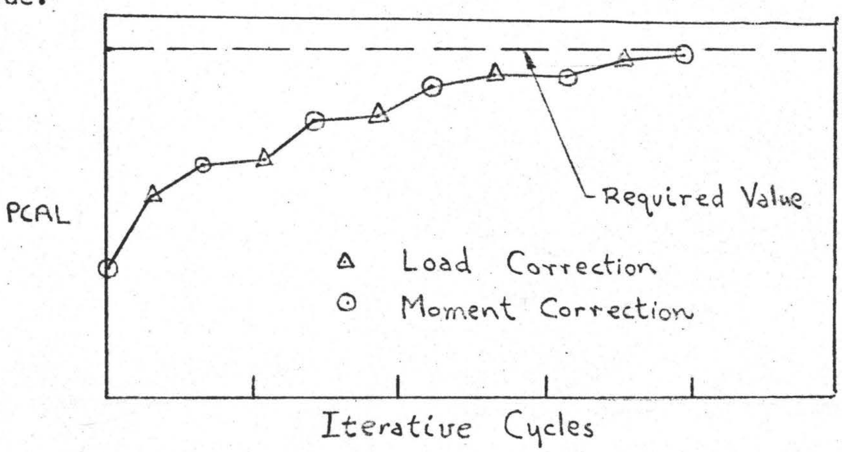

Fig. 3.11.

(ii) Determination of Free Creep

For each element, and for the given time increment, creep is computed from the Ross equation, with the constants "a" and "b" taking values dependent on the elastic strain at that element. This creep strain is now added to the elastic strain to give the value of the total strain in each element.

The creep for an element subjected to a change in strain over the previous time increment ~~was~~ is calculated by a superposition method, which may ~~be~~ give illustrated by ~~the~~ an ~~following~~ example.

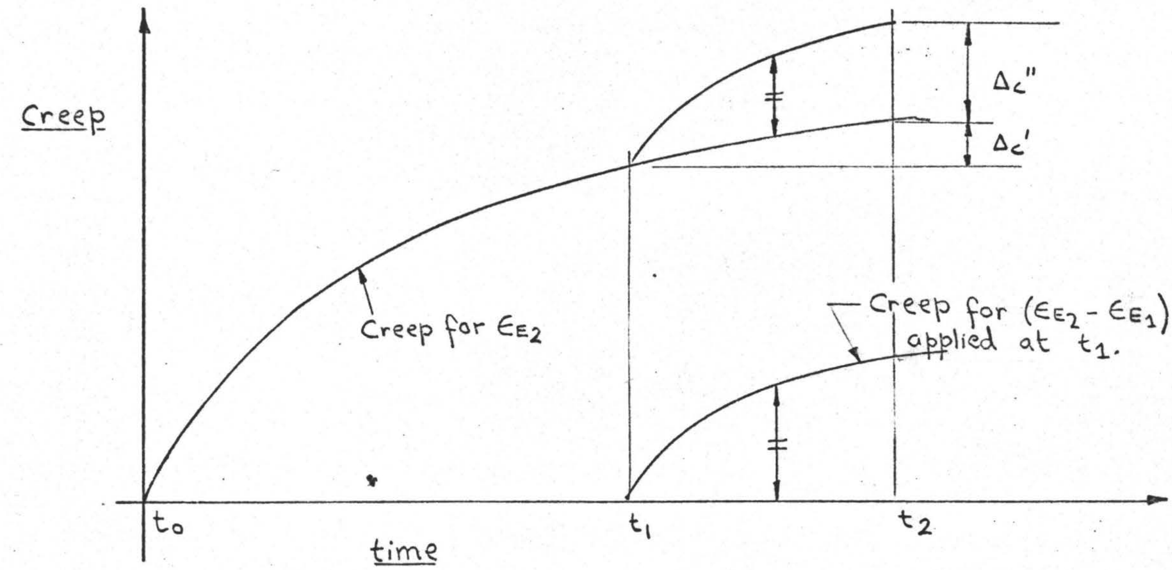

Fig. 3.12.

On board.

Consider an element initially subjected to an elastic strain ϵ_{E1}. At the end of one time increment, t_o to t_1, the elastic strain is found to have changed to ϵ_{E2}.

The creep for a subsequent time interval, t_1 to t_2, is found as the sum of two terms:

(a) the creep that would have occurred in the time interval t_1 to t_2 as if ϵ_{E2} had been on the element from t_0 to t_1. (i.e. $\Delta c'$ in the figure)

(b) the creep due to the strain difference $(\epsilon_{E2} - \epsilon_{E1})$, assuming this increment to have been newly applied. (i.e. the first part of the creep curve for this strain increment is used).

Thus, the creep strain increment Δc is given by

$$\Delta c = \Delta c'' + \Delta c'$$

as shown in Fig. 3.12. Step (b) was omitted for $\epsilon_{E2} < \epsilon_{E1}$, owing to a lack of sufficient data on creep recovery.

Thus, the assumed total strain distribution is as shown in the sketch Fig. 3.13.

It may be noted that this distribution is known to be incorrect; it is, however, known to be reasonably close, and a convenient first trial is thus provided by using the total strains at the extreme fibres.

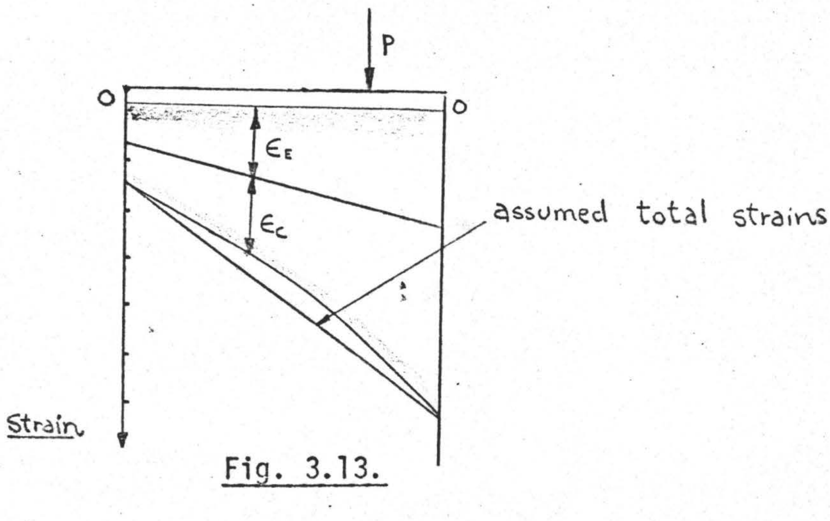

Fig. 3.13.

(iv) Satisfying Statics

The new elastic strain distribution is given by

$$\varepsilon_E = \varepsilon_t - \varepsilon_c$$

Since ε_t is the result of the assumption made in (iii), the elastic strain distribution will not generally be compatible with the applied load and moment. The load-balancing process, as used in (i) is brought into play again; this time, however, the corrections UP and UM are applied to the total strains, rather than to the elastic strains.

When the load balance has been completed, the new total strains at the end of the time interval are known, as are the new elastic strains, given by

$$\varepsilon_E = \varepsilon_t - \varepsilon_c$$

Thus, the creep for the next time interval can be computed on the basis of the new elastic strain distribution.

The process can be carried on for any desired number of time intervals.

For further information on the workings of the "element" method, the reader is referred to reference 11. The program used in this investigation appears in Appendix I. A comparison of the creep predicted by this method with that observed in the laboratory is contained in Chapter 5.

3.3.2. The "Continuous" Method

The "element" method, while powerful in that it is able to handle complex problems which necessitate the use of many time intervals, is relatively extravagant in its use of computer time and storage.

It is necessary, for example, to compute and store values of elastic strain and creep strain for each individual element. In addition, in the load-balancing process, the stress on each element must be computed separately, the total load and moment being found by summing the contributions of all the elements.

The continuous method was evolved in an attempt to save computer time and storage. This method considers the whole member cross-section as one unit, and represents elastic, creep, and total strains as continuous functions of position on the cross-section.

The general form and degree of these functions can be found. The actual computation is then reduced to a relatively simple and fast procedure which calculates the co-efficients of the terms in these functions.

The method goes through the stages explained in the general approach to the problem in section 1.5.

The first step is to choose axes and identify the member dimensions. Take the x-axis as shown in Fig. 3.14., so that the load P is applied at some point along its length. The prism's cross-section is rectangular, of area w x t. Note that at the point of application of P,

$$x = \frac{w}{2} + e_x$$

where e_x denotes eccentricity of the load in the x-direction.

(i) Determination of Initial Elastic Strains

The initial elastic strain distribution may be expressed as a linear function of x.

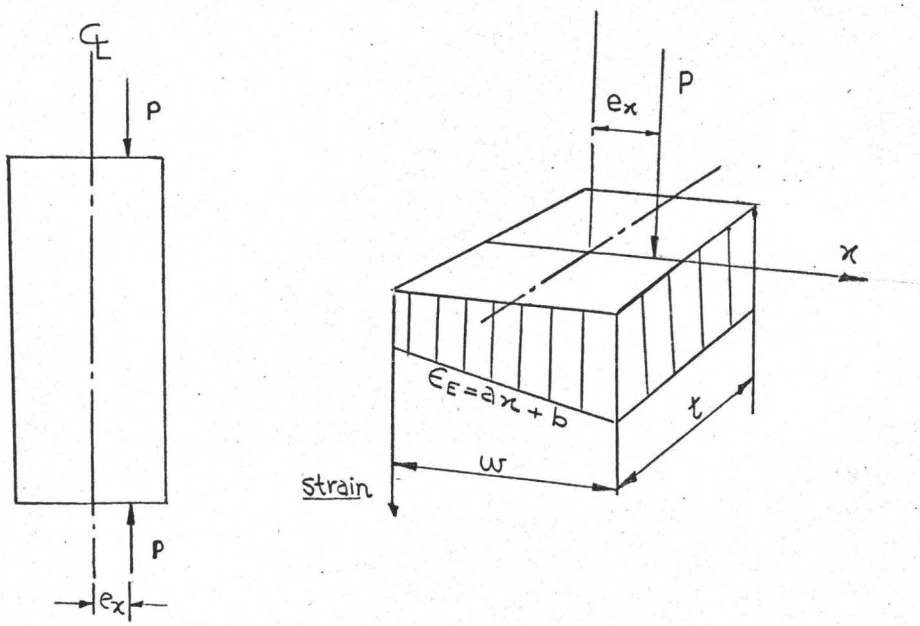

Fig. 3.14.

Thus, $\varepsilon_E = ax + b$

where ε_E denotes elastic strain, and "a" and "b" are constants.* The constants "a" and "b" may be found by solving directly the equations for resultant load and moment. This is a somewhat lengthy procedure which is especially tedious if stress is a function of a high degree in strain. Instead of this, an iterative procedure, rather similar in principle to that employed in the element method, was used, and will be described.

Suppose that the stress-strain relation of the concrete can be represented by a second degree curve of the type

$$\sigma = c_1 \varepsilon_E^2 + c_2 \varepsilon_E$$

where σ = stress, and c_1, c_2 are constants with units of stress. (This was done in Chapter 2).

* "a" and "b" have no connection with the Ross constants.

Since $\varepsilon_E = ax + b$

$$\sigma = c_1(a^2x^2 + 2abx + b^2) + c_2(ax + b)$$

$$= (c_1a^2)x + (2abc_1 + c_2a)x + (b^2c_1 + bc_2)$$

$$= k_1x^2 + k_2x + k_3$$

where $k_1 = c_1a^2$; $k_2 = 2abc_1 + c_2a$; $K_3 = b(bc_1 + c_2)$

The resultant force, PCAL, say, is given by

$$\text{PCAL} = t_0\int^W\sigma.dx$$

i.e. $\text{PCAL} = t(k_1w^3/3 + k_2w^2/2 + k_3w)$

Similarly, the resultant moment of the concrete stresses about "o" is BMCAL, where

$$\text{BMCAL} = t_0\int^W\sigma.x.dx$$

$$= t(k_1w^4/4 + k_2w^3/3 + k_3w^2/2)$$

Thus, the type and form of the functions for resultant load and moment are known and the constants k_1, k_2, k_3 can be calculated for any values of a, b, c_1, c_2.

Then, taking any likely values of a and b as a first trial, the equivalent load and moment can be easily computed.

The constants a and b can now be modified by error terms dependent on the magnitude and sign of the differences (P - PCAL) and (BM - BMCAL), where BM = P (w/2 + ex). These error terms can be applied in the same way as in the "element" method. Values of k_1, k_2, k_3 can be recomputed. This process is repeated until satisfactory convergence is achieved.

(ii) Determination of Free Creep

Consider the time interval from $T = 0$ to $T = T_1$. The Semi-log creep expression

$$C = A + B \log e(t)$$

will be used here in preference to Ross's formula, since the latter leads to greater mathematical complexity in this case.

A and B can both be expressed as second degree functions of elastic strain (see section 3.2.3.)

Thus, $A = c\varepsilon_E^2 + d\varepsilon_E + e$

$$B = f\varepsilon_E^2 + g\varepsilon_E + h$$

where c, d, e, f, g, h, are constants.

Since $\varepsilon_E = ax + b$, we may substitute to obtain

$$A = u_2 x^2 + u_1 x + u_o$$

$$B = v_2 x^2 + v_1 x + v_o$$

in which $u_2 = ca^2 \quad , \quad v_2 = fa^2$

$u_1 = a(2bc + d), \quad v_1 = a(2bf + g)$

$u_o = cb^2 + db + e, \; v_o = fb^2 + gb + h$

Thus, after some time T_1 under load, the creep strain will be

$$\varepsilon_c = x^2(u_2 + v_2 \log T_1) + x(u_1 + v_1 \log T_1) + (u_o + v_o \log T_1)$$

The total strain at time T_1 is then given by

$$\begin{aligned}\varepsilon_t &= \varepsilon_c + \varepsilon_E \\ &= x^2(u_2 + v_2 \log T_1) + x(a + u_1 + v_1 \log T_1) + (b + u_o + v_o \log T_1)\end{aligned}$$

If $K_4 = u_2 + v_2 \log T_1$

$K_5 = u_1 + v_1 \log T_1$

$K_6 = u_0 + v_0 \log T_1$

Then ε_t may be rewritten

$$\varepsilon_t = k_4 x^2 + (k_5 + a)x + (k_6 + b)$$

(iii) Restoration of Plane Sections

The same assumption as was made in the "element" method about the new total strain will be made here.

Thus, ε_t', the new total strain, will be linear in x.

i.e. $\varepsilon_t' = a'x + b'$, say

At its extremities, this line coincides with the line representing ε_t.

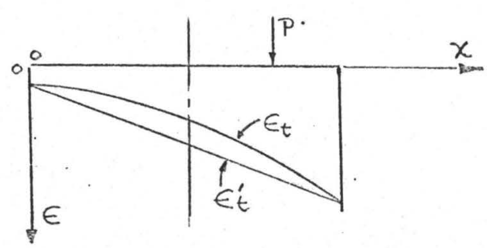

i.e. at $x = 0$

$b' = k_6 + b$

Similarly, for $x = w$

$$a'w + b' = w^2 k_4 + w(k_5 + a) + k_6 + b$$

i.e. $a' = wk_4 + k_5 + a$

(iv) Satisfying Statics

To "satisfy statics" it is necessary to find the stress distribution across the section, and to evaluate the equivalent load and moment. Statics will then be satisfied by altering the total strain distribution until equilibrium is achieved. This load-balancing process will be similar to that carried out for the initial elastic strains.

$$\text{Now} \quad \varepsilon_E = \varepsilon'_E - \varepsilon_C$$

$$= a'x + b' - k_4x^2 - k_5x - k_6$$

$$= -k_4x^2 + x(a' - k_5) + (b' - k_6)$$

$$\text{Put } k_7 = a' - k_5$$

$$k_8 = b' - k_6$$

Thus $\qquad \varepsilon_E = -k_4x^2 + k_7x + k_8$

Suppose that at time T_1, the concrete stress-strain relationship is given by

$$\sigma = C_3\,\varepsilon_E^2 + C_4\varepsilon_E$$

(C_3 and C_4 will differ from C_1 and C_2 owing to the concrete's gain in strength over the period $T = 0$ to $T = T_1$).

$$\text{Thus } \sigma = C_3(-k_4x^2 + k_7x + k_8)^2 + C_4(-k_4x^2 + k_7x + k_8)$$

leading to $\qquad \sigma = p_1x^4 + p_2x^3 + p_3x^2 + p_4x + p_5$

where $\quad p_1 = k_4{}^2C_3$

$$p_2 = -2C_3k_4k_7$$

$$p_3 = C_3(-2k_4k_8 + k^2{}_7) - C_4k_4$$

$$p_4 = 2C_3k_7k_8 + k_7C_4$$

$$p_5 = k_8(C_3k_8 + C_4)$$

PCAL, the load equivalent to this stress distribution is given by

$$PCAL = t_0\int^{w}\sigma.dx$$

$$= t(w^5p_1/5 + w^4p_2/4 + w^3p_3/3 + w^2p_4/2 + wp_5)$$

Also, $BMCAL = t_0\int^{w}_{0}\sigma.x.dx$, again taking moments about 0.

i.e. $$BMCAL = t(w^6p_1/6 + w^5p_2/5 + w^4p_3/4 + w^3p_4/3 + w^2p_5/2)$$

Iterating as before will bring PCAL and BMCAL to the desired values by altering the values of a' and b'.

Knowing the final values of a' and b' permits the final total strain distribution, and hence the new stress distribution to be calculated. This completes the calculation for one time interval.

It will be apparent, however, that the free creep is determined assuming that the initial elastic strain distribution remains constant throughout the time interval. For many practical problems, this means that the time period of interest will have to be broken into two or more time intervals.

The calculation for a second time interval is identical in principle, but involves more lengthy algebra. The process is outlined below:

Recall that $C = A + B \log e(T)$

$$\frac{dc}{dt} = \frac{B}{T}$$

(i) Determination of Free Creep

This is the first step in this case, as the initial elastic strain distribution is known (It is that given by the last part of the calculation for the first time interval).

If the second time interval is ΔT, and $T_2 = T_1 + \Delta T$, then the increment of creep taking place, ΔC, is given by

$$\Delta C = C_2 - C_1 = B\ (\log_e T_2 - \log_e T_1)$$

$$= B.\gamma \quad , \text{ say.}$$

Note that γ may be approximated to by $\Delta T/(T2 - \Delta T/2)^{+}$

Recall that

$$B = f\varepsilon_E^2 + g\varepsilon_E + h$$

and that $\varepsilon_E = -k_4x^2 + k_7x + k_8$

Thus

$$\dot{B} = r_1x^4 - r_2x^3 - r_3x^2 + r_4x + r_5$$

in which $r_1 = fk_4$ $\qquad$ $r_4 = 2fk_8k_7 = gk_7$

$r_2 = 2fk_4k_7$ $\qquad$ $r_5 = fk_8^2 + gk_8 + h$

$r_3 = 2k_4k_8f - k_7^2f + gk_4$

Hence $\Delta C = (r_1x^4 - r_2x^3 - r_3x^2 + r_4x + r_5)\gamma$

$$= q_1x^4 - q_2x^3 - q_3x^2 + a_4x + q_5)$$

where $q_i = \gamma . ri$

(ii) Restoration of Plane Sections

$$\varepsilon tn = \text{New total strain} = \varepsilon t' + \Delta C$$

$$= a'x + b' + q_1x^4 - q_2x^3 - q_3x^2 + q_4x + q_5$$

i.e. $\varepsilon tn = q_1x^4 - q_2x^3 - q_3x^2 + x(q_4 + a') + (q_5 + b')$

+ For $\Delta T = 10$ and $T_2 = 10$, the approximation is within 3% of the correct value. For higher values of T_2, the approximation is better. For example, for $T_2 = 90$, $\Delta T = 10$, the error is .1%.

In the same way as before, we choose new trial values of total strain which have the same value as εtn at $x = 0$ and $x = w$; as before, the distribution is linear between those values.

Let new total strains be $\varepsilon' tn = a''x + b''$

At $x = 0$, $\varepsilon t'n = \varepsilon tn$, leading to $b'' = q_5 + b'$

Similarily, conditions at $x = w$ give

$$a''w + b'' = q_1 w^4 - q_2 w^3 - q_3 w^2 + w(q_4 + a') + b''$$

$$\text{i.e.} \quad a'' = q_1 w^3 - q_2 w^2 - q_3 w + q_4 + a'$$

(iii) Satisfying Statics

Elastic strain = Total strain - creep in 2nd time interval

- creep in 1st time interval.

The equations for these three strain distributions are known. Thus

$$\varepsilon_E = a''x + b'' - q_1 x^4 + q_2 x^3 + q_3 x^2 - q_4 x - q_5$$

$$- k_4 x^2 - k_5 x - k_6$$

or
$$\varepsilon_E = -q_1 x^4 + q_2 x^3 + s_1 x^2 + s_2 x + s_3$$

where
$$s_1 = q_3 - k_4$$

$$s_2 = a'' - q_4 - k_5$$

$$s_3 = b'' - q_5 - k_6$$

If the concrete's stress-strain relationship is given by

$$\sigma = C_5 \varepsilon_E^2 + C_6 \varepsilon_E \quad \text{at time } T_2,$$

it can be shown that

$$\sigma = Y_1 x^8 + Y_2 x^7 + Y_3 x^6 + Y_4 x^5 + Y_5 x^4 + Y_6 x^3 + Y_7 x^2 + Y_8 x + Y_9$$

in which:

$$Y_1 = C_5 q_1^2$$

$$Y_2 = -2C_5 q_1 q_2$$

$$Y_3 = C_5 \ (q_2^2 - 2q_1 s_1)$$

$$Y_4 = C_5 \ (2q_2 s_1 - 2q_1 s_2)$$

$$Y_5 = C_5 \ (-2q_1 s_3 + 2q_2 s_2 + s_1^2) - C_6 q_1$$

$$Y_6 = C_5 \ (2s_1 s_2 + 2q_2 s_3) + C_6 q_2$$

$$Y_7 = C_5 \ (2s_1 s_3 + s_2^2) + C_6 s_1$$

$$Y_8 = C_5 \ (2s_2 s_3) + C_6 s_2$$

$$Y_9 = C_5 s_3^2 + C_6 s_3$$

Therefore, $PCAL = t \int_0^W \sigma . dx$

$$= t(Y_1 w^9/9 + Y_2 w^8/8 + Y_3 w^7/7 + Y_4 w^6/6 + Y_5 w^5/5 + Y_6 w^4/4 + Y_7 w^3/3 + Y_8 w^2/2 + Y_9 w)$$

Also, $BMCAL = t \int_0^W \sigma . x . dx$

$$= t(Y_1 w^{10}/10 + Y_2 w^9/9 + Y_3 w^8/8 + Y_4 w^7/7 + Y_5 w^6/6 + Y_6 w^5/5 + Y_7 w^4/4 + Y_8 w^3/3 + Y_9 w^2/2)$$

A final iterative process will balance the load and moment, and supply final values of the constants which define the stress and strain distributions.

The method may be extended to include a third time interval. The working for this additional stage appears in Appendix II.

The principle drawback of this approach should now be apparent. Since the expression for creep

$$C = A(\varepsilon_E) + B(\varepsilon_E) \log_e T$$

is of second degree in elastic strain, the degree of the elastic strain distribution is doubled for each additional time increment. (The way in which this occurs is explained fully in section 3.3.3.). Thus, for the second time interval the calculation is noticeably more laborious than for the first. A similar increase in complexity and in the degree of the functions describing creep and elastic strains is apparent in the third interval calculation, (see Appendix II). For subsequent time intervals, the calculation becomes so lengthy that another method, such as the "element" method, would be more practical.

For problems in which it is desirable to consider a large number of time intervals, the following procedure was adopted. This procedure avoids the problem raised by the progressive increase in complexity of the basic method.

The degree of complexity is limited to that obtained by the end of the second time interval. That is, ε_E is of fourth degree in x. To do this a second degree curve is fitted through the elastic strain distribution. Hence, the elastic strain distribution at the end of the second time interval, known to be of fourth degree in x is evaluated at several values of x. A second degree curve is then fitted through these points. The library subroutine DLESQ[+] accomplished this part of the procedure. We may now compute creep for the third time interval in the same way as for the second time interval, since elastic strain is of

+ DLESQ is a subroutine which uses a least-squares fit technique to fit a curve of any desired degree through a given set of points.

second degree in x, as it was at the start of the second interval. In this case, the values of the co-efficients replacing k_4, k_7 and k_8 (which define the elastic strain distribution) are obtained from DLESQ. This procedure may be repeated for any desired number of time intervals. Note, however, that when finding the new elastic strain at the end of a time interval, we now have

$$\varepsilon_E = a^n x + b^n - \Sigma\Delta C$$

where a^n, b^n describe the new total strain distribution, and $\Sigma\Delta C$ represents the sum of the creep increments occurring in all previous time intervals.

Thus, where the co-efficient q_i was used for the calculation for the second time interval, for the "nth" time interval we use instead

$$\sum_{i=1}^{n} q_{1n} = q_{12} + q_{13} \ldots\ldots\ldots + q_{1n}$$

where the second subscript denotes the number of the time interval.

A superposition method for calculating creep, similar to that used in the element method, can be incorporated in the continuous method. For the second and subsequent time intervals, the change in elastic strain distribution is plainly of fourth degree in x.

$$\text{i.e.}\quad \varepsilon_{E2} - \varepsilon_{E1} = -k_4 \bar{x} + (k_7 - a)x + (k_8 - b)$$

for the second time interval. For any later interval, from T_n to T_{n+1},

$$\varepsilon_{En} - \varepsilon_{En-1} = (-k_4^n + k_4^{n-1})x^2 + (k_7^n - k_7^{n-1})x + (k_8^n - k_8^{n-1})$$

Let $\theta_1 = -k_4$

$\theta_2 = k_7 - a$ for the second time interval

$\theta_3 = k_8 - b$

Let $\theta_1 = -k_4^n + k_4^{n-1}$

$\theta_2 = k_7^n - k_7^{n-1}$ for any later time interval, T_n

$\theta_3 = k_8^n - k_8^{n-1}$ to T_{n+1}.

(k_7^n denotes the value of k_7 after the time interval t_{n-1} to t_n, etc.)

Thus, the change in elastic strain, ε_E', say, is given by

$$\varepsilon_E' = \theta_1 x + \theta_2 x + \theta_3$$

for any time interval after the first.

The creep strain due to this elastic strain change, $\Delta C''$, say, is then

$$\Delta C'' = A(\varepsilon'_E) + B(\varepsilon'_E) \log_e (\Delta t)$$

As before, $A = C\varepsilon_E^2 + d\varepsilon_E + e$

$$B = f\varepsilon_E^2 + g\varepsilon_E + h$$

It can be shown that

$$\Delta C'' = \beta_1 x^4 + \beta_2 x^3 + \beta_3 x^2 + \beta_4 x + \beta_5$$

where $\beta_1 = \theta_1{}^2 (C + f \log_e (\Delta t))$

$$\beta_2 = 2\theta_1\theta_2 \; (C = f \log_e (\Delta t))$$

$$\beta_3 = (\theta_2^2 + 2\theta_1\theta_3) \; (C + f \log_e (\Delta t)) + \theta_2(d + g \log_e (\Delta t))$$

$$\beta_4 = 2\theta_3\theta_2(C + f \log_e (\Delta t)) + \theta_2(d + g \log_e (\Delta t))$$

$$\beta_5 = \theta_3^2 \; (C + f \log_e (\Delta t)) + \theta_3(d + g \log_e(\Delta t)) + e + h \log_e (\Delta t)$$

Thus the total creep during any time interval is

$$\Delta C = \Delta C' + \Delta C''$$

$$= x^4(q_1 + B_1) + x^3(\beta_2 - q_2) + x^2(\beta_3 - q_3) + x(q_4 + \beta_4) + (\beta_5 + q_5$$

This is a similar expression to that already used in the analysis. Thus, to include the effect of the change in élastic strain, it is only necessary to modify the values of q_i by adding or subtracting β_i. In this case, it can be seen that the complete superposition method is used for both increasing and decreasing stress. This is equivalent to assuming that the magnitude of creep strain under a relief of stress is the same as that for an increase in stress. Expressed in another way, this means that creep recovery is assumed to be of the same magnitude as creep, but of opposite sign. It is known that this assumption will lead to an overestimate of creep recovery.

It will be recalled that in the element method the creep $\Delta C''$ was not included for decreasing stress. Using the same procedure with this method would require solving the equation for ε_E'. That is, the values of x at which $\varepsilon_E' = 0$ would be found. Then the ranges in which elastic strain had decreased would be known. The "β's" would not be applied to the "q's" in these regions. This refinement would be desirable in cases in which major relief of stress was thought likely. For the plain concrete prisms used in the experimental program, however, large scale transfer of stress within the test period was thought to be unlikely.

A computer program was written to carry out the calculations for the continuous method. Superposition was included in the program, which was used to predict the creep of the eccentrically-loaded prisms used in the experimental program. The program, with an explanatory introduction, is reproduced in Appendix II. The results obtained using the program are compared with those observed in the experimental program, in Chapter 5.

3.3.3. The Progressive Increase in Complexity of the Unmodified Continuous Method

In many cases it would be desirable to extend the method so that several time intervals might be considered. If, for example, creep was being computed for a member which was to undergo variations in applied load and moment (the latter perhaps due to creep itself), it might be necessary to consider a large number of short time intervals. This is because the elastic strain distribution is implicitly assumed to be constant over any chosen time interval (although some allowance for variation can be made, as in the superposition method).

The difficulties which arise in trying to consider large numbers of time intervals by the continuous method will be considered.

First Time Interval

It will be recalled that the initial elastic strain distribution is linear, and was represented by the equation

$$\varepsilon_E = ax + b$$

"A" and "B", the constants in the equation

$$\varepsilon_c = A + B \log_e T \ldots\ldots\ldots\ldots (1)$$

are of second degree in ε_E. Hence, so is ε_c, computed for any time interval $T = 0$ to $T = T_1$. Since ε_E is linear in x, ε_c is of second degree in x.

The "new" total strain (i.e. the total strain for $T = T_1$) is linear in x, being represented by

$$\varepsilon_t = a'x + b'$$

The new elastic strain distribution, given by $(\varepsilon_t - \varepsilon_c)$, is thus seen to be of second degree in x.

Second Time Interval

Let the second time interval be of length $\Delta T = T_2 - T_1$. It may be recalled that the creep occurring during this interval was found using the equation

$$\Delta C = \frac{B}{T_2 - \Delta T/2} \cdot \Delta T \text{ .... } (2)$$

The additional creep, ΔC, is thus of second degree in elastic strain, since B is of the form

$$B = f\varepsilon_E^2 + g\varepsilon_E + h$$

The equation for ε_E, however, is now of second degree in x. Thus, ΔC is of fourth degree in x.

Again the total strain distribution, $\varepsilon t'n$, will be linear in x. Hence, the elastic strain at time T_2 will be given by

$$\varepsilon_E = \varepsilon tn' - \varepsilon_C - \Delta C$$

and will be of fourth degree in x.

ΔC for the third and subsequent time intervals will be calculated using the relation (2). Using similar reasoning to the above, it can be seen that ΔC for the third time interval will be of degree eight in x. Thus, the elastic strain distribution at the end of the third interval will also be of eighth degree in x. It can then be seen that ΔC for the fourth time interval will be of degree sixteen in x, and so on.

Thus, the degree and length of the equations for creep strain and elastic strain increase with the number of the time interval. In fact, these equations become so complex and involve such lengthy computations that for a large number of time intervals, the continuous method loses any advantage which it has over the element method.

It had been hoped that a method could evolve which would allow the same calculation to be carried out for each time interval. This would be especially well adapted to solving problems on the computer. Accordingly, efforts were made to overcome the problem presented by the progressive increases in complexity outlined above. These efforts are detailed below.

(i) Attempts to represent the creep constants "A" and "B" as linear functions of elastic strain.

The cause of the continual escalation in the degree of the functions for creep and elastic strain is the fact that both A and B are of second degree in elastic strain. If they were linear in elastic strain, computed creep would be linear, and hence no increase in complexity would arise.

It was thought that the plots of both "A" and "B" against elastic strain might be taken as made up of two linear segments, rather than of one second degree curve. Thus

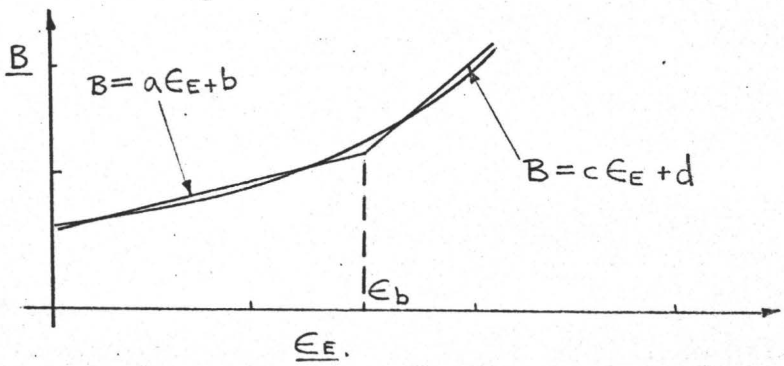

In this case, however, one is confronted by the problem of defining at what value of x on the member cross-section the "break" between the two portions of the line occurs. Equations can be devised which superficially appear to get round this difficulty. Such equations hold good for any value of ε_E.

e.g. for the case sketched on the preceeding page

$$B = \frac{[(\varepsilon_b + \varepsilon_E) + |\varepsilon_b - \varepsilon_E|]a}{2} + \frac{[(\varepsilon_E - \varepsilon_b) + |\varepsilon_E - \varepsilon_b|]c}{2} + b$$

will give the correct value for B for any ε_E.

Since, however

$$|ax + b| = + [(ax + b)^2]^{\frac{1}{2}}$$

it becomes evident that B is still represented by an equation containing powers of ε_E. These powers will cause increases in complexity as before.

(ii) Attempts to simplify the creep equations by neglecting terms which are "small" compared to the other terms.

An analysis was made of the magnitudes of the various terms in the creep occurring during the third time interval. It was hoped that the terms involving high powers of x (x^8, x^7, etc.) would prove to be "small" compared to the others, and that they could thus be neglected. It was also thought that similar high powers might be negligible for subsequent time intervals, and that the degree of the terms which had to be considered would thus tend to some limit.

The analysis of terms for the third interval creep, however, showed that, for typical numerical values found from the experimental program, the terms all lay in the same range (between .01 and 1). There was no apparent justification for neglecting some terms and retaining others.

These efforts having failed, the modified continuous method, incorporating the least-squares fit of a second degree curve to data obtained from a fourth degree function, was adopted. In this modified form, the continuous method can be applied to problems requiring the consideration of any number of time intervals. The modified continuous method is described fully in section 3.3.2.

The strains predicted by the "element" and "continuous" methods are compared with those observed in the experimental program in Chapter 5. The effects of certain errors on the accuracy of the predicted strains are considered in Chapter 4.

CHAPTER 4

ACCURACY OF THE COMPUTATIONAL METHODS AND POSSIBLE INACCURACIES IN THE EXPERIMENTAL PROCEDURE

4.1. Introduction

The approximate analysis of the errors in the computational methods, which is described in the next section, was not intended to be rigorous. Its purpose was to indicate the likely accuracy of the computational method. A completely rigorous treatment of the uncertainties discussed in section 4.2. was not justified since the effects of some of the possible sources of error could not be mathematically evaluated. Hence, it was decided that a combination of rigorously obtained statistical error data with rationally estimated values from other variables could misrepresent the overall accuracy.

Section 4.3. contains a discussion of errors whose effect could not be estimated quantitatively, but which would nevertheless affect the accuracy of the solutions obtained using the computational methods.

The various possible inaccuracies in the experimental procedures are discussed in section 4.4.

4.2. Approximate Quantitative Analysis of Errors in the Computed Solutions

The purpose of this analysis is to obtain an estimate of the probable accuracy of the values of total strain obtained by the two computational methods. To arrive at this estimate, differences between computed and measured strains due to the following factors are considered:

(i) errors arising from the scatter of points about the "least-squares fit" plots of concentric creep data according to the Ross and Semi-log methods.

(ii) errors occurring in the experimental measurement of strain

(iii) errors arising due to the scatter of points about the least squares fit curve representing the concrete's stress-strain relation.

It will be recalled from section 1.5. that the total strain ε_t, at any time t, is given by

$$\varepsilon_t = \varepsilon_E + \varepsilon_C + \varepsilon' + \varepsilon''$$

Looking first at the term ε_C, and considering the creep computation carried out by the element method, ε_C is found using the Ross formula,

$$\varepsilon_C = \frac{t}{a + bt}$$

It will also be recalled that both "a" and "b" were expressed as functions of initial elastic strain.

i.e. $a = f(\varepsilon_E)$; $b = g(\varepsilon_E)$

The error arising from the use of this expression is derived from two sources:

(a) the original Ross plots, obtained from the concentric creep bests, give rise to an error due to the deviation of the points from the best straight line drawn through them.

(b) errors also arise from the fact that "a" and "b" are both expressed as functions of elastic strain. Again, there is some scatter of the values of "a" and "b" about the line given by a least-squares fit.

The effect of these errors on the value of ε_C must now be calculated. The general method for estimating the uncertainty in a value which is a function of several variables will be used.

For any function $z = f(x,y)$, the error in z, called δz, is given by

$$\delta z = \frac{df}{dx} \delta x + \frac{df}{dy} \delta y$$

where δx, δy are the errors (assumed to be small) in x and y respectively*.

Thus, $\delta_C = C$, say, $= f(a,b,t,)$

$$\delta_C = \frac{\partial f}{\partial a} \delta a + \frac{\partial f}{\partial b} \delta b + \frac{\partial f}{\partial t} \delta t$$

The last item obviously drops out, since time is known exactly.

Now

$$\frac{\partial f}{\partial a} = \frac{-t}{(a + bt)^2}$$

and $$\frac{\partial f}{\partial b} = \frac{-t^2}{(a + bt)^2}$$

whence

$$\delta_C = \frac{-t}{(a + bt)^2} \delta a + \delta b \frac{-t^2}{(a + bt)^2} \quad \text{..............(i)}$$

The above equation may be evaluated for any set of values, a,b,t of interest.

A similar procedure may be used to compute the uncertainty in ε_C in the continuous method.

---

* This formula may be found in any text on error analysis. See, for example, D.C. Baird's "Experimentation", Prentice Hall, 1962.

In this case ε_C is calculated from the Semi-log expression

$$\varepsilon_C = A + B \log t$$

with "A" and "B" being functions of elastic strain.

Again

$$\delta_C = \frac{\partial f}{\partial A} (\delta A) + \frac{\partial f}{\partial B} \delta B$$

Here

$$\frac{\partial f}{\partial A} = 1 \qquad \text{and} \qquad \frac{\partial f}{\partial B} = \log t$$

giving

$$\delta_C = \delta A + \delta B \log t$$

Again, δ_C can readily be obtained for given values of δA, δB, and t.

The remaining three terms in the equation for total strain all involve the same error. That is, all result from the uncertainty of values of strain obtained from the concrete's stress-strain curve. If the error in a point obtained from this curve is $\delta\varepsilon_s$, then the total error in ε_t may be written

$$\delta\varepsilon_t = \delta_C + 3\delta\varepsilon_s + \Delta q \qquad \text{...............(ii)}$$

For this approximate analysis, $\delta\varepsilon_s$ was taken to be the maximum deviation of an experimentally-obtained point from the least-squares curve of stress versus strain. Δq is the term due to all other inaccuracies in the computational methods. Δq could not be evaluated quantitatively. (The factors included in this term are discussed in the remainder of this chapter.)

The term δ_C was evaluated by taking values of δ_a and δ_b from the least-squares curves of "a" and "b" against elastic strain for the range of stress of interest. Again, the deviation of an experimentally-obtained point from the least-squares curve was assumed to give an approximate measure of the error involved. Using these values of δ_a and δ_b, δ_c was computed for specific values of a, b, and t.

The equation for $\delta\varepsilon_t$ represents an estimate of the maximum possible difference between the "true" total strain and the computed value. In this case, however, the "true" total strain is not known. Instead, the computed total strain is compared with the corresponding measured strain. If $\delta\varepsilon_t$ is to represent the difference between these values, further terms must be added to the right hand side of (ii).

The measured strains were obtained as differences. A reading was taken from a standard invar bar (s_1, say), and a second reading was taken from the gauge points fixed to the concrete (s_2 say). The difference between the two readings (s_2 - s_1) was recorded. The change between this value of (s_2 - s_1) and one recorded at a later date indicates the magnitude of additional strain.

If each reading is taken to be accurate to one half of one division on the scale, δ_D, then it is apparent that

$$s_1 - s_2 = s_1 \pm \delta_D - s_2 \pm \delta_D$$

Hence the maximum possible error in the quantity (s_1 - s_2) is $\pm$ $2\delta_D$, or one division. The strain at any time is obtained as the difference between (s_1 - s_2) and some "base" value (i.e. the reading obtained from the concrete before any load was applied). This "base" value is also a difference, and is also subject to a maximum error of $2\delta_D$. Therefore the maximum error in a measured strain is $\pm 4\delta_D$, or two divisions.

Thus

$$\delta\varepsilon_t = (3\delta\varepsilon_s + \delta\varepsilon_C + 4\delta_D) + \Delta q$$

As mentioned earlier, Δq represents the effects of those factors which could not be evaluated numerically. Considering only the remaining terms in the equation, values of $\delta\varepsilon_t$ were calculated for each eccentrically-loaded prism. Error lines representing the deviation of strains computed by the "element" method (using Ross's creep formula) from those measured in the laboratory were drawn. (The values of $\delta\varepsilon_t$ were computed for four points across the section. These points were then joined up to give an error "band"). These error lines appear in Figures 5.5 and 5.6 The error lines do not take into account all factors which affect the computed total strain values. While the values used for $\delta\varepsilon_s$ and $\delta\varepsilon_C$ are only approximations to the maximum possible errors involved, it is thought that the error lines do serve a useful prupose in indicating the probable degree of accuracy of the element method.

The formulations of test data used in computing the predicted strains are discussed in the next section.

4.3. Uncertainties in the Predicted Strains due to the Methods of Presenting the Data used in the Computed Solutions.

4.3.1. Variation of Concrete Strength and Stress-Strain Relation with Time

The concrete stress-strain relation obtained from instrumented cylinder tests performed at the time of first loading the creep prisms, was assumed to vary with time in the manner explained in Chapter 2.

This method is equivalent to "scaling-up" the ordinates (or stress values) on the stress-strain curve. All stress values are multiplied by the same factor for a given age of concrete. For example, for concrete at an age of 136 days (that is, after 100 days under load) the stress values are all multiplied by the factor 1.2. Therefore, the stress corresponding to any given strain at 136 days is 1.2 times the stress corresponding to the same strain at 36 days. A comparison of the elastic strain recovery of the concentric creep prisms (measured on off-loading) with the elastic recovery predicted using the above assumptions, showed that , in all cases, the predicted recovery was greater than that measured. The percentage error was not always the same, and increased with increasing stress. (The measured and computed strains appear in Table A-3-2 of Appendix III). This indicates that use of one factor for the entire stress strain curve is not completely realistic.

It is thought that a more accurate modification of the concrete stress-strain curve to account for increased age and strength could be devised. To do this, instrumented cylinders would be tested at various ages. An analysis of the changes in the shape of the stress-strain curve as a function of time could then be made. These changes could then be formulated in an equation which expressed the change in stress for a given strain as a function of strain and time. This equation would probably not be linear in elastic strain. (It is assumed in Chapter 2 that the relation is linear in elastic strain). A second degree function of elastic strain would probably be applicable. It is also likely that the equation would not be linear with time, as was assumed in Chapter 2. Data from a larger number of cylinder tests would allow formulation of a more realistic relationship.

The effect of sustained load on the "elastic" stress-strain relationship is more difficult to evaluate, although it is generally recognized that it will cause some change.

4.3.2. The Relationship of the Creep Constants to the Initial Elastic Strains.

Both the continuous and element methods require that the creep constants (from either the Ross formula or the Semi-log formula) be expressed as continuous functions of the initial elastic strain due to the applied load. For the Ross constants, "a" and "b", this requirement was satisfied, since the relationship could be approximated fairly closely by a curve of second degree in elastic strain. The Semi-log constants, "A" and "B", were not so suitable, as Fig. 3.8. shows. The constant "A" is especially unsatisfactory. Because of the scatter of the points, and because data for only four points was available, it was very difficult to express A realistically as a function of initial elastic strain. For elastic strains below that corresponding to a stress of 750 p.s.i., the shape of the "A" versue elastic strain curve is open to conjecture. Two choices are available.

(i) as ε_E approaches zero, the trend for A to decrease algebraically, shown by the experimentally-obtained points, continues.

(ii) as ε_E approaches zero, A also approaches zero. Theoretically, there should be zero creep at any time for zero applied stress.

i.e. for zero applied stress

$$C = A + B \log (T) = 0 \text{ , for any } T.$$

Therefore, $A = -B \log (T)$ for any T. Since A and B are not themselves functions of time, this implies that both A and B are zero for zero stress (i.e. $\varepsilon_E = 0$). This indicates that (ii) is the correct assumption to make.

The Semi-log formula, however, is not a theoretical law. It is an empirical formula devised to fit experimental data. It does not necessarily reflect observed creep behaviour perfectly at all levels of applied stress. In addition, it was found in a previous analysis[11] that the experimentally-obtained points did not appear to indicate that the values of A and B at $\varepsilon_E = 0$ should necessarily be zero. Accordingly, the second-degree curve used in the analysis was that which gave a least-squares fit of the four experimentally-obtained points. That is, the point $A = 0$ at $\varepsilon_E = 0$ was not included in the least-squares fit of the data. It is recognized that the values of A given by this equation for strains corresponding to stressed below 750 p.s.i. are thus doubtful. Owing to the lack of experimental data in this range, however, no other assumption could be made. As a check on the influence which this might have on the strains predicted by the continuous method, the element method had the Semi-log formula incorporated in it. The strains predicted by the three methods:

(i) continuous method using Semi-log formula

(ii) element method using Ross formula

(iii) element method using Semi-log formula.

are compared and discussed in Chapter 5. It is recommended that in future work, at least six concentric creep tests be performed in the range of stress of interest. This should give sufficient data to plot realistic curves of the creep constants against initial elastic strain.

4.3.3. The Method of Computing Creep under a Relief of Stress

An additional source of error in both methods is the way in which creep for varying stress is computed.

In the continuous method, it is assumed that creep under a relief of stress is of the same magnitude as creep under a stress increase. In actual fact, it is known to be markedly less. It would thus be expected that the creep recovery of those parts of the prisms undergoing a relief of stress would be overestimated by the continuous method. In other words, the total creep strains of parts undergoing relief of stress would be underestimated.

The superposition method of creep calculation used in the element method was known to overestimate creep for decreasing stress by ignoring creep recovery.

4.3.4. Other Factors Affecting the Computational Methods

(i) Number of Strips used in the Element Method.

Twenty strips were used in obtaining the computed strains. Previous studies involving the "element" method indicate that the errors incurred in dividing the member cross-section in this way are slight[11]. (It was found that very little difference in the computed answers was obtained by greatly increasing the number of elements). In the present investigation, solutions were obtained initially using twelve strips.

The differences in the total strains computed in this way compared to those obtained using twenty elements, were all in the region of one half of one percent.

(ii) The Effect of Assuming Conditions to Remain Constant over Finite Time Intervals.

Both creep and the concrete strength are continuous functions of time. In both methods of analysis, it is assumed that the elastic strain distribution across the member remains constant over the time interval considered.

In view of these factors, it is apparent that more accurate answers will result from the use of shorter time intervals. Ten-day intervals were used for both the element and continuous methods. A determination of the strains for prism E-1500 by the element method and using five-day intervals indicated that little gain in accuracy would result from consideration of shorter time intervals.

(iii) Errors Due to Computer Convergence Tolerances.

In both methods, strains were adjusted until the calculated and applied values of load and moment were within 1% of the known values. Owing to the assumption made regarding a first trial of total strain, the calculated loads and moments approached the "true" values from above, in each case. Thus, the accepted values of strain at the end of each time interval were slightly higher than the true values. This in turn would lead to high values of computed creep for the succeeding time interval. Trial runs of both programs with the convergence limit increased to 5% gave surprisingly little loss of accuracy (about 3% of the computed strains).

(iv) Error in Eccentricity of Eccentrically-loaded Prisms

It was assumed that the eccentricity of the applied loads did not vary with time due to creep deflection of the prisms. A calculation carried out to estimate roughly the deflection that would occur indicated that such deflection would be negligible. (The value for the prism under the greatest load was approximately 1% of the intended eccentricity. This error would not be equivalent to a 1% difference in the computed creep).

4.4. Discussion of Errors in Test Results Arising from Inaccuracies in Experimental Set-up.

There were several factors which, by nature of the experimental procedure, could influence the results obtained. It was not found to be feasible to make any numerical estimate of the discrepancies which these factors caused, since, unlike the errors involved in the computational process, their effects were difficult to evaluate realistically. Since the results of the various tests indicate consistent trends, and since the predicted creep values differ from those observed by a margin no greater than that which might reasonably occur due to computational error, it is thought that these factors, which are detailed below, probably had little effect on the test results.

(i) Accuracy of Forms

The forms used for casting the prisms were constructed so that each dimension was correct to a 1/32 of an inch. The breadth measured to the trowelled surface of some of the prisms was found to be in error by slightly more than this (the worst measured value was 1/20 of an inch).

The non-trowelled faces all had smooth regular surfaces.

(ii) Positioning of Load Seat Plates on Ends of Prisms

The seat plates were attached to the ends of the creep prisms using plaster of Paris. A straight edge and spirit level were used to help align the plates properly on the prism ends. The plates were 6 inch ± .003 in. square. It was thought that the effect of any unintentional eccentricity would be partly or wholly eliminated by the practice of averaging the strain readings. This does not apply, however, to misalignment of the load in the direction of the intended eccentricity. The maximum error in this case was likely to be 1/32 of an inch (the same as the accuracy of the forms).

(iii) Load Fluctuations and Load Cell Accuracy

It had been noted that the loads were not allowed to drop more than 5% below their intended value. The practice of applying an initial slight overload was adopted in order that the "time-average" load should be approximately correct.

After the termination of the tests, the load cells were recalibrated in the 120-kip capacity Tinius Olsen testing machine, as described in Chapter 2. The maximum error at working load was found to be 1.6% of the working load in the worst case. None of the loads, however, was indicated as being more than 3% from its nominal value during the last 90 days of the 137 day tests. In addition, any change in the "at load" readings of the load cells would most probably occur during this last portion of the test period. Thus, the total deviation of each load from its nominal level would be, at the worst, equal to (1.6 + 3)%, i.e. within the prescribed 5%.

The case of the load cell for the specimen E-1000 has been discussed in Chapter 2. It appears that this cell functioned satisfactorily until at least 40 days after the initial application of load. The analysis by both prediction methods was, therefore, restricted to this period.

(iv) Changes in Ambient Relative Humidity and Temperature.

The wax coating of the concrete specimen was intended to eliminate the effect of changes in atmospheric humidity during the best period. No allowance was made for the effect of changes in the atmospheric temperature. During the test period, the temperature in the test area varied only between 70°F and 80°F.

(v) Effect of Differential Drying of the Specimen between the Ages of 21 and 33 Days.

Drying out of the surface layers of the concrete between the time moist-curing ceased and the time of wax-coating could have set-up stresses in the concrete which might have influenced measured strains. It is thought that this was unlikely. In all cases, shrinkage and swelling of the unloaded prisms approximately cancelled each other out. It thus seemed unlikely that any major residual stresses remained.

CHAPTER 5

PREDICTED AND MEASURED CREEP OF THE ECCENTRICALLY-LOADED CONCRETE PRISMS

5.1. Introduction

In this chapter a comparison between test results and those calculated using the two prediction methods is presented. The redistributions of stress calculated by the two methods are also discussed. The two methods are compared and possible extensions of them are discussed.

5.2. The Results form the Eccentric Creep Tests

The test procedure for the eccentrically-loaded concrete prisms is discussed in Chapter 2.

Strain readings were taken from the gauge points located on the creep prisms. From each set of readings, a total strain distribution across the member was plotted. Such a strain distribution was obtained by fitting a best straight line through the experimentally-obtained points (i.e. through the points obtained from both sides of the specimen, as well as those from the tension and compression faces).

The total strain distributions obtained in this way are shown in Figures 5.1. and 5.2. for various times after application of the load. The extreme fibre strains given by these "best straight lines" were used in preference to actual measured values, since they should define the total strain more accurately. The actual readings of strain taken from the four eccentrically-loaded creep prisms appear in Tables A-3-3 and A-3-4 of Appendix III.

Figures 5.1. and 5.2. show that in all cases the strain gradient across the member increases with time. In addition, the

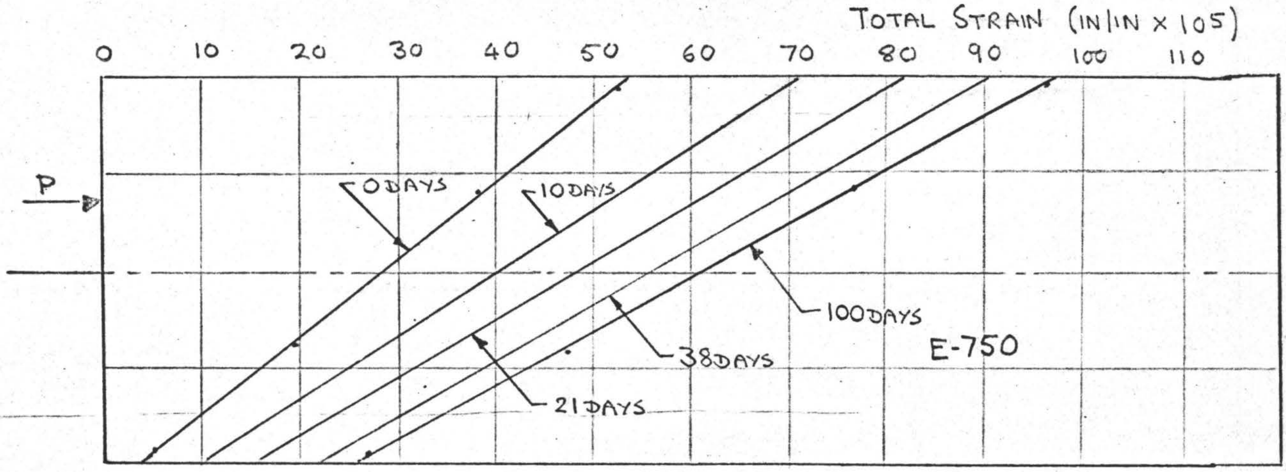

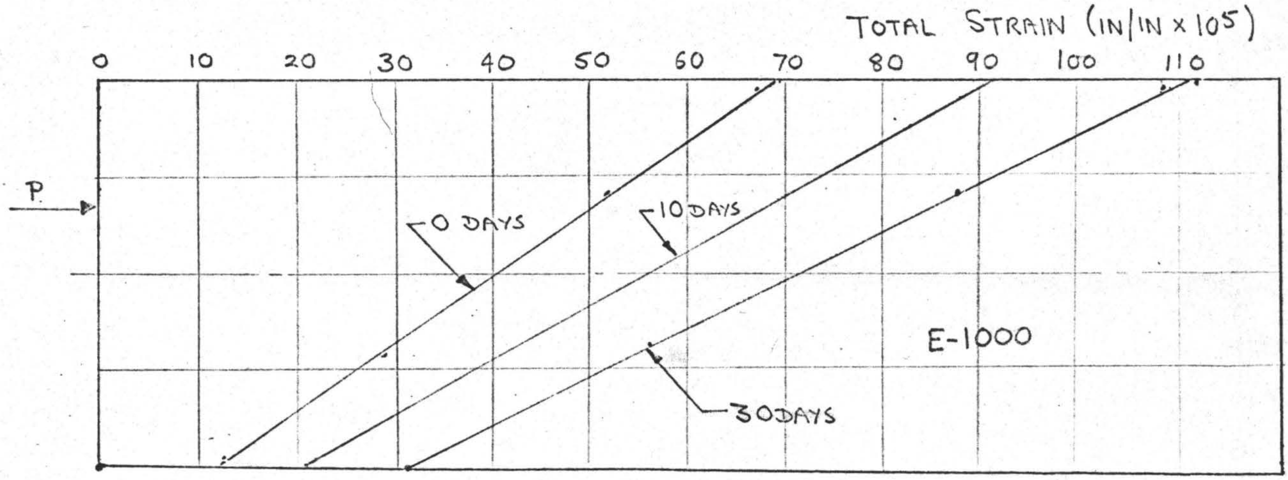

Fig. 5.1. STRAIN DISTRIBUTIONS OF E-750 AND E-1000 AFTER VARIOUS PERIODS UNDER LOAD.

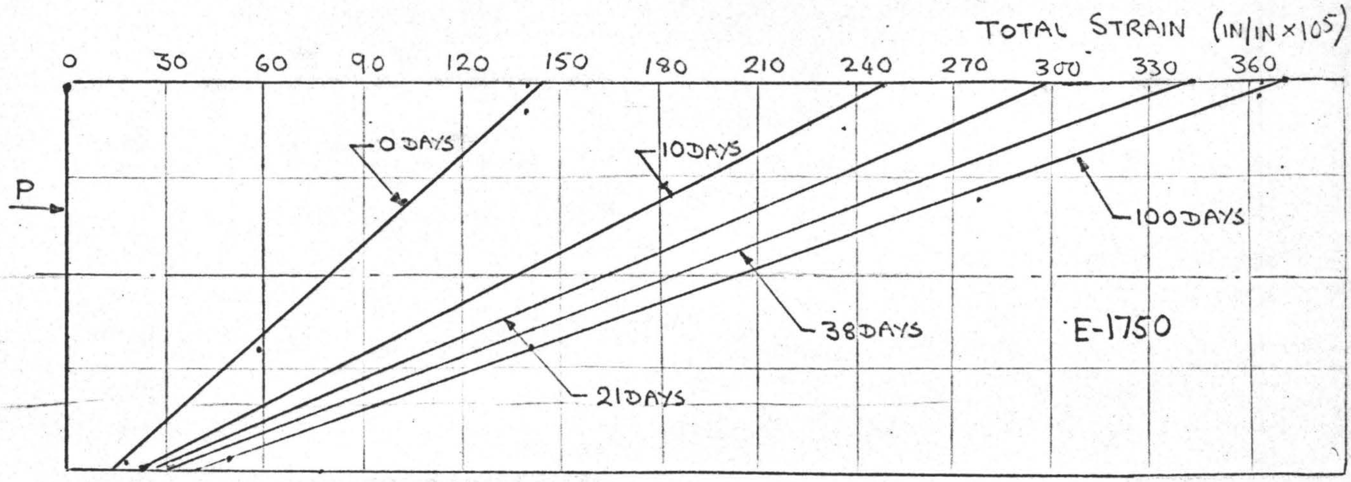

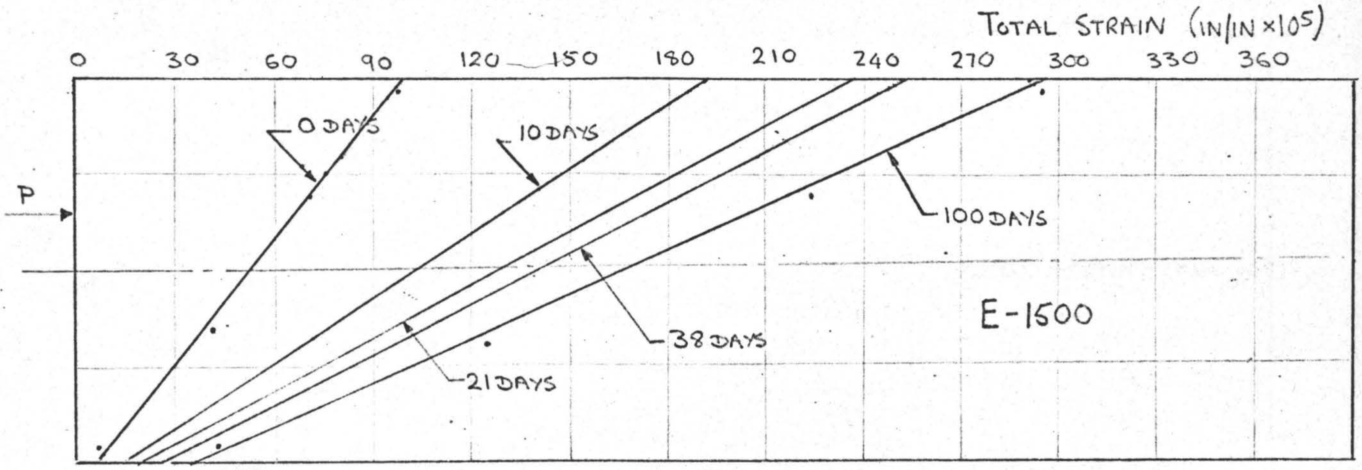

Fig. 5.2. STRAIN DISTRIBUTIONS OF E-1750 AND E-1500 AFTER VARIOUS PERIODS UNDER LOAD.

rate of increase of strain gradient is higher for higher values of average stress.

5.3. Prediction of Effects of Eccentric Creep

Initially, two methods were used to predict the effects of creep of the four eccentrically-loaded prisms. These were (i) the element method, incorporating the Ross creep formula, and (ii) the continuous method, incorporating the Semi-log creep formula. Later in order to determine the effect on accuracy of using the Semi-log formula, it was also used in the element method in place of the Ross formula. In this second form, the element method is referred to as the "element (ii)" method. In its original form, the element method is referred to as the "element (i)" method. All three methods adopted a standard ten day interval for prediction of the creep effects. It is therefore implicitly assumed that the elastic strain distribution is constant over each ten day period.

5.3.1. Predicted Strains

The extreme fibre creep strains predicted by all three methods are shown in Figures 5.3. and 5.4. These values were obtained as output from the FORTRAN computer programs run for each method. The observed extreme fibre creep strains are also shown, for comparison purposes. The four sets of total strains are tabulated in Tables 5.1. and 5.2. The abbreviations used in this table are as follows:

"O" denotes observed strains (from the "best straight lines" mentioned in 5.1.)

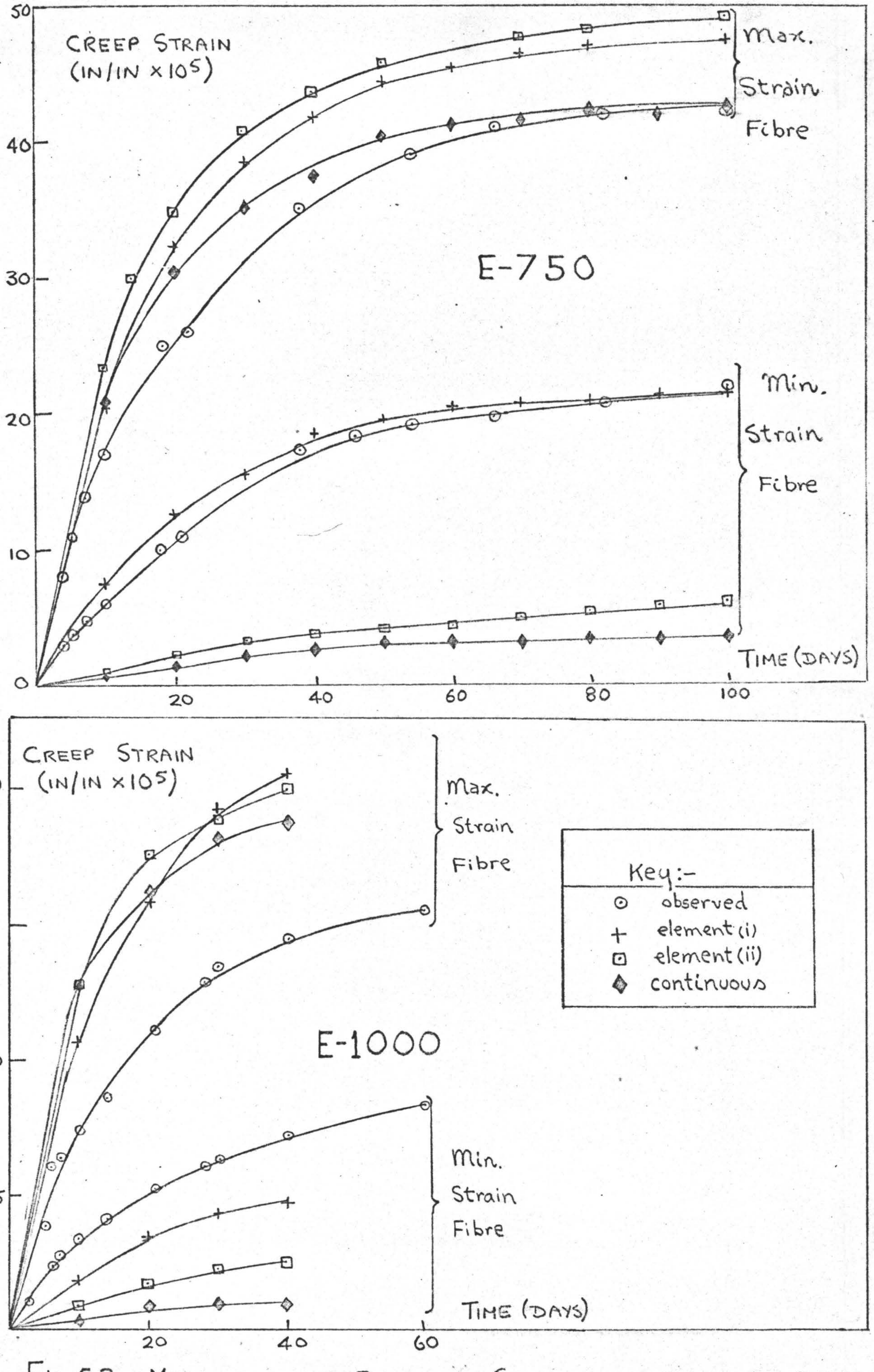

Fig. 5.3 MEASURED AND PREDICTED STRAINS FOR E-750 AND E-1000

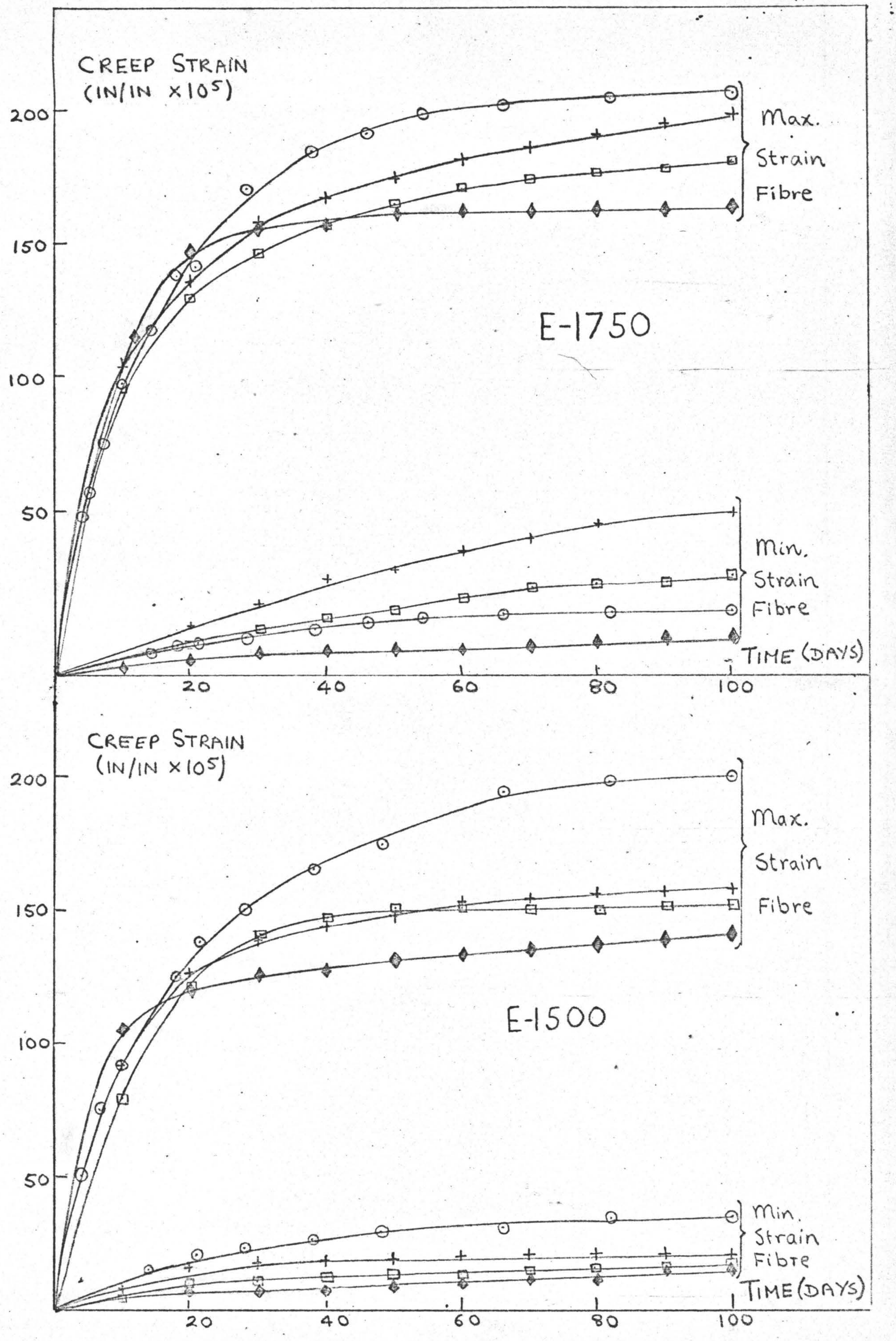

Fig. 5.4 MEASURED AND PREDICTED STRAINS FOR E-1500 AND E-1750

"E(i)" denotes strains predicted by element (i) method
"E(ii)" denotes strains predicted by element (ii) method
"CTS." denotes strains predicted by the continuous method
"C" denotes maximum compression fibre strains
"T" denotes minimum compression fibre strains

The element (i) method gives the best agreement with the observed strains in all but two of the plots. For the minimum compression fibre of specimen E-750, the predicted creep strain is so close to that obtained from the experimental results, that the two plots practically overlap. From the other plots, it appears that the margin of error at the maximum compression fibre stays constant or diminishes slightly from about 50 days onward.

The creep strains at the maximum compression fibres predicted by the continuous method, although generally lower than those obtained using the element (i) method, are reasonably close to those observed. For the maximum compression fibre of E-750, in fact, the continuous method gives a particularly good prediction of creep strain. For the minimum compression fibres, however, the continuous method always gives the lowest predicted strains. For E-750 and E-1000 in particular, these predicted strains are much lower than those observed. It was thought that this discrepancy was due to the uncertainty of the Semi-log constants "A" and "B" for low values of elastic strain. This suspicion was confirmed by the results of the element (ii) method, which show similarly low values of minimum compression strain.

The total strain distributions predicted by the element (i) and continuous methods for the prisms E-750, E-1500 and E-1750 after 100 days under load, and for E-1000 after 30 days under load, are plotted in Figures 5.5. and 5.6. The element (ii) method strain distributions are omitted for the sake of clarity. The error bands for the element (i) method have been included in the graphs. (The derivation of these error bands is described in Chapter 4). It can be seen

Time (days)	E-750								E-1000							
	Face "C"				Face "T"				Face "C"				Face "T"			
	0	E(i)	E(ii)	CTS	0	E(i)	E(ii)	CTS	0	E(i)	E(ii)	CTS	0	E(i)	E(ii)	CTS
0	54.0	53.6	53.6	50.7	4.0	8.2	8.2	8.9	69.0	72.0	72.0	66.2	12.0	11.3	11.3	9.1
10	72.0	74.0	77.8	71.6	10.0	15.8	9.5	9.1	92.0	103.6	103.6	104.3	21.0	16.7	14.0	9.7
20	80.0	85.1	88.5	81.2	15.0	21.1	10.4	10.3	101.0	120.8	124.5	115.0	26.0	21.4	16.1	10.8
30	85.0	92.2	94.6	85.8	19.0	23.9	11.3	11.1	111.0	129.2	128.2	121.0	31.0	24.1	17.6	11.5
40	90.0	95.7	97.1	89.0	21.0	25.6	12.1	11.6	113.0	135.1	131.8	123.8	33.0	25.6	18.7	11.7
50	92.0	97.8	98.7	91.1	23.0	26.7	12.3	12.0								
60	94.0	99.0	100.3	91.9	24.0	27.4	12.4	12.0								
70	95.0	100.1	101.0	92.2	24.0	27.9	13.1	12.1								
80	96.0	100.7	101.6	92.9	25.0	28.2	13.4	12.3								
90	96.0	101.1	102.3	92.7	25.0	28.4	13.9	12.4								
100	97.0	100.6	102.5	93.1	25.0	28.9	14.3	12.5								

Strains in in/in x 10^5

TABLE 5.1. COMPARISON OF OBSERVED AND PREDICTED TOTAL STRAINS FOR E-750 and E-1000

Time (days)	E-1500								E-1750							
	Face "C"				Face "T"				Face "C"				Face "T"			
	0	E(i)	E(ii)	CTS	0	E(i)	E(ii)	CTS	0	E(i)	E(ii)	CTS	0	E(i)	E(ii)	CTS
0	101.0	110.1	110.1	107.0	6.0	15.5	15.5	11.2	145.0	134.5	134.5	129.9	14.0	14.8	14.8	12.3
10	188.0	201.5	189.7	211.0	16.0	23.6	19.8	15.1	257.0	251.0	242.3	257.9	21.0	25.7	21.4	15.2
20	232.0	237.4	229.8	226.1	23.0	24.7	25.5	17.0	292.0	282.5	276.9	296.9	26.0	34.0	26.8	19.2
30	252.0	248.2	250.9	231.4	28.0	33.0	26.6	18.3	326.0	304.1	291.8	304.9	28.0	41.0	32.0	20.9
40	270.0	253.9	257.1	234.1	29.0	34.1	27.4	18.6	343.0	314.7	302.9	306.9	31.0	50.6	37.1	22.1
50	279.0	259.2	259.5	239.0	30.0	35.0	28.7	19.6	353.0	321.6	311.4	310.9	33.0	54.7	40.1	22.4
60	289.0	262.4	259.7	241.2	32.0	35.8	29.3	21.5	358.0	328.6	317.3	311.9	34.0	61.8	44.2	23.0
70	295.0	263.5	259.8	242.6	32.0	36.0	30.4	22.4	361.0	333.4	321.6	312.8	35.0	65.6	47.9	24.9
80	298.0	265.5	259.9	245.1	33.0	36.6	30.6	23.7	363.0	338.4	324.4	322.1	36.0	72.3	49.6	25.2
90	299.0	266.6	260.2	247.3	34.0	36.9	31.6	25.4	364.0	342.1	326.3	323.2	38.0	75.9	51.7	25.4
100	300.0	267.3	260.9	249.2	35.0	37.2	33.1	25.7	372.0	346.2	328.5	323.3	39.0	82.2	52.9	25.8

Strains in in/in x 10^5

TABLE 5.2. COMPARISON OF OBSERVED AND PREDICTED TOTAL STRAINS FOR E-1500 and E-1750

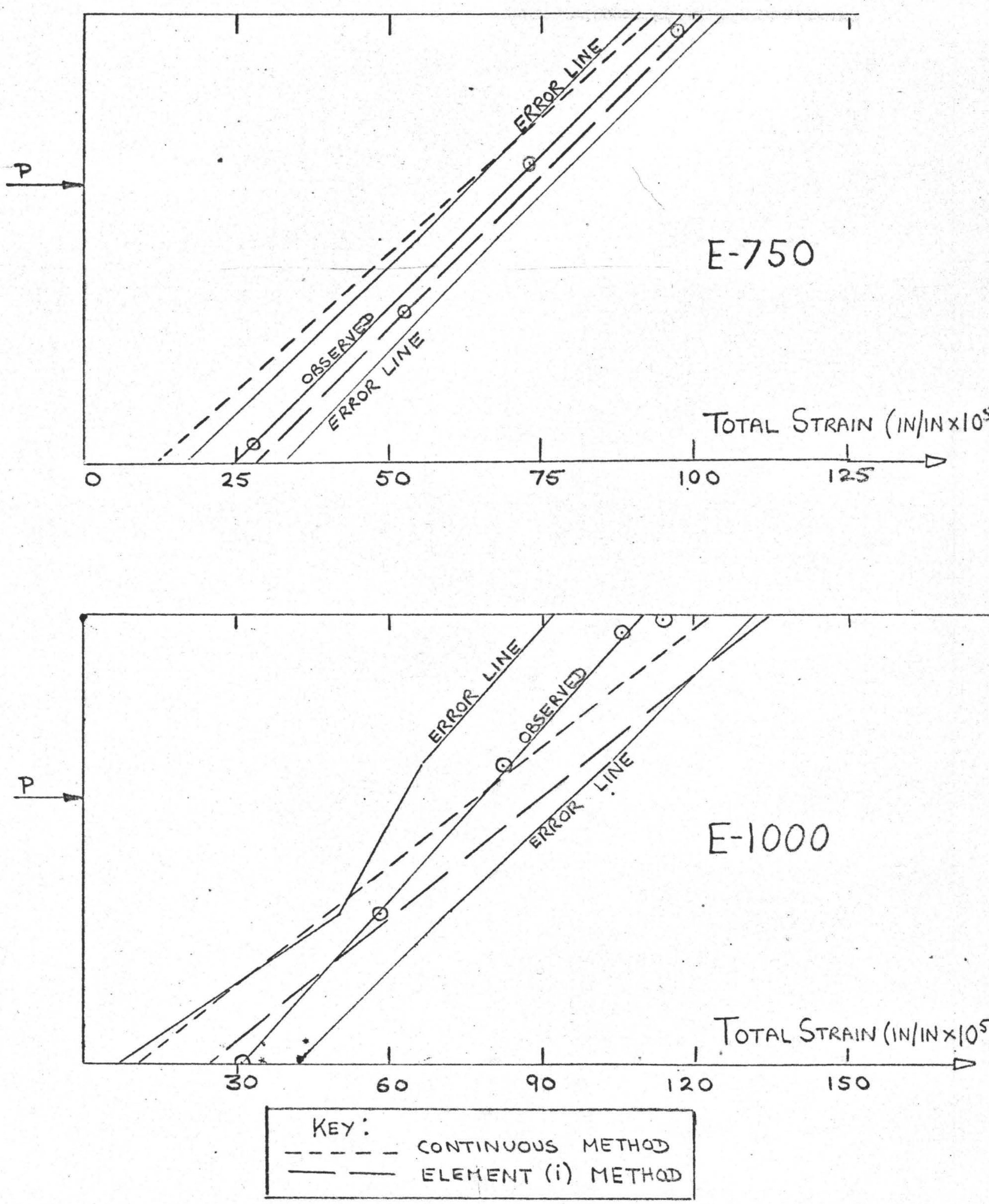

Fig. 5.5. OBSERVED AND PREDICTED TOTAL STRAINS AFTER 100 DAYS UNDER LOAD FOR E-750 AND AFTER 40 DAYS FOR E-1000

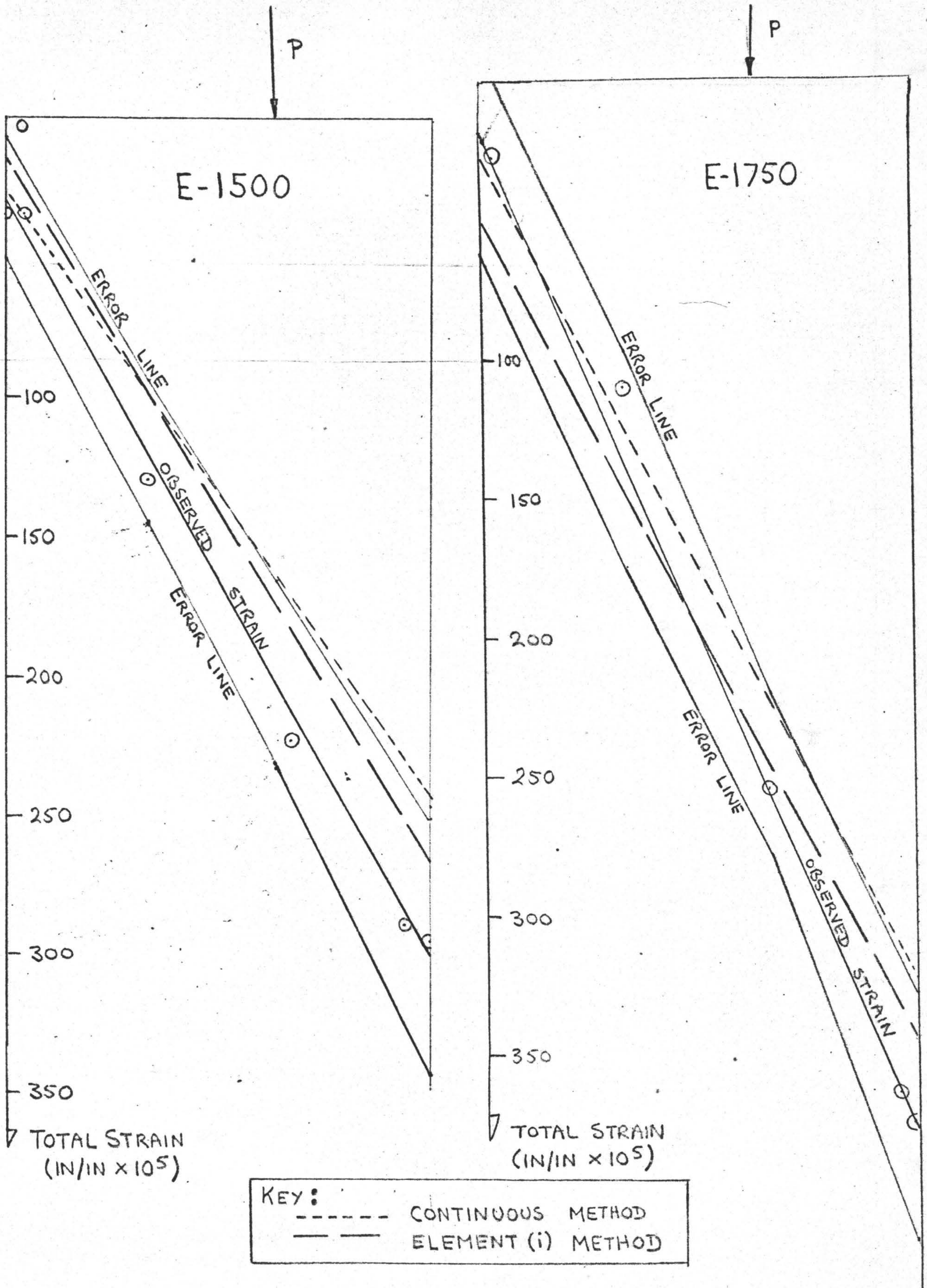

Fig. 5.6. OBSERVED AND PREDICTED TOTAL STRAINS AFTER 100 DAYS UNDER LOAD FOR SPECIMENS E-1500 AND E-1750

the distributions given by the continuous method fall outside the error bands, indicating the lower general accuracy of this method. Because of the difficulty in assigning a realistic value to the errors in the Semi-log constants, "A" and "B", no error bands were included for the continuous method.

5.3.2. Predicted Redistribution of Stress

The redistribution of stress, which accompanies creep of concrete under non-uniform stress, is of interest. Both the element and continuous methods can be used to obtain the stress distribution across a member at any given time after initial application of the load. The continuous method computes the coefficients which define the equation of the stress distribution as a part of its load balancing procedure. The element method computes the elastic strain on each element, and this value is easily converted to stress within the program.

The stress distributions at the time of first load, as computed by the element method, are shown for all specimens in Figures 5.7. and 5.8. The stress distributions computed by both the element (i) and continuous methods for specimens E-750, E-1500 and E-1750, after 100 days under load are also shown in the figures. For the specimen E-1000, the initial stress distribution, and the distribution after 40 days under load are shown in Figure 5.8. Both of these distributions were computed by the continuous metood. (In this case, the computed redistribution is slight by both methods, and the element (i) method solution is omitted for clarity).

In all cases, the transfer of stress from the extreme fibres into the interior of the prism is evident.

5.4. Discussion of the Prediction Methods

Both the continuous and element methods can effectively carry out the same calculation for total strain and stress distributions of a member subjected to sustained non-uniform stress. The discrepancies in

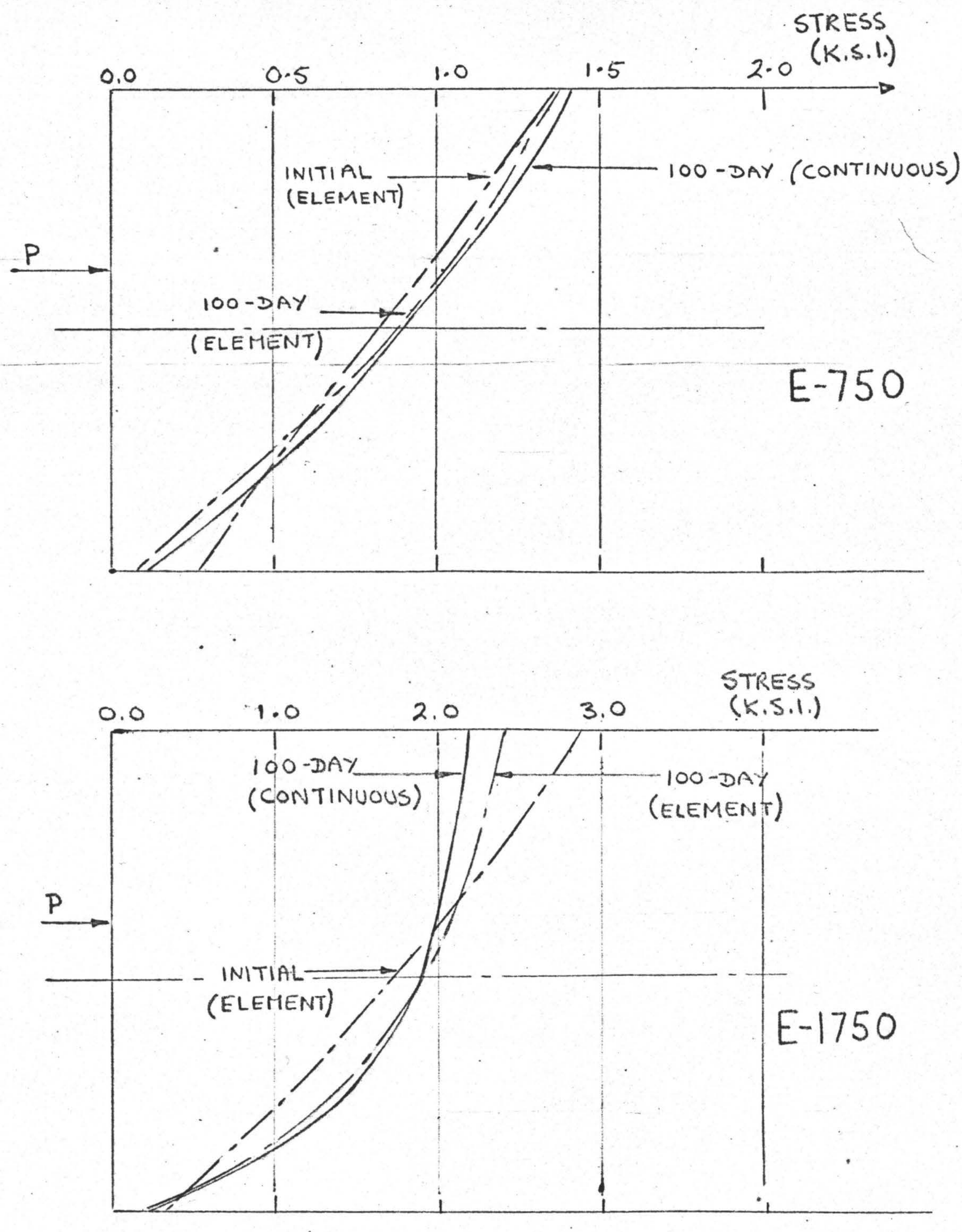

Fig. 5.7. STRESS DISTRIBUTIONS ON INITIAL LOADING AND AFTER 100 DAYS UNDER LOAD FOR SPECIMENS E-750 AND E-1750

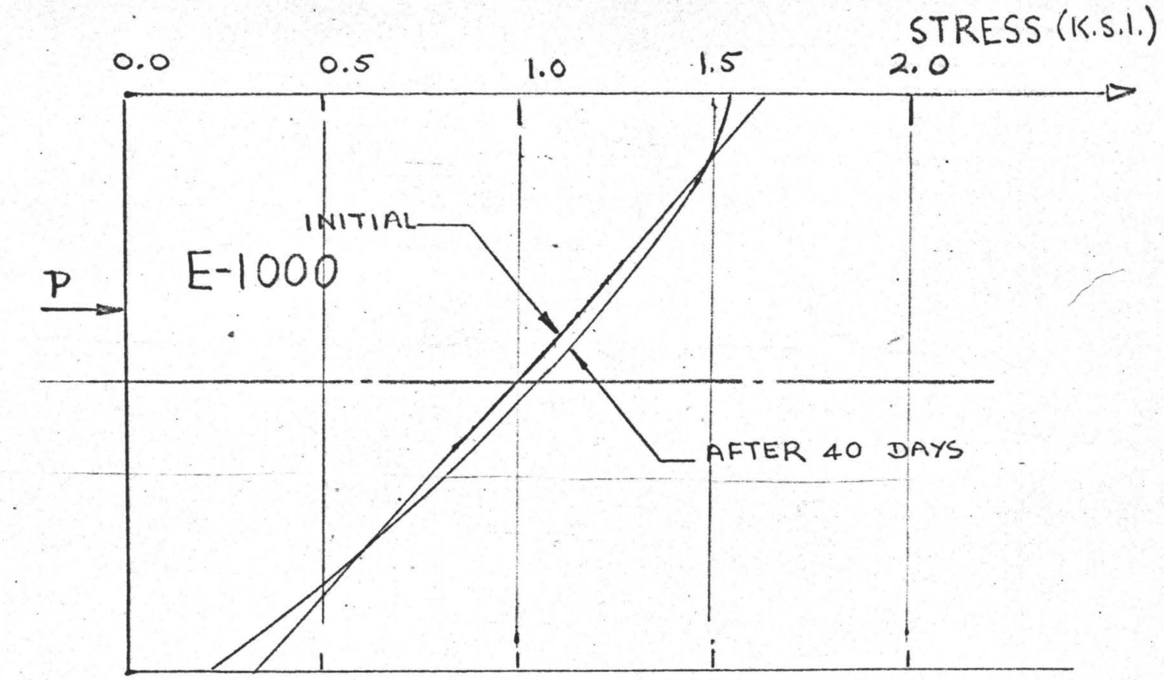

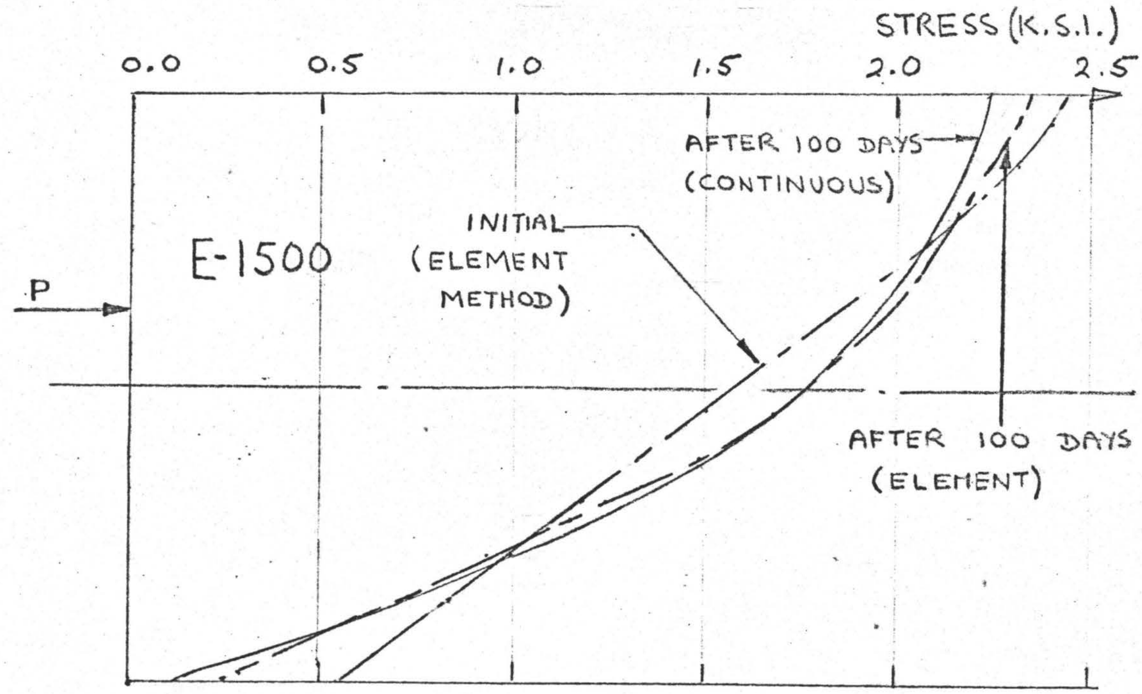

Fig. 5.8. STRESS DISTRIBUTIONS ON INITIAL LOADING AND AFTER SOME TIME UNDER LOAD FOR SPECIMENS E-1000 AND E-1500

certain values of strain predicted by the continuous method appear to be largely due to uncertainty of the values of the Semi-log creep constants "A" and "B", for low values of elastic strain. Thus, this lack of accuracy is not a defect of the continuous method, but merely an indication that more concentric creep data is needed to accurately express "A" and "B" as functions of elastic strain.

Both the continuous and element methods possess useful flexibility in that they can handle any number of time intervals. This means that variations in applied load and moment can be dealt with easily. The new values of load and moment are simply identified at the desired time, and the creep and elastic strains are altered accordingly in the subsequent time interval.

It had been intended to take into account the initial overload of the prism E-1750. The Ross and Semi-log plots, however, only give a good fit of the creep data for periods of ten days or more under load. Thus the effect of the initial overload, followed by load reduction four days later, could not be predicted by either of the two methods. If a major change in applied load or moment had occurred at some later time, it could have been taken into account quite easily by either method.

Another useful feature of both methods is that a member's cross-section properties can be altered in the course of the analysis. In the element method, the process is especially simple, since computations are carried out for each individual element. If the strain distribution across the member indicates that a particular element is in tension, then the force and moment contributions of that element can be set to zero.

(Or if it is assumed that the concrete can take some tension, an appropriate value of tensile force can be used). For the continuous method, it would be necessary to solve the equation for elastic strain (i.e. find at what value of x, xy say, elastic strain was zero). If the concrete can take no tension, the calculation will then proceed as before, but with a new section width, equal to (w - xy) instead of w.

This ability to deal with varying section properties would be useful when considering members under-going sustained loading to failure, since their cross-sections frequently develop cracks. It is cautioned, however, that the method of assuming a "first trial" value of the total strain at the end of a time interval would need to be changed for problems involving members approaching failure. As already noted in Chapter 3, this first approximation gives a computed load which is greater than the true value. Under near-failure conditions, the computed load would fail to converge in the load-balancing procedure. In such cases, it is necessary to change the first assumed value of total strain so that the computed load is less than the known applied load. The simplest way of doing this is to use as a first trial the total strain distribution from the previous time interval. For either method, this modification is quite simple. For the plain concrete prisms considered here, however, this assumption would cause a waste of computer time, since it represents a bad "first trial" value. This, in turn, necessitates more load-balance cycles before convergence is obtained.

Both methods can be adapted to handle problems involving members with steel reinforcement. Such a version of the element method is already in existence. (see reference 11)

In the continuous method, knowing (or assuming) a strain distribution across a reinforced concrete member permits the strain at the level of the steel to be determined. Hence, the stress in the steel can be computed. PCAL and BMCAL would then include terms representing respectively the load and moment contributions of the reinforcing steel.

The simple modifications necessary to take account of reinforcing steel are therefore not extensive.

The FORTRAN computer programs for both methods were run on the IBM 7040 computer at the McMaster Computer Centre. Typical times for the two programs, with each using ten time intervals, were as follows:

"Element" method	2 min. 41 sec.
"Continuous" method	2 min. 58 sec.

The continuous method, however, was more economical in storage space than the element method. In a typical run, the continuous method used 3402 locations, compared to 4036 locations for the element method.

CHAPTER 6

CONCLUSION

6.1. Introduction

An investigation was conducted into the effects of creep of concrete under non-uniform stress. An important feature of creep in such cases is that due to the non-linearity of the creep-stress relation, a redistribution of stress takes place. This effect is important in practice.

The purpose of the investigation was to devise and test methods of predicting the time-dependent strains and stresses in members subjected to sustained non-uniform stresses. The investigation included both experimental and theoretical work.

6.2. The Experimental Program

In the experimental program, four plain concrete prisms were subjected to different sustained concentric loads. This set of tests was used to provide data for use in the application of the theoretical approach. Four identical prisms were subjected to different sustained eccentric loads. It was intended that the strains of these prisms be compared with those predicted by the theoretical approach.

A record was kept of the prisms' strains over a period of four and a half months. Additional information was required for use in the theoretical approach. This information consisted of

(i) the concrete stress-strain relationship

(ii) the concrete strength

(iii) the manner in which (i) and (ii) changed with time

(iv) non-load induced strain changes produced in the prisms

(i), (ii), and (iii) were provided by tests of standard concrete cylinders, some of which were instrumented in order that the concrete's stress-strain curve might be obtained.

(iv) was obtained by measuring the strains on unloaded prisms (identical to the creep prisms) placed in the test area.

In view of the many factors which can influence the measured creep of concrete, efforts were made to ensure similarity in the concrete test prisms and cylinders, and consistency in the test procedure. To this end, all of the concrete specimens were made using the same concrete mix. All the creep test prisms and the companion unloaded prisms had the same dimensions. Forms were carefully checked for accuracy. To eliminate the effect of varying atmospheric humidity on the test results, all of the concrete specimens were sealed by wax-coating at the same age.

6.3. Theoretical Approach

The purpose of the theoretical approach was to devise a procedure by which the distributions of total strain and of stress across a plain concrete prism subjected to sustained eccentric load could be predicted. Such a procedure would provide the basis for a method which could provide the same information for reinforced concrete members. Two methods were presented:

(a) an "element" method, which considers the eccentrically-loaded member as an assembly of smaller concentrically-loaded elements, held together according to the condition that plane cross-sections must remain plane. This method was a modification of a technique already in existence.

(b) a "continuous" method, which deals with the member cross-section as one unit. This method considers the mathematical functions representing stress, creep strain and total strain distributions. To the author's knowledge, such a method had not been presented before.

Both methods used the data listed in (i) to (iv), plus the results of the concentric creep tests, to arrive at a solution. For each method, a computer program was written to calculate the strain and stress distributions of the eccentrically-loaded prisms at any time after the application of the loads. In both cases, the predicted total strains were reasonably close to the measured values. A lack of accuracy in some of the solutions given by the continuous method was found to be due to a method of representing the creep data. This, in turn, was caused by a lack of sufficient data for creep under low stresses.

6.4. Uses of the Prediction Methods and Suggestions for Further Research

Both of the methods possess useful flexibility in that they can deal with fairly complex problems involving variations of the applied load and/or moment with time. In addition, both can be modified fairly easily to deal with members having steel reinforcement. It is cautioned, however, that the method of formulating the data used by both methods affects the accuracy of the computed answers. In order that such formulations be as realistic as possible, an extensive range of back-up tests is required. In particular, a comprehensive set of concentric creep tests, covering the stress range of interest is required.

In order to make results obtained from one test program applicable to other situations, it would be necessary to determine quantitatively the effect of such variables as member size and shape, and atmospheric conditions. In addition, some more accurate method of predicting creep recovery would be desirable, since present methods are known to be only approximate. Research along these lines would allow a wider application of the two prediction methods presented here.

6.5. Resume

The problem of predicting the stresses and strains in a plain concrete member subjected to sustained non-uniform stress was investigated. Two theoretical approaches, using experimentally-obtained data, were applied to the problem. Both were found to give satisfactory answers, and both can be easily modified for use with reinforced concrete members. A fairly large amount of test data is required for both methods. This includes information on the concrete's strength, stress-strain relation, and shrinkage characteristics, as well as results from creep tests under uniform stress. The methods are at present applicable only to situations in which such data are available.

APPENDIX I

THE FORTRAN PROGRAM FOR THE ELEMENT METHOD

Names of Variables:

The meanings of the variables named in the program are listed below. Any other variables are either defined in Chapter 3, or by the context in which they appear.

BAX	Applied bending moment
BMXCAL	Calculated bending moment
CYL	Concrete cylinder strength
ISEC	Iteration limit for load-balance cycles
M	Number of elements
P	Applied load
PCAL	Calculated load
CPEEP(J)	Total creep on a particular cross-section element
T_1, T_2	Times defining an increment of time
UC, UT	Extreme fibre strains
U(J)	Total strain on a particular cross-section element

SUBROUTINES:

ALOAD	Calculation of the internal force on a cross-section
CREEP	Calculation of creep during a time interval
XMOM	Calculation of internal bending moments

FUNCTIONS:

CONCF	Concrete stress-strain formula
A, AA, B, BB	Ross creep co-efficients

```
$JOB    WATFOR  003336 GRAY D C
$IBFTC
C        PROGRAM FOR PREDICTION OF CREEP OF CONCRETE UNDER
C        A STRESS GRADIENT
C     MODIFIED VERSION OF PROG FOR SUSTAINED LOADING OF LONG
C       COLUMNS DEVELOPED BY DR DRYSDALE
        DIMENSION DELX(40),DX(40),U(40),UU(10,40),CPEEP(40),PEEP(10,40)
       1 UE1(40),UUE1(10,40)
  401 READ(5,402) P,DPP,CYL,XCECC,ISEC,M,UC,UT
      WRITE(6,402)P,DPP,CYL,XCECC,ISEC,M,UC,UT
  402 FORMAT (4F10.3,2I3,2F12.5)
      READ(5,504) TIMIT
  504 FORMAT(F10.3)
      COMMON UC,UT
      FCII=CYL
      T0=0.0
      T1=0.0
      T2=0.0
      N=1
      DO46 J=1,M
      PEEP(N,J) =0.0
   46 CONTINUE
       DO 48 J=1,M
      CPEEP(J)=0.0
   48 CONTINUE
      GO TO 436
  711 P=P+DPP
        WRITE (6,707) P
  707 FORMAT(5X,F10.2)
      GO TO 436
  702 READ(5,703) T2,P,DECIDE
  703 FORMAT(3F10.2)
      WRITE(6,704) T1,T2,P
  704 FORMAT(10X,2F10.2,10X,F10.2)
      CALL CREEP(T0,T1,T2,U,UU,CPEEP,PEEP,M)
      IF (T2-120.) 10,10,11
   11 CYL=FCII*1.15
      GO TO 436
   10 CYL=FCII*(1.0+0.15*T2/120.)
  436 ZX=0.0
      LP=0
  437 LP=LP+1
      CALL ALOAD(UC,UT,PCAL,P,M,CPEEP,T2,U,CYL)
      CALL XMOM(UC,UT,BMXCAL,BAX,XCECC,ZX,P,M,CPEEP,T2,U,CYL)
      PERROR=ABS(P-PCAL)/P
      XBMER=ABS(BAX-BMXCAL)/BAX
      IF(PERROR-0.05) 206,206,205
  206 IF(XBMER-0.10) 180,180,205
  205 IF(LP-ISEC) 437,207,207
  207 CONTINUE
      WRITE (6,404)
  404 FORMAT(10X,17HNO GO-P TOO LARGE//   )
      GO TO 699
  180 WRITE(6,190)XCECC,PCAL,P,BMXCAL,BAX,UC,UT
  190 FORMAT(F10.3,4F10.2,2F9.3)
      GO TO 43
  699 WRITE(6,700)
  700 FORMAT(10X,23HCREEP BUCKLING OCCURRED//)
```

```
      WRITE (6,800) PCAL
  800 FORMAT(6H PCAL=,F10.3)
      WRITE(6,801) T2,LP
  801 FORMAT(4H T2=,F5.1,4H LP=,I3)
      GO TO 401
   43 IF (T2-TIMIT) 715,13,13
  715 GO TO 702
   13 GO TO 401
      END
$IBFTC ALOAD
      SUBROUTINE ALOAD(UC,UT,PCAL,P,M,CPEEP,T2,U,CYL)
      DIMENSION U(40),CPEEP(40)
      DM=M
      PCAL=0.0
      DO 200 J=1,M
      DJ=J
      U(J)=UC-(DJ-0.5)/DM*(UC-UT)
      W=U(J)-CPEEP(J)
      WRITE(6,40) J,W
   40 FORMAT(10H FOR EL NO,I2,14H ELASTIC STRN=,F9.3)
  203 PCAL=PCAL+36./DM*CONCF(W,CYL)
  200 CONTINUE
  141 UP=ABS(UC-UT)*(P-PCAL)/(8.*P)
  140 UC=UC+UP
      UT=UT+UP
      WRITE(6,20)
   20 FORMAT(13H ALOAD CALLED)
      WRITE(6,30) PCAL
   30 FORMAT(6H PCAL=,F10.3)
      RETURN
      END
$IBFTC XMOM
      SUBROUTINE XMOM(UC,UT,BMXCAL,BAX,XCECC,ZX,P,M,CPEEP,T2,U,CYL)
      DIMENSION U(40),CPEEP(40)
      DM=M
      BMXCAL=0.
      DO 210 J=1,M
      DJ=J
      U(J)=UC-(DJ-0.5)/DM*(UC-UT)
      W=U(J)-CPEEP(J)
      IF (W-1.) 209,213,213
  209 GO TO 210
  213 BMXCAL=BMXCAL+36./DM*(3.-(DJ-0.5)/DM*6.)*CONCF(W,CYL)
      WRITE(6,55) BMXCAL
   55 FORMAT(8H BMXCAL=,F12.3)
  210 CONTINUE
      BAX=P*XCECC
  171 UMX=ABS(UC-UT)*(BAX-BMXCAL)/(8.*BAX)
  158 UT=UT-UMX
      UC=UC+UMX
      RETURN
      END
$IBFTC CREEP
      SUBROUTINE CREEP(T0,T1,T2,U,UU,CPEEP,PEEP,M)
      DIMENSION U(40),UU(10,40),PEEP(10,40),CPEEP(40),UE1(40),
     1   UUE1(10,40)
      COMMON UC,UT
      IF (T1) 61,61,62
```

```
   61 DO 52 J=1,M
      CLU=U(J)
   64 CPEEP(J)=T2/(A(CLU)+B(CLU)*T2)
   58 UE1(J) =CLU
      U(J)=CLU+CPEEP(J)
   52 CONTINUE
      GO TO 55
   62 DO 54 J=1,M
      CLU=U(J)-CPEEP(J)
   66 OLDU=CLU-UE1(J)
      IF (OLDU) 96,96,97
   96 CROLD=0.0
      GO TO 98
   97 CROLD=(T1-T0)/(AA(OLDU)+BB(OLDU)*(T1-T0))
   98 CPEEP(J)=CPEEP(J)+(T2-T1)*A(CLU)/(A(CLU)+B(CLU)*T1)**2.
     1+CROLD
   59 UE1(J)=CLU
   54 U(J)=CLU+CPEEP(J)
   55 T0=T1
      T1=T2
      UC=U(1)-0.5*(U(2)-U(1))
      UT=U(12)+0.5*(U(12)-U(11))
      RETURN
      END
$IBFTC CONCF
      FUNCTION CONCF(W,CYL)
C      QU=STRAIN IN IN/IN*10**-4
      QU=W/10.0**2.
      CONCF=(CYL/4.253)*(-0.36848/10.0**2.+0.25857*QU-(0.76875/10.0**
     1 *QU**2.-(0.24895/10.0**3.)*QU**3.+(0.49157/10.0**5.)*QU**4.)
      RETURN
      END
$IBFTC A
      FUNCTION A(CLU)
      FL=CLU/100.
       A=.79890-0.12568*FL+.49846/100.*FL*FL
      A=A/10.
      RETURN
      END
$IBFTC B
      FUNCTION B(CLU)
      FL=CLU/100.
       B=0.42394-0.58099E-01*FL+0.21345E-02*FL*FL
      B=B/100.
      RETURN
      END
$IBFTC BB
      FUNCTION BB(OLDU)
      FL=OLDU/100.
      BB=0.42394-0.58099E-01*FL+0.21345E-02*FL*FL
      BB=BB/100.
      RETURN
      END
$IBFTC AA
      FUNCTION AA(OLDU)
      FL=OLDU/100.
      AA=.79890-0.12568*FL+.49846/100.*FL*FL
      AA=AA/10.
```

```
      RETURN
      END
$ENTRY
                                        CD TOT    0177
```

APPENDIX II

THE CONTINUOUS METHOD

2A-1 Extension of the Unmodified Continuous Method to Three Time Intervals

The following continues from the working for the first two time intervals described in section 3.3.2.

Recall that at the end of the second time interval the elastic strain distribution was given by

$$\varepsilon_E = -q_1x^4 + q_2x^3 + s_1x^2 + s_2x + s_3$$

As for the second time interval, the creep for the third time interval is given by an expression of the type

$$\Delta C = B\gamma$$

where $\gamma = \log_e T_3 - \log_e T_2$, in which T_3 is the time at the end of the third intefval.

Since $B = f\varepsilon_E^2 + g\varepsilon_E + h$, and putting $z_1 = -q_1$, it can be shown that

$$\Delta C = \gamma\left(\sum_{i=0}^{8} \phi_i . x^i\right)$$

where $\phi_0 = s_3^2f + s_3g + h$

$\phi_1 = s_1g + 2s_3s_2$

$\phi_2 = s_2^2f + sfs_1s_3 + s_1g$

$\phi_3 = q_2g + 2fs_3q_2 + 2s_2s_1f$

$\phi_4 = 2fs_3z_1 + 2fs_2q_2 + fs_1^2 + gz_1$

$\phi_5 = 2fs_1q_2 + 2fs_2z_1$

$$\phi_6 = 2z_1s_1f + q_2^2f$$

$$\phi_7 = 2fz_1q_2$$

$$\phi_8 = fz_1^2$$

Let the new total strain at the end of the third interval be given by

$$\varepsilon_t = a'''x + b'''$$

The elastic strain at the end of the third interval is thus

$$\varepsilon_E = a'''x + b''' - \Delta C(\text{2nd interval})$$

$$- \Delta C(\text{3rd interval}) - \varepsilon_C(\text{1st interval})$$

$$= a'''x + b''' - \left(\sum_{i=0}^{8} \phi_i x^i\right) - (q_1x^4 - q_2x^3 - q_3x^2$$

$$+ q_4x + q_5) - (k_4x^2 + k_5x + k_6)$$

or

$$\varepsilon_E = -\phi_8x^8 - \phi_7x^7 - \phi_6x^6 - \phi_5x^5 - \rho_1x^4 - \rho_2x^3 - \rho_3x^2$$

$$- \rho_4x - \rho_5$$

in which

$$\rho_1 = \phi_4 + q_1$$

$$\rho_2 = \phi_3 - q_2$$

$$\rho_3 = \phi_2 - q_3 + k_4$$

$$\rho_4 = \phi_1 + q_4 + k_5 - a'''$$

$$\rho_5 = \phi_0 + q_5 + k_6 - b'''$$

Let the concrete's stress-strain relationship at time T_3 be given by

$$\sigma = C_7(\varepsilon_E)^2 + C_8(\varepsilon_E)$$

$$= \sum_{i=0}^{16} \alpha_i x^i$$

in which it can be shown that

$$\alpha_0 = C_7\rho_5^2 - C_8\rho_5$$

$$\alpha_1 = 2C_7\rho_4\rho_5 - C_8\rho_4$$

$$\alpha_2 = C_7\ (2\rho_3\rho_5 + \rho_4^2) - C_8\rho_3$$

$$\alpha_3 = 2C_7(\rho_2\rho_5 + \rho_3\rho_4) - C_8\rho_2$$

$$\alpha_4 = C_7(\rho_3^2 + 2\rho\ \rho_4 + 2\rho_1\rho_5) - C_8\rho_1$$

$$\alpha_5 = 2C_7(\rho_3\rho_2 + \rho_1\rho_4 + w_5\rho_5) - C_8\phi_5$$

$$\alpha_6 = C_7(\rho_2^2 + 2\rho_1\rho_3 + 2w_5\rho_4 + 2w_6\rho_5) - C_8\phi_6$$

$$\alpha_7 = 2C_7(\rho_1\rho_2 + \phi_5\rho_3 + \phi_6\rho_4 + \phi_7\phi_5) - C_8\phi_7$$

$$\alpha_8 = C_7(\rho_1^2 + 2\phi_5\rho_2 + 2\phi_6\rho_3 + 2\phi_7\rho_4 + 2\phi_8\rho_5) - C_8\phi_8$$

$$\alpha_9 = 2C_7(\phi_5\rho_1 + \phi_6\rho_2 + \phi_7\rho_3 + \phi_8\rho_4)$$

$$\alpha_{10} = C_7(\phi_5 + 2\phi_6\rho_1 + 2\phi_7\rho_2 + 2\phi_8\rho_3)$$

$$\alpha_{11} = 2C_7(\phi_8\rho_2 + \phi_7\rho_1 + \phi_6\phi_5)$$

$$\alpha_{12} = C_7(\phi_6^2 + 2\phi_7\phi_5 + \phi_8\rho_1)$$

$$\alpha_{13} = 2C_7(\phi_6\phi_7 + \phi_5\phi_8)$$

$$\alpha_{14} = C_7(\phi_7^2 + 2\phi_6\phi_8)$$

$$\alpha_{15} = 2C_7\phi_7\phi_8$$

$$\alpha_{16} = C_7\phi_8^2$$

The force equivalent to this distribution is PCAL, given by

$$PCAL = t_o\int^W \sigma . dx$$

$$= t\sum_{i=0}^{16} \frac{\alpha_i W^{i+1}}{i+1}$$

Also, BMCAL $= t\int_0^W \sigma . x . dx$

$$= t \sum_{i=0}^{16} \frac{\alpha_i . W^{i+2}}{i+2}$$

Load-balancing iterations, as applied before, will bring PCAL and BMCAL to the correct values by adjusting a'" and b"', which define the total strain distribution. The α_i defining the distribution of stress will then also be known.

2A-2 Fortran Program to Predict the Effects of Creep of Plain Concrete Prisms under Sustained Eccentric Load

(i) Nomenclature:

Generally, variable names consisting of one letter, or a letter and a number, or a letter and one or more subscript(s), are equivalent to the corresponding lower case symbols used in Chapter 3.

e.g. E in the program denotes "e" from Chapter 3

P_3 in the program denotes p_3 from Chapter 3

Y(3) in the program denotes y_3 from Chapter 3

Q(1,3) in the program denotes q_{13} from Chapter 3, etc.

Exceptions to this rule and other names are listed below along with the equivalent symbol from Chapter 3.

BR(I)	θ_i
RCAL	BMCAL/W
BET(I)	β_i
EL(N)	ε_E evaluated at x = n

PERR(21, 22)	Function subprogram to calculate the fractional difference in z_1, z_2
GF(T_1, T_o)	Function subprogram to compute concrete's gain in strength in period T_1, T_o
NO	(Number of time interval) -1
TIMIT	Period under load of interest
CON1, CON2, etc.	k_1, k_2 etc.
W, DEP	Section dimensions w, t
XEC	ρX, load eccentricity
DELT	ΔT

Other variable names are either defined by the context they appear in or else have the same meaning as in the "element" method program.

(ii) Introduction to the Program

The program goes through the procedure described in Chapter 3. The various co-efficients which define the distributions of stress, and creep, elastic and total strains are computed in the same order as in Chapter 3.

The program is split into two main components:

(a) a main program

(b) a subroutine, GRAFT, in which the working for the co-efficients "Q" is carried out. In this subroutine, the superposition terms BET(I), corresponding to β_i, are computed and applied to the "Q" values.

```
$JOB           003336 GRAY D C
$IBJOB         NODECK
$IBFTC
C        **PROGRAM FOR CTS METHOD OF CALCULATING EFFECTS OF
C        ECCENTRIC CREEP IN PLAIN CONCRETE PRISMS
C        ***CAN BE USED FOR ANY NO. OF TIME INTERVALS
C        **INCLUDES SUPERPOSITION METHOD FOR CREEP UNDER VARYING STRESS
    6 READ(5,10) A,B,C1,C2,W,P,XEC
   10 FORMAT(2F12.2,2E12.4,3F10.2)
       WRITE(6,10) A,B,C1,C2,W,P,XEC
      READ(5,50) C,D,E,F,G,H
   50 FORMAT(6E12.5)
      WRITE(6,50) C,D,E,F,G,H
      READ(5,60) TO,DELT,ISEC
   60 FORMAT(2F10.2,I5)
      WRITE(6,60) TO,DELT,ISEC
      READ(5,70) DEP
   70 FORMAT(F10.2)
      READ(5,70) TIMIT
      LP=0
      BM=P*(XEC+W/2.)
  437 LP=LP+1
      CON1=C1*A*A
      CON2=(2.*B*C1+C2)*A
      CON3=(C2+C1*B)*B
      PCAL=W*(CON3+W*(CON2/2.+W*CON1/3.))
      PCAL=DEP*PCAL
      UP=ABS(A*W)*(P-PCAL)/(8.*P)
      B=B+UP
      CON2=(2.*B*C1+C2)*A
      CON3=(C2+C1*B)*B
      BMCAL=    (CON3/2.+W*(CON2/3.+W*CON1/4.))*W*W
      BMCAL=DEP*BMCAL
      UM=ABS(A*W)*(BM-BMCAL)/(8.*BM)
      B=B-UM
      A=A+2.*UM/W
      UC=A*W+B
      PERR=ERROR(P,PCAL)
       BMERR=ERROR(BM,BMCAL)
      IF (PERR-0.05) 206,206,205
  206 IF (BMERR-0.05) 180,180,205
  205 IF (LP-ISEC) 437,207,207
  207 WRITE(6,20) ISEC
   20 FORMAT(19H NON CONVERGENCE IN ,I3,7H CYCLES)
      CALL EXIT
  180 WRITE(6,30) P,PCAL,B,UC
   30 FORMAT(2F10.5,2F12.5)
C     INITIAL ELASTIC STRAINS NOW KNOWN
      T1=TO+DELT
       U2=C*A*A
      U1=(2.*B*C+D)*A
      U0=(C*B+D)*B+E
      V2=F*A*A
      V1=(2.*B*F+G)*A
      V0=(F*B+G)*B+H
      CON4=U2+V2*ALOG(T1)
      CON5=U1+V1*ALOG(T1)
      CON6=U0+V0*ALOG(T1)
```

```
C       NEXT VALUES OF A,B GIVE POST-CREEP VALUES------------
C       BEFORE LOAD BALANCE
      A=W*CON4+CON5+A
      B=B+CON6
      C3=C1*GF(T1,T0)
      C4=C2*GF(T1,T0)
      LP=0
  537 LP=LP+1
      WRITE(6,82) C3
   82 FORMAT(4H C3=,E11.4)
      WRITE(6,83) CON4
   83 FORMAT(6H CON4=,E11.4)
      CON7=A-CON5
      CON8=B-CON6
      P1=C3*CON4*CON4
      P2=-2.*CON4*CON7*C3
      P3=C3*(CON7*CON7-2.*CON4*CON8)-C4*CON4
      P4=CON7*(2.*C3*CON8+C4)
      P5=CON8*(C3*CON8+C4)
      WRITE(6,81) P1,P2,P3,P4,P5
   81 FORMAT(13H P1 TO P5 ARE,6E11.4)
       PCAL=W*(P5+W*(P4/2.+W*(P3/3.+W*(P2/4.+W*P1/5.))))
      PCAL=DEP*PCAL
      WRITE(6,30) P,PCAL
      UP=ABS(A*W)*(P-PCAL)/(8.*P)
      B=B+UP
      CON8=B-CON6
      P3=C3*(CON7*CON7-2.*CON4*CON8)-C4*CON4
      P4=CON7*(2.*C3*CON8+C4)
      P5=CON8*(C3*CON8+C4)
      BMCAL=    (P5/2.+W*(P4/3.+W*(P3/4.+W*(P2/5.+W*P1/6.))))*W*W
      BMCAL=DEP*BMCAL
      UM=ABS(A*W)*(BM-BMCAL)/(8.*BM)
      B=B-UM
      A=A+2.*UM/W
      UC=A*W+B
      PERR=ERROR(P,PCAL)
      BMERR=ERROR(BM,BMCAL)
      IF (PERR-0.05) 306,306,305
  306 IF (BMERR-0.05) 280,280,305
  305 IF (LP-ISEC) 537,307,307
  307 WRITE(6,20) ISEC
      CALL EXIT
  280 WRITE(6,30) P,PCAL,B,UC
C     THIS IS END OF CALCN FOR 1ST TIME INTERVAL
C     THIS IS CALC FOR 2ND TIME INTERVAL
      DIMENSION Z1(9),Z2(9)
      READ(5,70) DELT
      T2=T1+DELT
      NO=0
      COMMON/BLOK1/F,G,H,DELT,C3,C4,Y(9),T2,W,LP,NO,Q(5,12)/BLOK2/
     1 CON7,CON8,C,D,E,BR(3),S1,S2,S3
      DO 4 I=1,5
    4 Q(I,1)=0.0
   99 NO=NO+1
      C3=C1*GF(T2,T0)
      C4=C2*GF(T2,T0)
      LP=0
```

```
      IF(NO-1) 63,63,64
   63 BR(1)=-CON4
      BR(2)=CON7-A
      BR(3)=CON8-B
   64 CONTINUE
  637 LP=LP+1
      CALL GRAFT (A,B,CON4,CON5,CON6)
      DO 2 I=1,9
      A2=I
    2 Z1(I)=Y(I)/(10.-A2)
      PCAL=DEP*W*(Z1(9)+W*(Z1(8)+W*(Z1(7)+W*(Z1(6)+W*(Z1(5)
     1  +W*(Z1(4)+W*(Z1(3)+W*(Z1(2)+W*Z1(1)))))))))
      WRITE(6,70) PCAL
      UP=ABS(A*W)*(P-PCAL)/(8.*P)
      B=B+UP
      LP=LP+1
      CALL GRAFT (A,B,CON4,CON5,CON6)
      DO 3I=1,9
      A2=I
    3 Z1(I)=Y(I)/(11.-A2)
      RCAL=DEP*W*(Z1(9)+W*(Z1(8)+W*(Z1(7)+W*(Z1(6)+W*(Z1(5)
     1  +W*(Z1(4)+W*(Z1(3)+W*(Z1(2)+W*Z1(1)))))))))
      BMCAL=W*RCAL
      WRITE(6,30) BM,BMCAL
      UM=ABS(A*W)*(BM-BMCAL)/(8.*BM)
      WRITE(6,51) UM,UP
   51 FORMAT(4H UM=,E12.5,4H UP=,E12.5)
      B=B-UM
      A=A+2.*UM/W
      UC=A*W+B
      WRITE(6,84) A,UC
   84 FORMAT(3H A=,F10.5,4H UC=,F10.5)
      PERR=ERROR(P,PCAL)
      BMERR=ERROR(BM,BMCAL)
      IF (PERR-0.05) 406,406,405
  406 IF (BMERR-0.05) 380,380,405
  405 IF (LP-ISEC) 637,407,407
  407 WRITE(6,20) ISEC
      CALL EXIT
  380 WRITE(6,30) P,PCAL,B,UC,T2
C      NEXT PART IS FOR THIRD AND SUBSEQUENT TIME INTERVALS
      DOUBLE PRECISION X(6),EL(6),A1(8),B1(3)
      M=NO+1
      DO 5 I=1,6
      X(I)=I
    5 EL(I)=S3+X(I)*(S2+X(I)*(S1+X(I)*(Q(2,M)-X(I)*Q(1,M))))
      CALL DLESQ(A1,B1,X,EL,2,6)
      WRITE(6,98) B1(1),B1(2),B1(3)
   98 FORMAT(12H COEFFS ARE ,3F10.5)
      IF (NO-2) 61,62,62
   62 BR(1)=-B1(3)+CON4
      BR(2)=B1(2)-CON7
      BR(3)=B1(1)-CON8
   61 CON4=-B1(3)
      CON7=B1(2)
      CON8=B1(1)
      IF (T2-TIMIT) 97,96,96
   97 READ(5,70) DELT
```

```
      T2=T2+DELT
      T1=T1+DELT
      GO TO 99
   96 GO TO 6
      END
$IBFTC GRAFT
       SUBROUTINE GRAFT(A,B,CON4,CON5,CON6)
      COMMON/BLOK1/F,G,H,DELT,C3,C4,Y(9),T2,W,LP,NO,Q(5,12)/BLOK2/
     1 CON7,CON8,C,D,E,BR(3),S1,S2,S3
      DIMENSION R(5),BET(5),T(5)
      IF(NO-1) 96,96,97
   96 CON7=A-CON5
      CON8=B-CON6
   97 CONTINUE
      WRITE(6,52) CON7,CON8
   52 FORMAT (6H CON7=,E12.5,6H CON8=,E12.5)
      R(1)=F*CON4*CON4
      R(2)=2.*F*CON4*CON7
      R(3)=F*(2.*CON4*CON8-CON7*CON7)+G*CON4
      R(4)=(2.*F*CON8+G)*CON7
      R(5)=CON8*(F*CON8+G)+H
      IF(LP-2) 34,35,35
   34 B=B+R(5)*DELT/(T2-DELT/2.)
      A=A+(R(4)+W*(-R(3)+W*(-R(2)+W*R(1))))*DELT/(T2-DELT/2.)
   35 CONTINUE
      M=NO+1
      DO 1 I=1,5
    1 Q(I,M)=R(I)*DELT/(T2-DELT/2.) +Q(I,NO)
      FAC=C+F*ALOG(DELT)
      GAC=D+G*ALOG(DELT)
      BET(1)=BR(1)*BR(1)*FAC
      BET(2)=2.*BR(1)*BR(2)*FAC
      BET(3)=(BR(2)*BR(2)+2.*BR(1)*BR(3))*FAC+BR(2)*GAC
      BET(4)=2.*BR(3)*BR(2)*FAC+BR(2)*GAC
      BET(5)=BR(3)*BR(3)*FAC+BR(3)*GAC+E+H*ALOG(DELT)
      DO 2 I=1,5
    2 T(I)=Q(I,M)
      T(1)=T(1)+BET(1)
      T(2)=T(2)-BET(2)
      T(3)=T(3)-BET(3)
      T(4)=T(4)+BET(4)
      T(5)=T(5)+BET(5)
      S1=T(3)-CON4
      S2=A-T(4)-CON5
      S3=B-T(5)-CON6
      Y(1)=C3*T(1)*T(1)
      Y(2)=-2.*C3*T(1)*T(2)
      Y(3)=C3*(T(2)*T(2)-2.*T(1)*S1)
      Y(4)=C3*2.*(T(2)*S1-T(1)*S2)
      Y(5)=C3*(-2.*T(1)*S3+2.*T(2)*S2+S1*S1)-C4*T(1)
      Y(6)=C3*(2.*S1*S2+T(2)*S3+S3*T(2))+C4*T(2)
      Y(7)=C3*(2.*S1*S3+S2*S2)+C4*S1
      Y(8)=S2*(2.*S3*C3+C4)
      Y(9)=S3*(C4+C3*S3)
      RETURN
      END
$IBFTC ERROR
      FUNCTION ERROR(Z1,Z2)
```

```
      ERROR=ABS(Z1-Z2)/Z1
      RETURN
       END
$IBFTC GF
      FUNCTION GF(T1,T0)
      GF=1.+(T1-T0)*.0015
      RETURN
       END
```

CD TOT   0240

APPENDIX III

TABULATION OF EXPERIMENTAL RESULTS

The readings of strain for the concentrically-loaded creep prisms are entered in Table A-3-1. The readings of elastic recovery of these prisms, measured immediately on off-loading after 137 days under load, are entered in Table A-3-2. The elastic recovery strains predicted using the assumptions described in Chapter 2 are also tabulated for comparison purposes.

Tables A-3-3 and A-3-4 contain the strain readings taken from the various locations on the member cross-setions. These locations are identified below.

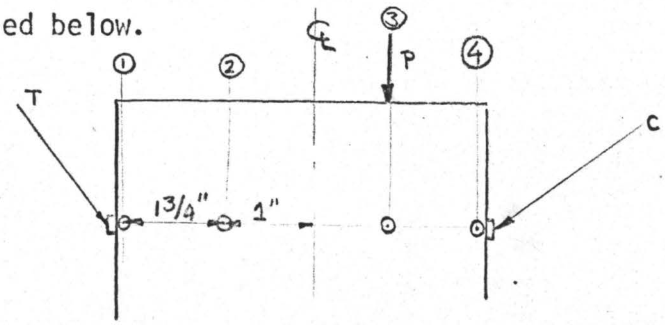

When no strains are recorded for one location on a particular prism, it is because the gauge points at that location proved defective. (That is, it was not possible to repeat the readings to within one half of a division). The readings entered under the headings "1", "2", "3", and "4" are normally averages of the readings at these locations on opposite faces. The readings under "T" and "C" are readings from single sets of gauge points.

The strains entered in the "elastic recovery" section are those measured immediately after off-loading at 137 days.

Time Since Loading (days)	Creep Strains x 10^5 (in/in)			
	C-750	C-1500	C-2250	C-3000
4	7.0	15.0	45.0	97.0
5	7.8	17.5	49.0	122.5
7	10.0	22.5	63.0	150.0
10	13.0	30.9	90.0	210.0
14	16.8	36.2	103.0	235.0
18	17.5	40.4	118.6	250.0
21	19.8	45.8	122.8	256.0
28	22.8	49.2	130.0	267.5
38	24.8	53.9	137.2	276.0
46	25.8	57.5	135.7	283.7
54	31.3	58.6	141.5	289.0
66	33.0	63.8	151.5	291.0
82	33.3	64.1	152.0	291.7
100	33.5	64.5	154.5	295.0
137	34.5	67.0	160.5	306.0

TABLE A-3-1 Creep of the Concentrically-Loaded Prisms

Specimen	C-750	C-1500	C-2250	C-3000
Recovery (137 days)	18.5	35.3	58.5	66.5
Predicted Recovery	23.5	47.0	75.0	102.0

TABLE A-3-2 Measured and Predicted Recovery Strains

TABLE A-3-3 Strains of Prisms E-750, E-1500

Specimen	E-750						E-1500					
Location	T	1	2	3	4	C	T	1	2	3	4	C
Time Since Loaded	CREEP STRAINS (IN/INX10 ^{5})											
4	-	2.0	4.0	5.0	7.0	-	5.0	4.5	18.5	39.0	48.0	53.0
5	-	4.0	5.0	6.0	10.0	-	5.0	4.5	22.5	43.5	49.0	58.0
7	-	6.0	6.0	9.0	14.0	-	7.0	5.5	29.5	55.5	63.0	73.0
10	-	7.0	9.0	12.0	17.0	-	9.0	8.0	40.0	74.0	89.0	97.0
14	-	9.0	14.0	17.0	20.0	-	10.0	8.5	46.5	85.0	106.0	114.0
18	-	12.0	15.0	19.0	22.0	-	11.0	9.5	52.5	95.0	117.0	123.0
21	-	12.0	16.0	20.0	24.0	-	12.0	11.0	60.5	105.5	128.0	139.0
28	-	15.0	18.0	24.0	29.0	-	14.0	12.5	66.0	117.0	139.0	148.0
38	-	17.0	22.0	26.0	33.0	-	15.0	13.5	70.5	123.5	158.0	162.0
46	-	17.0	22.5	27.0	35.0	-	17.0	15.0	73.5	129.0	167.0	168.0
54	-	18.0	24.5	28.0	36.5	-	19.0	18.5	82.5	133.5	187.0	184.0
66	-	18.0	26.0	29.0	39.0	-	21.0	22.5	89.0	140.5	194.0	193.0
82	-	19.0	27.0	30.0	40.5	-	23.0	24.0	97.5	145.0	198.0	200.0
100	-	20.0	28.0	32.0	42.0	-	25.0	26.0	98.5	150.0	201.0	203.0
137	-	21.0	29.5	34.0	44.5	-	25.0	27.0	101.0	154.0	203.0	205.0
Initial Elastic Strains	-	8.0	25.0	41.0	55.0	-	8.0	9.0	34.0	77.0	92.0	94.0
Elastic Recovery	-	4.0	15.0	28.5	41.0		5.0	5.5	21.0	42.5	62.0	63.5

TABLE A-3-4 Strains of Prisms E-1000, E-1750

Specimen	E-1750						E-1000					
Location	T	1	2	3	4	C	T	1	2	3	4	C
Time Since Loaded	CREEP STRAINS (IN/INX10^5)											
3	-	-	-	-	-	-	4.0	-	7.0	7.0	10.0	11.0
4		1.0	14.0	24.0	50.0	48.0	-	-	-	-	-	-
5		2.0	16.0	27.0	56.0	50.0	-	-	-	-	-	-
6	-	-	-	-	-	-	9.0	-	12.5	15.5	17.0	19.0
7		3.0	20.0	41.0	72.0	68.0	9.0	-	12.5	13.5	17.5	19.0
10	-	-	-	-	-	-	10.0	-	13.5	17.0	21.5	23.0
14		7.0	41.0	85.0	134.0	125.0	9.0	-	13.5	17.0	24.0	23.0
18		8.0	46.0	94.0	143.0	158.0	-	-	-	-	-	-
21		9.0	53.0	110.0	165.0	175.0	15.0	-	23.5	25.5	31.5	33.0
28		9.0	56.0	119.0	180.0	195.0	18.0	-	27.0	27.5	33.5	37.0
30	-	-	-	-	-	-	19.0	-	28.0	28.5	35.5	39.0
38		10.0	61.0	130.0	195.0	200.0	21.0	-	30.0	32.5	38.0	41.0*
46		16.0	67.0	129.0	194.0	180.0	*40 Day Strains					
54		18.0	68.0	125.0	189.0	198.0						
66		28.0	73.0	146.0	199.0	204.0						
82		30.0	78.0	156.0	202.0	210.0						
100		32.0	79.0	158.0	209.0	217.0						
137		34.0	80.5	161.0	211.0	220.0						
Initial Elastic Strain	-	18.0	56.0	98.0	154.0	158.0	12.0	-	30.0	54.0	70.0	72.0
Elastic Recovery	-	7.0	27.5	50.5	61.0	62.0	8.0	-	19.0	32.0	40.0	42.0

REFERENCES

1. ACI Bibliography No. 7, "Shrinkage and Creep in Concrete", American Concrete Institute, Detroit, 1967.

2. CACA Bibliography, "Creep and Shrinkage of Concrete", Cement and Concrete Association, London, England.

3. Neville, A.M., "Properties of Concrete:, Sir Isaac Pitman, London, 1963.

4. Theory of Thomas, described by Neville, A.M. in "Theories of Creep in Concrete", ACI Journal, Proceedings, V.52, September 1955, p. 47-60.

5. Powers, T.C., discussion of "Mechanisms of Creep in Concrete", by C.E. Kesler and I. Ali, ACI Publication SP-9,"Symposium on Creep of Concrete", p. 1-31.

6. Neville, A.M., and Meyers, B.L., "Creep of Concrete: Influencing Factors and Prediction", ACI Publication SP-9, "Symposium on Creep of Concrete", p. 1-31.

7. "Design and Control of Concrete Mixtures", Portland Cement Association, Published by the Portland Cement Association, 1967.

8. Mattock, A.H., and Hansen, T.C., "Influence of Size and Shape of Member on Shrinkage and Creep of Concrete", Portland Cement Association Research and Development Laboratories, Bulletin D103.

9. Ross, A.D., "Concrete Creep Data", Structural Engineer, V15, No. 8, August 1937, p. 314-326.

10. Freudenthal, A.M. and Roll, F., "Creep and Creep-recovery of Concrete under High Compressive Stress", ACI Journal, Proceedings, V54, No. 12, June 1958, p. 1111-1142.

11. Drysdale, R.G., "The Behaviour of Slender Reinforced Concrete Columns Subjected to Sustained Biaxial Bending", Ph.D. thesis, University of Toronto, 1967.

12. Troxell, G.E., Raphael, J.M., and Davis, R.E., "Long-Time Creep and Shrinkage Tests of Plain and Reinforced Concrete", Proceedings, ASTM, V. 58, 1958, p. 1101-1120.

13. Pickett, G., "The Effect of Moisture Content on the Creep of Concrete Under a Sustained Load", ACI Journal, Proceedings, V.38, No. 6, February 1942, p. 333-355.

14. Kesler, C.E., and Ali, I., "Mechanisms of Creep in Concrete" ACI Publication SP-9, "Symposium on Creep of Concrete", p. 35-55.